

---

# Mesonic Excitations in an Inhomogeneous Phase of the Nambu–Jona-Lasinio Model

---

Mesonische Anregungen in einer Inhomogenen Phase des Nambu–Jona-Lasinio–Modells  
Master-Thesis von Jamil Hirsch  
November 2013



TECHNISCHE  
UNIVERSITÄT  
DARMSTADT

Fachbereich Physik  
Institut für Kernphysik  
NHQ

Mesonic Excitations in an Inhomogeneous Phase of the Nambu–Jona-Lasinio Model  
Mesonische Anregungen in einer Inhomogenen Phase des Nambu–Jona-Lasinio–Modells

Vorgelegte Master-Thesis von Jamil Hirsch

1. Gutachten: Priv.-Doz. Dr. Michael Buballa
2. Gutachten: Prof. Dr. Jochen Wambach

Tag der Einreichung:

---

## Abstract

---

We study the inhomogeneous phase with chiral density wave modulation within the framework of the two-flavor Nambu–Jona-Lasinio model. Using mean-field methods we determine the dressed quark propagator for the inhomogeneous phase and calculate constituent quark masses. The polarization loop of the Bethe-Salpeter equation playing a crucial role in acquiring mesonic propagators and masses is investigated. Numerically evaluable expressions for the polarization loop are derived and results of calculations for simple scenarios are shown.

---

## Zusammenfassung

---

Wir untersuchen im Rahmen des mit zwei Quarkflavours ausgestatteten Nambu–Jona-Lasinio-Modells eine inhomogene, durch eine chirale Dichtewelle modulierte, Phase. Unter Verwendung von Molekularfeld-Methoden ermitteln wir den gedressten Quarkpropagator für die genannte inhomogene Phase und berechnen die Amplitude der Modulation. Die Polarisations-Schleife der Bethe-Salpeter-Gleichung, welche eine entscheidende Rolle für die Erarbeitung von Mesonenpropagatoren und -massen spielt, wird untersucht. Numerisch auswertbare Ausdrücke für die Polarisations-Schleife werden hergeleitet und es werden Ergebnisse von Rechnungen für einfache Szenarien gezeigt.

---

## **Erklärung zur Eigenständigkeit**

---

Hiermit versichere ich, die vorliegende Masterarbeit ohne Hilfe Dritter nur mit den angegebenen Quellen und Hilfsmitteln angefertigt zu haben. Alle Stellen, die aus Quellen entnommen wurden, sind als solche kenntlich gemacht. Die schriftliche und elektronische Fassung stimmen überein. Diese Arbeit hat in gleicher oder ähnlicher Form noch keiner Prüfungsbehörde vorgelegen.

Darmstadt, den 28.11.2013

---

(Jamil Hirsch)

---

## Acknowledgment

---

I would like to thank my supervisor Priv.-Doz. Dr. Michael Buballa for the time he took to have detailed and in-depth discussions with me. I thank Prof. Dr. Jochen Wambach for the opportunity to conduct this research in the NHQ group. Furthermore I thank my colleagues in office 302 for a very pleasant atmosphere and the members of the NHQ group for their help with mathematical, numerical and technical issues.

---

## Contents

---

<b>1. Introduction</b>	<b>5</b>
1.1. Overview . . . . .	6
<b>2. The NJL Model in Vacuum</b>	<b>8</b>
2.1. The NJL Lagrangian . . . . .	8
2.2. Gap Equation . . . . .	10
2.3. Mesons . . . . .	11
2.4. Numerical Results . . . . .	13
<b>3. The NJL Model in Medium</b>	<b>14</b>
3.1. Gap Equation . . . . .	14
3.2. Mesons . . . . .	15
3.3. Numerical Results . . . . .	16
<b>4. Inhomogeneous Phase</b>	<b>17</b>
4.1. Dressed quark propagator . . . . .	17
4.2. Gap Equation . . . . .	21
4.3. Mesons . . . . .	23
4.4. Numerical Results . . . . .	27
<b>5. Summary, Conclusion and Outlook</b>	<b>35</b>
<b>Appendices</b>	<b>37</b>
<b>A. Miscellaneous</b>	<b>38</b>
<b>B. Vacuum Calculations</b>	<b>39</b>
<b>C. Medium Calculations</b>	<b>45</b>
<b>D. Inhomogeneous Phase Calculations</b>	<b>48</b>
<b>Bibliography</b>	<b>65</b>

---

## 1 Introduction

---

The Standard Model of particle physics is today's most prominent theory for explaining the existing particles and interactions on their most basic level, except for gravity. Among the three other interactions, electromagnetic, weak and strong, the strong one is responsible for the binding of quarks, the most fundamental constituents of matter.

Up to the early 1960's nuclear physicists thought that the large ensemble of known, strongly interacting particles was elementary, yet their origin was unexplained. In 1964 Gell-Mann [1] introduced his idea of the existence of a few underlying elementary particles, quarks and anti-quarks, which composed all strongly interacting particles. A decade later quantum chromodynamics (QCD) [2] was introduced and is today the most accepted theory describing quarks and their interaction.

Quarks are spin 1/2 point-like particles with mass which interact due to massless spin 1 gluons. Quarks come in different flavors and have electrical charge. In analogy to the role of the electrical charge for electromagnetic interactions, quarks and gluons carry a so-called color charge. The fact that gluons can carry color charge, unlike photons which do not carry electrical charge, leads to a more complicated nature of the strong interaction since gluons can interact with each other.

The two most prominent features of QCD originating from the nature of strong interaction are confinement [3] and asymptotic freedom [4, 5]. Asymptotic freedom means that the interaction of quarks and gluons gets weaker with decreasing distances or equivalently increasing energies. This is related to interesting low-energy properties of QCD like confinement. Confinement states that at low energies quarks and gluons only appear in bound states and cannot be observed freely. Another important feature of QCD is the chiral symmetry [6] and its spontaneous breaking responsible for the high masses of hadrons despite very low quark masses.

Consequently, the investigation of QCD matter and the mapping of the QCD phase diagram [8] depicted in Figure 1.1 is of particular interest and nuclear physicists have made an enormous effort to achieve progress in this field of research. The QCD phase diagram shows the phase structure of QCD matter, which is described by the thermodynamical variables temperature  $T$  and chemical potential  $\mu$ . The chemical potential  $\mu$  is related to the net baryon density. As mentioned above, in the low-energy regime, i.e. at low temperature and net density, QCD matter exists in form of confined hadrons. With the help of heavy ion colliders like LHC and RHIC it is experimentally possible to explore the region along the temperature axis for zero net density. Ab initio calculations in lattice QCD were able to provide useful insight on the phase transition, more precisely crossover transition, from confined to deconfined QCD matter, or quark-gluon plasma, at a temperature of about 170 MeV [9].

Nevertheless, heavy ion collisions and lattice QCD are not able to describe areas of the QCD phase diagram, where the density is nonzero. The sign-problem [10] prohibits lattice calculations for nonzero net baryon density and only recent developments have allowed progress in

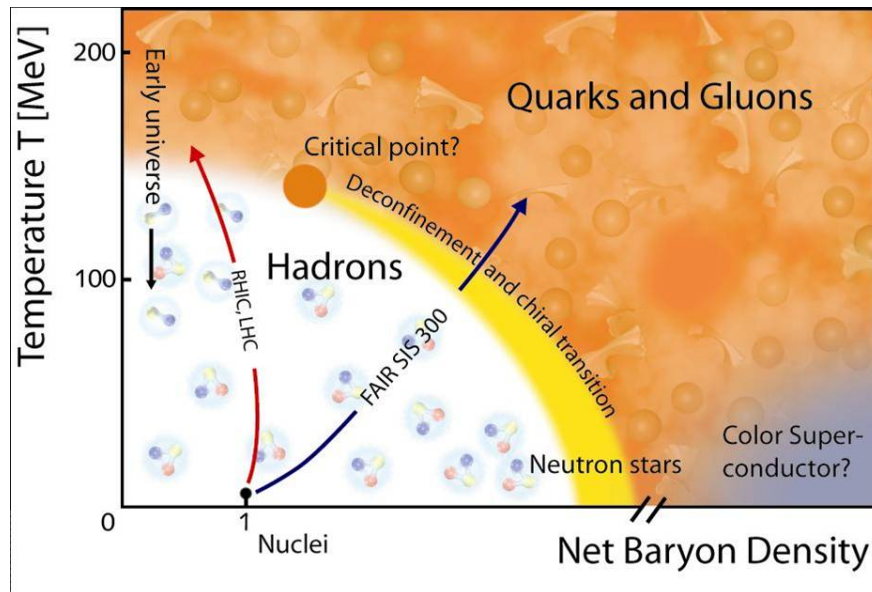


**Figure 1.1.:** A conjecture about the QCD phase diagram [7].

this direction [11]. Experimentally the QCD phase diagram area of low temperature and intermediate to high density cannot be accessed as of today.

In order to explore the QCD phase diagram at low temperatures and intermediate to high net baryon densities, one has to turn to effective theories. Effective theories describe only certain features of exact theories while neglecting others and therefore are more manageable. The phase structure of QCD matter is believed to be multi-variant at low temperatures and intermediate to high net baryon densities [12, 13]. While the formation of a color-superconducting phase [14] is expected in the area of high densities, the area of intermediate densities can be described as an inhomogeneous phase, characterized by spatially dependent properties of the system, an idea introduced by Overhauser in 1960 [15].

One effective model of QCD is the Nambu and Jona-Lasinio (NJL) model [16, 17], which we would like to discuss in the context of inhomogeneous phases in this thesis. The NJL model features no gluons but shares important symmetries with QCD. NJL model analyses of the low temperature and intermediate to high density region of the QCD phase diagram have been done in-detail [12]. Quarks and their properties in inhomogeneous phases as well as inhomogeneous phases by themselves have been studied [18, 19].

The aim of this work is to study properties of mesonic excitations in an inhomogeneous phase of the QCD phase diagram within the framework of the NJL model.

---

## 1.1 Overview

---

In chapter 2 we will introduce the reader to the NJL model in vacuum. We will show, how the dynamical mass generation of quarks is described and how mesons are built from quarks. Some simple results for their masses will be given.



---

In chapter 3 we move our discussion from the vacuum into the medium, through the introduction of finite temperature and chemical potential. We will discuss, which changes to the mass gap and the description of the mesons occur due to introduction of temperature and chemical potential then show some results at the end of this chapter.

In chapter 4 we take another step forward and allow an inhomogeneous phase to occur. We calculate the dressed quark propagator and analyze the gap equation and self-energy of quarks. We discuss our investigation regarding mesons in the inhomogeneous phase and present findings.

In chapter 5 we conclude this thesis with a summary, a discussion of our results and problems and an outlook.

---

## 2 The NJL Model in Vacuum

---

The NJL model was derived by Yoichiro Nambu and Giovanni Jona-Lasinio with the aim to “develop a dynamical theory of elementary particles in which nucleons and mesons are derived in a unified way from a fundamental spinor field”[16, 17]. Later on, after the quarks and the phenomenon of confinement had been discovered, this model was reinterpreted as an effective theory for interacting quarks. Therefore the NJL model does not take confinement into account. Chiral symmetry on the other hand is a feature of the NJL model.

---

### 2.1 The NJL Lagrangian

---

A simple form of the NJL Lagrangian, describing the two lightest quarks, up and down, can be given by

$$\mathcal{L} = \bar{\psi}(i\cancel{\partial} - \underline{m})\psi + G_S \left[ (\bar{\psi}\psi)^2 + (\bar{\psi}i\gamma^5\vec{\tau}\psi)^2 \right]. \quad (2.1)$$

The first term is the Dirac Lagrangian of a free relativistic particle, while the second term describes the four-point interactions of the quarks.  $\psi$  is the incoming and  $\bar{\psi} = \psi^\dagger\gamma_0$  the outgoing quark-antiquark field. They have 4 components in Dirac space with additional  $N_f = 2$  flavor and  $N_c = 3$  color degrees of freedom, resulting in  $4N_fN_c$ -dimensional spinor fields.  $\underline{m} = \text{diag}(m_u, m_d)$  is the bare or current quark mass. For simplicity we assume that up quark and down quark have the same mass  $m$ .  $G_S$  is the coupling constant and has the dimension of  $[\text{energy}]^{-2}$ .  $(\bar{\psi}\psi)^2$  is a scalar and  $(\bar{\psi}i\gamma^5\vec{\tau}\psi)^2$  a pseudoscalar four-point interaction. Although NJL Lagrangian can generically be extended to more quark flavors or interaction channels, we will restrict ourselves to the above NJL Lagrangian.

---

### Symmetries

---

Symmetries are very important features of physical systems. If a physical system undergoes a transformation, i.e. translation or rotation in space, which leaves certain properties of the physical system unchanged, these properties are called invariants of the system. They are symmetric under given transformation. In the following we want to discuss some symmetries the NJL Lagrangian shares with QCD and to which conservation laws these symmetries lead according to Noether’s theorem.

The first symmetry of the NJL Lagrangian is its invariance under a global phase transition of the kind

$$\psi \rightarrow \psi e^{-i\alpha} \quad \text{and} \quad \bar{\psi} \rightarrow \bar{\psi} e^{i\alpha} \quad \text{for} \quad \alpha \in \mathbb{R}. \quad (2.2)$$

The conserved quantity of this invariance is the baryon number.

We assumed that both, up and down quark, have the same mass, thus we can describe them as isospin partners. The NJL Lagrangian then is invariant under rotations in the isospin space

$$\psi \rightarrow \psi e^{-\frac{i}{2}\alpha_a\tau_a} \quad \text{and} \quad \bar{\psi} \rightarrow \bar{\psi} e^{\frac{i}{2}\alpha_a\tau_a} \quad \text{for} \quad \alpha_a \in \mathbb{R}, \quad a = 1, 2, 3. \quad (2.3)$$

This invariance corresponds to the conservation of isospin.

In the chiral limit ( $m = m_d = m_u = 0$ ) the NJL Lagrangian additionally becomes invariant under unitary transformations of the kind

$$\psi \rightarrow e^{-\frac{i}{2}\gamma^5\alpha_a\tau_a}\psi \quad \text{and} \quad \bar{\psi} \rightarrow \bar{\psi}e^{-\frac{i}{2}\gamma^5\alpha_a\tau_a} \quad \text{for} \quad \alpha_a \in \mathbb{R}. \quad (2.4)$$

The combination of the last two symmetries is referred to as chiral symmetry. It is explicitly broken by the non-zero quark mass in the NJL Lagrangian. Since the bare quark mass is quite small, the chiral symmetry can be considered as approximately fulfilled. However, the interaction terms of the NJL Lagrangian dynamically generate an effective quark mass, even in the chiral limit. This phenomenon is referred to as spontaneous breaking of the chiral symmetry.

---

## Feynman Rules

---

In quantum field theories it is customary to use Feynman diagrams to write down equations and physical processes. We now want to discuss the basic Feynman diagrams and rules used in this work. First of all, there is the bare quark propagator

$$\text{-----}\overleftarrow{p}\text{-----} = iS_0(p) = i\frac{\not{p} + m}{p^2 - m^2 + i\epsilon} \quad (2.5)$$

the standard propagator for a Dirac fermion. Here we used the Feynman slash notation  $\not{p} = \gamma^\mu p_\mu$ . As mentioned above, the interaction channels of the NJL Lagrangian generate mass. Then the quark is called dressed, having an effective or constituent mass  $M$ . It is described by the dressed quark propagator

$$\text{-----}\overleftarrow{p}\text{-----} = iS(p) = i\frac{\not{p} + M}{p^2 - M^2 + i\epsilon}. \quad (2.6)$$

The couplings are depicted as interaction vertices

$$\begin{array}{c} \diagup \\ \diagdown \end{array} \bullet \begin{array}{c} \diagdown \\ \diagup \end{array} = 2iG_S\Gamma_M \otimes \Gamma_M \quad (2.7)$$

with

$$\Gamma_M = \begin{cases} \Gamma_\sigma = \mathbb{1}_{\text{Dirac}} \otimes \mathbb{1}_{\text{color}} \otimes \mathbb{1}_{\text{flavor}} & \text{scalar channel} \\ \Gamma_\pi = i\gamma^5 \otimes \mathbb{1}_{\text{color}} \otimes \tau_a & \text{pseudo-scalar channel } (a \in [1, 2, 3]) \end{cases} \quad (2.8)$$

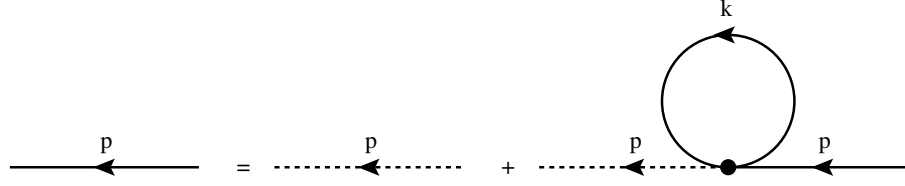
As usual for fermionic theories, for a closed fermion loop with momentum label  $k$  we have

$$- \int \frac{d^4k}{(2\pi)^4} \text{Tr}[\dots], \quad (2.9)$$

where the trace contains the propagators of the loop. For more details regarding Feynman rules and diagrams, see [20].

## 2.2 Gap Equation

As a first application, we want to calculate the effective quark mass, which is generated via self-coupling of the quarks. We will derive an expression for the constituent quark mass from the self-consistent Dyson equation



$$\text{Solid line } p \leftarrow = \text{Dashed line } p \leftarrow + \text{Dashed line } p \leftarrow \text{---} \text{Loop } k \text{---} \text{Dashed line } p \leftarrow \quad (2.10)$$

Using the Feynman rules for the propagators given above, we can rewrite this diagrammatic expression into the formula

$$iS(p) = iS_0(p) + iS_0(p)(-i\Sigma)iS(p). \quad (2.11)$$

Multiplying with  $S_0^{-1}(p)$  from the left and  $S^{-1}(p)$  from the right we arrive at

$$M = m + \Sigma \quad (2.12)$$

where  $\Sigma$  denotes the self-energy. Here we ignored  $i\epsilon$  and used  $\not{p}^2 = p^2$ . Using the Feynman rules, the self-energy  $\Sigma$  translates into the formula

$$\Sigma = 2G_S \left( \mathbb{1} \int \frac{d^4k}{(2\pi)^4} \text{Tr}[\mathbb{1}iS(k)] + i\gamma^5 \tau_a \int \frac{d^4k}{(2\pi)^4} \text{Tr}[i\gamma^5 \tau_a iS(k)] \right) \quad (2.13)$$

where the trace has to be taken over color-, flavor- and Dirac-space. Detailed evaluation of this expression<sup>1</sup> yields

$$\Sigma = 8G_S N_f N_c M I_1(M), \quad (2.14)$$

with the integral<sup>2</sup>  $I_1(M)$  being

$$I_1(M) \equiv I_1^{\text{vac}}(M) = i \int \frac{d^4k}{(2\pi)^4} \frac{1}{k^2 - M^2 + i\epsilon} = \frac{1}{4\pi^2} \int_0^\infty dk \frac{k^2}{\sqrt{k^2 + M^2}}. \quad (2.15)$$

---

### Regularization

---

The integrand of  $I_1^{\text{vac}}(M)$  diverges, since the upper bound of integration is infinity. Throughout this work we will frequently encounter such divergencies. In order to calculate the integrals, one has to regularize them with the result that those divergencies vanish. In the following we want to present some of the commonly used regularization schemes.

<sup>1</sup> See appendix B on page 39.

<sup>2</sup> For details of calculation see appendix B on page 42.

---

## Sharp Three-Momentum Cutoff

---

A simple limitation to values of  $|\vec{k}|$  up to  $\Lambda$ .

$$\int \frac{d^4k}{(2\pi)^4} f(k, m) \longrightarrow \int_{-\infty}^{+\infty} \frac{dk_0}{2\pi} \int_{|\vec{k}| < \Lambda} \frac{d^3k}{(2\pi)^3} f(k, m) \quad (2.16)$$

The integral gets finite and can be calculated easily. The drawback of this method is that the Lorentz invariance is lost because the non-invariant  $\vec{k}$  is restricted and the resulting integration domain is not invariant under translations.

---

## Sharp Four-Momentum Cutoff

---

This regularization scheme is similar to the Three-Momentum Cutoff. It involves a Wick rotation and it preserves Lorentz invariance, since the limiting value is imposed on the invariant  $k^2$ .

$$\int \frac{d^4k}{(2\pi)^4} f(k, m) \longrightarrow i \int_{\sqrt{\vec{k}^2 + k_4^2} < \Lambda} \frac{d^3k}{(2\pi)^3} \frac{dk_4}{2\pi} f(\vec{k}, ik_4, m), \quad (2.17)$$

where we substituted  $k_4 = -ik_0$ . The disadvantage of this technique is, that we put an unphysical restriction on the inhomogeneous phase which we want to study in this work.

---

## Pauli-Villars regularization

---

This scheme does not use a sharp momentum cutoff, but changes the asymptotic behaviour of the integrand. Additional terms are added to the integrand which contribute hardly for small momenta but have the same behaviour as the integrand for high momenta, evening out divergencies for high momenta.

$$\int \frac{d^4k}{(2\pi)^4} f(k, m) \longrightarrow \int \frac{d^4k}{(2\pi)^4} \sum_{\alpha=0}^n c_{\alpha} f(k, m_{\alpha}) \quad (2.18)$$

We will use the Pauli-Villars regularization [21] with different regulator terms throughout this work.

---

## 2.3 Mesons

---

Now that we know how to calculate the constituent quark masses, we take the next step and build mesons out of these constituent quarks. In the NJL model mesons are described as a state of quark-antiquark-scattering. The mathematical description of this process is given by the Bethe-Salpeter equation [22]. This equation describes the bound states of two particles by iterating the interaction of these particles infinitely many times. As Feynman diagram the equation reads

$$\text{Diagram 1} = \text{Diagram 2} + \text{Diagram 3} \quad (2.19)$$

where the double lines depict propagating mesons. This diagram is translated into

$$iT_M = iK_M + iK_M(-i\Pi_M)iT_M. \quad (2.20)$$

Here  $M \in \{\sigma, \pi^a\}$  denotes the type of mesons we want to study in this work. The elements of this equation are

- the  $q\bar{q}$ -scattering matrix

$$iT_M = \Gamma_M it(q) \Gamma_M, \quad (2.21)$$

- the scattering kernel

$$iK_M = \Gamma_M 2iG_S \Gamma_M, \quad (2.22)$$

- the polarization loop

$$J_M(q) = \Gamma_M \Pi_M \Gamma_M. \quad (2.23)$$

Inserting these expressions into eq. (2.20) we get

$$it(q) = \frac{2iG_S}{1 - 2G_S J_M(q)}.^3 \quad (2.24)$$

Based on its connection to the scattering matrix of the Bethe-Salpeter equation, this expression is referred to as the meson propagator. Thus it should have the same properties as a propagator, i.e. it has a pole at the meson mass  $m_M$

$$1 - 2G_S J_M(q)|_{q=m_M} \stackrel{!}{=} 0. \quad (2.25)$$

This relation allows us to calculate the meson mass. In order to calculate a numerical value for the mass we will have to evaluate the polarization loop  $J_M(q)$ .<sup>4</sup> We get two slightly different expressions, one for each meson

$$J_{\pi_a}(q) = 4N_f N_c I_1^{vac}(M) - 2N_f N_c q^2 I_2^{vac}(q, M) \quad (2.26)$$

and

$$J_\sigma(q) = 4N_f N_c I_1^{vac}(M) - 2N_f N_c (q^2 - 4M^2) I_2^{vac}(q, M). \quad (2.27)$$

We already know  $I_1^{vac}(M)$  from our calculations regarding the mass gap. The new integral  $I_2^{vac}(q, M)$  is given by

$$I_2^{vac}(q, M) = i \int \frac{d^4k}{(2\pi)^4} \frac{1}{[k^2 - M^2 + i\epsilon][(k+q)^2 - M^2 + i\epsilon]}. \quad (2.28)$$

<sup>3</sup> For detailed derivation please see B on page 39.

<sup>4</sup> Details of the calculation are on page 40 in appendix B.

## 2.4 Numerical Results

To conclude the description of the NJL model in vacuum, we will show some numerical results based on the calculations done so far. We have calculated the current quark mass and the mass of the pion. The results are presented in Table 2.1. The  $k_0$ -integration and add-on simplification of  $I_1^{\nu ac}(M)$  and  $I_2^{\nu ac}(q, M)$  have been done analytically<sup>5</sup>. For the remaining integration we used the Pauli-Villars regularization scheme with the following corrections to the integrand  $f(k, M)$ :

$$f(k, M) \rightarrow f(k, M) - 2f(k, \sqrt{M^2 + \Lambda^2}) + f(k, \sqrt{M^2 + 2\Lambda^2}). \quad (2.29)$$

The parameters have been fitted to a pion mass of 140.0 MeV. Due to this fact we retain the same value of the pion mass for every parameter set. All five parameter sets have been fitted to different values of the pion decay constant [23], which relate to different corrections to the theoretical description. Parameter set A reflects the experimentally measured pion decay constant. The results for the constituent quark mass agree with [23]. The much higher constituent quark mass reflects the spontaneous chiral symmetry breaking due to dynamical mass generation via self-coupling of the quarks. There are no explicit results for  $m_\sigma$  given in [23], thus not allowing any comparison. However, the same calculation has been done in [24] and the results agree with each other.

Set	A	B	C	D	E
$m$ [MeV]	6.13	6.40	6.77	6.70	6.54
$\Lambda$ [MeV]	800	800	800	820	852
$G_S \Lambda^2$	2.90	3.07	3.49	3.70	4.16
$M$ [MeV]	260.457	303.067	395.042	446.249	549.364
$m_\pi$ [MeV]	140.0	140.0	140.0	140.0	140.0
$m_\sigma$ [MeV]	530.2	613.4	794.7	896.3	1101.4

**Table 2.1.:** Parameters and results of the calculation for five different parameter sets. In the upper half of the table the five different parameter sets taken from [23] are presented. In the lower half the calculated masses are shown. The results agree with [23, 24]. The  $\sigma$ -masses are taken from [24].

<sup>5</sup> Details are on pages 42 and 43 of appendix B.

---

### 3 The NJL Model in Medium

---

In the last chapter we discussed the basics of the NJL model in vacuum, i.e. zero temperature  $T$  and chemical potential  $\mu$ . Since we want to study mesons in medium, we will focus on the NJL model within the framework of a thermal field theory [25] introducing non-zero temperature  $T$  and chemical potential  $\mu$ . This is commonly done by using the Matsubara technique, we replace the energy-integration of appearing integrals by a sum over so-called Matsubara frequencies. This substitution is written as

$$i \int \frac{d^4k}{(2\pi)^4} f(k) \rightarrow -T \sum_m \int \frac{d^3k}{(2\pi)^3} f(i\omega_m + \mu, \vec{k}). \quad (3.1)$$

Since we deal with quarks, which are fermions, and mesons, which are bosons, we will need both types of Matsubara frequencies. Fermionic Matsubara frequencies are given by  $\omega_m = (2m + 1)\pi T$ , bosonic ones by  $\omega_n = 2n\pi T$  with  $m, n \in \mathbb{Z}$ .

---

#### 3.1 Gap Equation

---

The formula for the constituent quark mass in medium can be calculated analogously to the vacuum case. The gap equation will keep the form we derived in our vacuum calculations, although the integral  $I_1(M)$  will now depend not only on  $M$ , but also on  $T$  and  $\mu$ :

$$M = m + 8N_f N_c G_S M I_1(T, \mu, M), \quad (3.2)$$

where the integral reads  $I_1(T, \mu, M)$

$$I_1(T, \mu, M) \equiv I_1^{med}(M) = -T \sum_m \int \frac{d^3k}{(2\pi)^3} \frac{1}{(i\omega_m + \mu)^2 - E_k^2} \quad (3.3)$$

with  $E_k = \sqrt{\vec{k}^2 + M^2}$ . All expressions in medium are functions of  $T$  and  $\mu$ . We will omit these as arguments of the occurring functions and integrals and rather use the superscript *med* to symbolize the dependency of  $T$  and  $\mu$ . Before we can calculate numerical values for the constituent quark mass, we have to simplify  $I_1^{med}(M)$  analytically<sup>1</sup>. The result reads

$$I_1^{med}(M) = I_1^{vac}(M) + \int \frac{d^3k}{(2\pi)^3} (n_{E_k} + \bar{n}_{E_k}), \quad (3.4)$$

where we defined the occupation number densities for quarks  $n_{E_k} \equiv n_F(E_k - \mu)$  and antiquarks  $\bar{n}_{E_k} \equiv n_F(E_k + \mu)$  with the Fermi-Dirac distribution

$$n_F(x) = \frac{1}{1 + e^{\frac{x}{T}}}. \quad (3.5)$$

Concerning regularization there are no changes here. The second term – which we refer to as the medium part – drops to 0 for high values of  $k = |\vec{k}|$ , thus we do not need to regularize it. The regularization of the vacuum part has been discussed in the last chapter.

---

<sup>1</sup> Which is done in appendix C on page 45.



## 3.2 Mesons

The description of mesons in medium is almost analogous to the case of mesons in vacuum. The main difference is that we have to evaluate the polarization loop with the Matsubara formalism and keep in mind to endow the four-momentum of the meson with a bosonic Matsubara frequency. Solving the Bethe-Salpeter equation, we get the meson propagator

$$it(i\omega_n, \vec{q}) = \frac{2iG_S}{1 - 2G_S J_M(i\omega_n, \vec{q})}, \quad (3.6)$$

where  $i\omega_n$  is a bosonic Matsubara frequency. The polarization loop reads

$$J_M(i\omega_n, \vec{q}) = -N_f N_c T \sum_m \int \frac{d^3k}{(2\pi)^3} \text{Tr}_{\text{Dirac}} [\Gamma_M S(i\omega_m + i\omega_n + \mu, \vec{k} + \vec{q}) \Gamma_M S(i\omega_m + \mu, \vec{k})]. \quad (3.7)$$

The meson-specific polarization loops are given by

$$J_\pi(i\omega_n, \vec{q}) = 4N_c N_f I_1^{\text{med}}(M) - 2N_c N_f ((i\omega_n)^2 - \vec{q}^2) I_2^{\text{med}}(i\omega_n, \vec{q}, M) \quad (3.8)$$

and

$$J_\sigma(i\omega_n, \vec{q}) = 4N_c N_f I_1^{\text{med}}(M) - 2N_c N_f ((i\omega_n)^2 - \vec{q}^2 - 4M^2) I_2^{\text{med}}(i\omega_n, \vec{q}, M). \quad (3.9)$$

We have shown the expression for  $I_1^{\text{med}}(M)$  in eq. (3.3). The other integral is

$$I_2^{\text{med}}(i\omega_n, \vec{q}, M) = -T \int \frac{d^3k}{(2\pi)^3} \sum_m \frac{1}{(i\omega_m + \mu) - \vec{k}^2 - M^2} \times \frac{1}{(i\omega_m + i\omega_n + \mu)^2 - (\vec{k} + \vec{q})^2 - M^2}. \quad (3.10)$$

This expression can be simplified<sup>2</sup>. Moreover we need to make the continuous extension  $i\omega_n \rightarrow q_0 + i\epsilon$  where  $\epsilon$  is infinitesimal positive, in order to be able to calculate numerical values for the meson masses. For  $\epsilon \rightarrow 0$  the integral  $I_2^{\text{med}}(q_0, \vec{q}, M)$  is given by

$$I_2^{\text{med}}(q_0, \vec{q}, M) = \int \frac{d^3k}{(2\pi)^2} \left[ \left( \frac{1}{E_k} - \frac{n_{E_k} + \bar{n}_{E_k}}{2E_k E_{k,q}} s_E \right) \frac{1}{q_0^2 - s_E^2} - \frac{n_{E_k} + \bar{n}_{E_k}}{2E_k E_{k,q}} d_E \frac{1}{q_0^2 - d_E^2} \right], \quad (3.11)$$

with  $E_k$  as defined in the previous section,  $E_{k,q} = \sqrt{(\vec{k} + \vec{q})^2 + M^2}$  and their sum  $s_E = E_{k,q} + E_k$  and difference  $d_E = E_{k,q} - E_k$ . In contrast to the vacuum case, where  $I_2^{\text{vac}}(q, M)$  depended on  $q^2$ , in the medium case it depends on  $q_0$  and  $\vec{q}$  separately. However, we want to study the case of resting mesons, i.e.  $\vec{q} = 0$ . If we do so,  $d_E = 0$  and  $I_2^{\text{med}}(q_0, \vec{q} = 0, M)$  becomes

$$I_2^{\text{med}}(q_0, \vec{q} = 0, M) \equiv I_2^{\text{med}}(q_0, M) = \int \frac{d^3k}{(2\pi)^3} \frac{1 - (n_{E_k} + \bar{n}_{E_k})}{E_k (q_0^2 - 4E_k^2) + i\epsilon}, \quad (3.12)$$

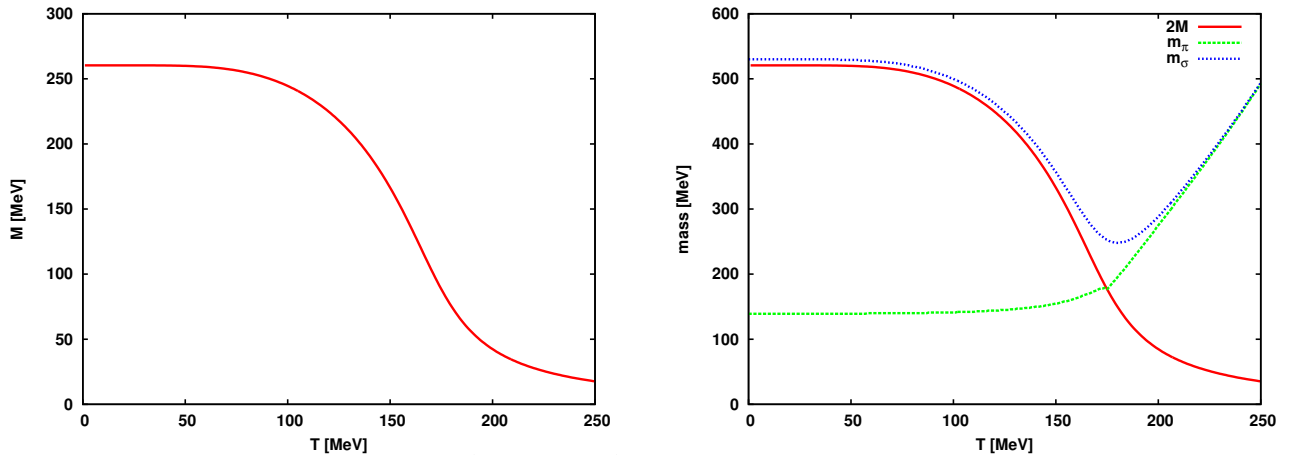
which will be regulated like  $I_1^{\text{med}}(M)$ . Equivalent to the vacuum case we have the following relation for calculating the meson masses in medium

$$1 - 2G_S J_M \left( q_0 = \sqrt{m_M^2 + \vec{q}^2}, \vec{q} \right) = 1 - 2G_S J_M(m_M) \stackrel{!}{=} 0. \quad (3.13)$$

<sup>2</sup> Shown in appendix C on page 46

### 3.3 Numerical Results

In the course of the calculation we used Parameter set [A]<sup>3</sup> and the same Pauli-Villars regularization as in the vacuum case. First let us discuss the results for the constituent quark mass  $M$  shown in Subfigure 3.1(a). For  $T = 0$  the mass corresponds to its vacuum value of about 260 MeV. As the temperature rises, the value of the current quark mass  $M$  falls off, eventually approaching 0 MeV for high enough temperatures. This corresponds to the transition from the phase with broken chiral symmetry into the phase with restored chiral symmetry shown in the QCD phase diagram in Figure 1.1 along the temperature axis. Since  $M$  is a continuous and differentiable function of  $T$ , this is called a crossover. The results for the masses of  $\pi$ - and  $\sigma$ -meson are shown in Subfigure 3.1(b). At low temperatures we can see that the  $\pi$ -mass corresponds very well to its vacuum value of 140 MeV, while the  $\sigma$ -mass is approximately twice as much as the constituent quark mass  $M$  and agrees with its vacuum value of about 530 MeV. As the crossover happens, the pion gains mass and becomes degenerate in mass with the  $\sigma$ -meson. These results agree with [24].



(a) Constituent quark mass  $M$  as a function of temperature  $T$  at chemical potential  $\mu = 0$ . As  $T$  increases, the constituent quark mass drops which corresponds to the crossover transition from the phase with broken chiral symmetry to the phase with restored chiral symmetry.

(b) Masses of the pion- and sigma-meson as a function of  $T$  at  $\mu = 0$ . For comparison, twice the constituent quark mass has been plotted as well.

**Figure 3.1.:** Numerical results for the quark mass (a) and meson masses (b).

<sup>3</sup> cf. Table 2.1

---

## 4 Inhomogeneous Phase

---

In the introduction we mentioned that the occurrence of so-called inhomogeneous phases in the QCD phase diagram is expected for low temperatures  $T$  and intermediate quark chemical potentials  $\mu$ . In the following we want to study mesons in such an inhomogeneous phase, which is characterized by a spatially dependent order parameter.

---

### 4.1 Dressed quark propagator

---

#### Coordinate space

---

Since we want to study mesons which are built from quarks via the Bethe-Salpeter equation, we will need the dressed quark propagator in inhomogeneous phases, which we want to derive in the following. Once again we start our calculation from the NJL Lagrangian in coordinate space

$$\mathcal{L}_{NJL} = \bar{\psi}(i\cancel{\partial} - \underline{m})\psi + G_S \left[ (\bar{\psi}\psi)^2 + (\bar{\psi}i\gamma^5\tau_a\psi)^2 \right], \quad (4.1)$$

where  $S_0^{-1} = (i\cancel{\partial} - \underline{m})$  is the inverse bare quark propagator. We apply a mean-field approximation to the chiral condensates allowing them now to be functions of the three-dimensional space

$$\bar{\psi}\psi = \phi_S(\vec{x}) + \delta\phi_S, \quad \bar{\psi}i\gamma^5\tau_a\psi = \phi_P^a(\vec{x}) + \delta\phi_P^a. \quad (4.2)$$

Plugging these expressions into the NJL Lagrangian and neglecting terms with  $\delta\phi_i^2$ , the NJL Lagrangian in mean-field approximation can be written as

$$\begin{aligned} \mathcal{L}_{MF} &= \bar{\psi} \left[ i\gamma^\mu \partial_\mu - m + 2G_S(\phi_S(\vec{x}) + i\gamma^5\tau_a\phi_P^a(\vec{x})) \right] \psi - G_S \left[ \phi_S^2(\vec{x}) + \phi_P^2(\vec{x}) \right] \\ &= \bar{\psi}S^{-1}\psi - \mathcal{V}, \end{aligned} \quad (4.3)$$

with the inverse dressed propagator  $S^{-1}$

$$S^{-1} = i\gamma^\mu \partial_\mu - m + 2G_S(\phi_S(\vec{x}) + i\gamma^5\tau_a\phi_P^a(\vec{x})). \quad (4.4)$$

The dressed propagator includes the interaction, which arises from the condensates. In a next step we introduce a Hamiltonian via splitting  $\gamma^\mu \partial_\mu = \gamma^0 \partial_0 + \gamma^i \partial_i$ , yielding

$$\mathcal{L}_{MF} = \bar{\psi}\gamma^0(i\partial_0 - \mathcal{H})\psi - \mathcal{V}, \quad (4.5)$$

with the hermitian effective mean-field Hamiltonian

$$\mathcal{H} = \gamma^0 \left[ -i\gamma^i \partial_i + m - 2G_S(\phi_S(\vec{x}) + i\gamma^5\tau_a\phi_P^a(\vec{x})) \right]. \quad (4.6)$$

At this point we want to make a restriction. We set a constant direction for the vector  $\phi_P^a(\vec{x})$ , i.e.  $\phi_P^1(\vec{x}) = \phi_P^2(\vec{x}) = 0$  and  $\phi_P^3(\vec{x}) \equiv \phi_P(\vec{x})$ . This restriction means that neither up quarks nor

down quarks are favored. The mean-field Hamiltonian can be reduced to a direct product of two Hamiltonians  $\mathcal{H}_\pm$  in flavor space

$$\mathcal{H} = \gamma^0 \left[ -i\gamma^i \partial_i + m - 2G_S(\phi_S(\vec{x}) + i\gamma^5 \tau_3 \phi_P(\vec{x})) \right] = \mathcal{H}_+ \otimes \mathcal{H}_-, \quad (4.7)$$

with

$$\mathcal{H}_\pm = \gamma^0 \left[ -i\gamma^i \partial_i + m - 2G_S(\phi_S(\vec{x}) \pm i\gamma^5 \phi_P(\vec{x})) \right]. \quad (4.8)$$

Making use of the chiral representation of the Dirac matrices we can write

$$\mathcal{H}_+ = \begin{pmatrix} i\sigma^i \partial_i & m - 2G_S(\phi_S(\vec{x}) + i\phi_P(\vec{x})) \\ m - 2G_S(\phi_S(\vec{x}) - i\phi_P(\vec{x})) & -i\sigma^i \partial_i \end{pmatrix}, \quad (4.9)$$

$$\mathcal{H}_- = \begin{pmatrix} i\sigma^i \partial_i & m - 2G_S(\phi_S(\vec{x}) - i\phi_P(\vec{x})) \\ m + 2G_S(\phi_S(\vec{x}) + i\phi_P(\vec{x})) & -i\sigma^i \partial_i \end{pmatrix}. \quad (4.10)$$

Now we define an inhomogeneous mass function  $M(\vec{x})$  and its complex conjugate  $M^*(\vec{x})$

$$M(\vec{x}) = M_+(\vec{x}) = m - 2G_S(\phi_S(\vec{x}) + i\phi_P(\vec{x})), \quad (4.11)$$

$$M^*(\vec{x}) = M_-(\vec{x}) = m - 2G_S(\phi_S(\vec{x}) - i\phi_P(\vec{x})). \quad (4.12)$$

Then we can write  $\mathcal{H}_\pm$  as follows

$$\mathcal{H}_+ = \begin{pmatrix} i\sigma^i \partial_i & M(\vec{x}) \\ M^*(\vec{x}) & -i\sigma^i \partial_i \end{pmatrix} \quad (4.13)$$

$$\mathcal{H}_- = \begin{pmatrix} i\sigma^i \partial_i & M^*(\vec{x}) \\ M(\vec{x}) & -i\sigma^i \partial_i \end{pmatrix}. \quad (4.14)$$

---

## Momentum space

---

The next step will be to transform the inverse propagator in coordinate space

$$S^{-1} = \begin{pmatrix} S^{-1(+)} & 0 \\ 0 & S^{-1(-)} \end{pmatrix} = \begin{pmatrix} -M^*(\vec{x}) & i(\partial_0 + \sigma^i \partial_i) & 0 & 0 \\ i(\partial_0 - \sigma^i \partial_i) & -M(\vec{x}) & 0 & 0 \\ 0 & 0 & -M(\vec{x}) & i(\partial_0 + \sigma^i \partial_i) \\ 0 & 0 & i(\partial_0 - \sigma^i \partial_i) & -M^*(\vec{x}) \end{pmatrix} \quad (4.15)$$

to momentum space via a Fourier transformation. To make the calculation feasible, the problem is discretized by imprisoning the described system into a volume  $V$ , which will be sent to infinity in the end, thus allowing for a continuous spectrum of momenta again. Imposing periodical boundary conditions on the spinors, they can be written in Fourier series as follows

$$\psi(x) = \frac{1}{\sqrt{V}} \sum_{p_n} \psi_{p_n} e^{-ip_n x} = \frac{1}{\sqrt{V}} \sum_{\omega_n} \sum_{\vec{p}_n} \psi_{p_n} e^{-i(\omega_n \tau - \vec{p}_n \cdot \vec{x})}, \quad (4.16)$$

$$\bar{\psi}(x) = \frac{1}{\sqrt{V}} \sum_{p_n} \bar{\psi}_{p_n} e^{+ip_n x} = \frac{1}{\sqrt{V}} \sum_{\omega_n} \sum_{\vec{p}_n} \bar{\psi}_{p_n} e^{+i(\omega_n \tau - \vec{p}_n \cdot \vec{x})}, \quad (4.17)$$

with  $p^0 = E_n = i\omega_n$  and  $x^0 = t = -i\tau$ . At this point one has to make an ansatz for the inhomogeneous mass function. Since it represents both condensates, it has to represent their mathematical structure, too. We assume here, that the condensates are modulated periodically

$$M(\vec{x}) = \sum_{\vec{q}_k} M_{\vec{q}_k} e^{+i\vec{q}_k \cdot \vec{x}}, \quad (4.18)$$

$$M^*(\vec{x}) = \sum_{\vec{q}_k} M_{\vec{q}_k}^* e^{-i\vec{q}_k \cdot \vec{x}}, \quad (4.19)$$

with discrete momenta  $\vec{q}_k$  which represent the periodicity of the condensates in form of a reciprocal lattice. Carrying out the transformation and including the chemical potential  $\mu$  in the course of the calculation, which has been done in [19], one arrives at the following expression for the inverse dressed quark propagator in momentum space

$$S_{\vec{p}_m, \vec{p}_n}^{-1(\pm)} = \gamma^0 (i\omega_m \delta_{\vec{p}_m, \vec{p}_n} - \mathcal{H}_{\vec{p}_m, \vec{p}_n}^{(\pm)} + \mu \delta_{\vec{p}_m, \vec{p}_n}) \delta_{\omega_m, \omega_n}, \quad (4.20)$$

with

$$\mathcal{H}_{\vec{p}_m, \vec{p}_n}^{(\pm)} = \begin{pmatrix} -\vec{\sigma} \cdot \vec{p}_m \delta_{\vec{p}_m, \vec{p}_n} & \sum_{\vec{q}_k} M_{\vec{q}_k} \delta_{\vec{p}_m, \vec{p}_n + \vec{q}_k} & 0 & 0 \\ \sum_{\vec{q}_k} M_{\vec{q}_k}^* \delta_{\vec{p}_m, \vec{p}_n - \vec{q}_k} & \vec{\sigma} \cdot \vec{p}_m \delta_{\vec{p}_m, \vec{p}_n} & 0 & 0 \\ 0 & 0 & -\vec{\sigma} \cdot \vec{p}_m \delta_{\vec{p}_m, \vec{p}_n} & \sum_{\vec{q}_k} M_{\vec{q}_k}^* \delta_{\vec{p}_m, \vec{p}_n - \vec{q}_k} \\ 0 & 0 & \sum_{\vec{q}_k} M_{\vec{q}_k} \delta_{\vec{p}_m, \vec{p}_n + \vec{q}_k} & \vec{\sigma} \cdot \vec{p}_m \delta_{\vec{p}_m, \vec{p}_n} \end{pmatrix}. \quad (4.21)$$

As we can see from the off-diagonal elements, only those momenta  $\vec{p}_m, \vec{p}_n$  are coupled with each other which differ by a momentum  $\vec{q}_k$ . None of the momenta  $\vec{p}_i$  in the first Brillouin zone of the reciprocal lattice are coupled with each other. As a consequence the full inverse propagator can be divided into block diagonal sub-propagators, one for each momentum of the first Brillouin zone.

---

### Chiral density wave

---

For now we stay restricted to a one-dimensional modulation of the condensates, namely the chiral density wave, resulting in  $M(\vec{x}) = M e^{i\vec{q} \cdot \vec{x}}$  ( $M \in \mathbb{R}$ ). Then  $S^{-1(+)}$  and  $S^{-1(-)}$  are not quite identical and a sub-propagator will take the following form

$$\mathcal{S}_{\vec{p}}^{-1(+)} = \begin{pmatrix} \ddots & & & & \\ & 0 & \mathbb{1} & 0 & 0 \\ & \mathbb{1} & 0 & 0 & 0 \\ & 0 & 0 & 0 & \mathbb{1} \\ & 0 & 0 & \mathbb{1} & 0 \\ & & & & \ddots \end{pmatrix} \begin{pmatrix} \ddots & & & & \\ & i\omega_m + \vec{\sigma} \cdot \vec{p} + \mu & 0 & 0 & 0 \\ & 0 & i\omega_m - \vec{\sigma} \cdot \vec{p} + \mu & -M & 0 \\ & 0 & -M & i\omega_m + \vec{\sigma} \cdot (\vec{p} + \vec{q}) + \mu & 0 \\ & 0 & 0 & 0 & i\omega_m - \vec{\sigma} \cdot (\vec{p} + \vec{q}) + \mu \\ & & & & \ddots \end{pmatrix} \quad (4.22)$$

$$\mathcal{S}_{\vec{p}}^{-1(-)} = \begin{pmatrix} \ddots & & & & & & & & \\ & 0 & \mathbb{1} & 0 & 0 & & & & \\ & \mathbb{1} & 0 & 0 & 0 & & & & \\ & 0 & 0 & 0 & \mathbb{1} & & & & \\ & 0 & 0 & \mathbb{1} & 0 & & & & \\ & & & & & \ddots & & & \end{pmatrix} \begin{pmatrix} \ddots & & & & & & & & \\ & i\omega_m + \vec{\sigma} \cdot \vec{p} + \mu & 0 & 0 & -M & & & & \\ & 0 & i\omega_m - \vec{\sigma} \cdot \vec{p} + \mu & 0 & 0 & & & & \\ & 0 & 0 & i\omega_m + \vec{\sigma} \cdot (\vec{p} + \vec{q}) + \mu & 0 & & & & \\ -M & 0 & 0 & 0 & i\omega_m - \vec{\sigma} \cdot (\vec{p} + \vec{q}) + \mu & & & & \\ & & & & & \ddots & & & \end{pmatrix} \quad (4.23)$$

with

$$\vec{p} = \begin{pmatrix} p_x \\ p_y \\ p_z \end{pmatrix}, \quad \vec{q} = \begin{pmatrix} 0 \\ 0 \\ q \end{pmatrix}. \quad (4.24)$$

$\vec{p}$  denotes an arbitrary momentum of the Brillouin zone and we dropped the  $\delta_{\omega_m, \omega_n}$  for legibility. Our aim is to calculate the propagator, therefore we will have to invert these matrices. It suffices to look at one block<sup>1</sup> of a sub-propagator, i.e. the  $8 \times 8$  block from eq. (4.22), naming it  $S^{-1(+)}(\vec{p} + \vec{q}, \vec{p})$ , since the results can be easily generalized. At this point we changed the notation  $S_{\vec{p}, \vec{p} + \vec{q}}^{-1(+)}$  from [19] to  $S^{-1(+)}(\vec{p} + \vec{q}, \vec{p})$ , which is more convenient for this work. The latter notation denotes that  $S^{-1(+)}(\vec{p} + \vec{q}, \vec{p})$  is the propagator of a quark changing its momentum from  $\vec{p}$  to  $\vec{p} + \vec{q}$  by scattering off the inhomogeneous condensate. The (-)-case can be handled analogously and therefore we will only present its results. In order to invert  $S^{-1(+)}(\vec{p} + \vec{q}, \vec{p})$ , we first diagonalize  $\mathcal{H}^{(+)}(\vec{p} + \vec{q}, \vec{p}) = U \mathcal{H}_{diag} U^{-1}$ .  $\mathcal{H}_{diag}$  has eigenvalues [26]

$$\lambda_i = \pm \sqrt{\vec{p}^2 + M^2 + \frac{\vec{q}^2}{4} \pm \sqrt{\vec{q}^2 M^2 + (\vec{p} \cdot \vec{q})^2}}. \quad (4.25)$$

For the inverse propagator we then have

$$\begin{aligned} S^{-1(+)}(\vec{p} + \vec{q}, \vec{p}) &= \gamma^0 [i\omega_m - \mathcal{H}^{(+)}(\vec{p} + \vec{q}, \vec{p}) + \mu] \\ &= \gamma^0 [i\omega_m - U \mathcal{H}_{diag} U^{-1} + \mu] \end{aligned} \quad (4.26)$$

$$= \gamma^0 U [i\omega_m - \mathcal{H}_{diag} + \mu] U^{-1}, \quad (4.27)$$

where the expression in brackets is a diagonal matrix. Inverting this matrix yields the propagator

$$S^{(+)}(\vec{p} + \vec{q}, \vec{p}) = U \cdot \text{diag} \left( \left\{ \frac{1}{i\omega_m - \lambda_i + \mu} \right\} \right) \cdot U^{-1} \cdot \gamma^0. \quad (4.28)$$

Each eigenvalue appears twice in this  $8 \times 8$  block. Since the propagator is quite a lengthy expression<sup>2</sup>, we refrain from showing the full expression here, but rather present the structure of the propagator in Dirac-space

$$S^{(+)}(\vec{p} + \vec{q}, \vec{p}) = \begin{pmatrix} 0 & (1^{(+)}) & 0 & 0 \\ (2^{(+)}) & 0 & 0 & (3^{(+)}) \\ (4^{(+)}) & 0 & 0 & (5^{(+)}) \\ 0 & 0 & (6^{(+)}) & 0 \end{pmatrix}, \quad (4.29)$$

<sup>1</sup> For the sake of simplicity we call it one block, although it consists of 2 blocks in Dirac-Space and 1 full and 2 half blocks in momentum space. Since the Dirac-space is shifted in respect to the momentum space, we actually diagonalize and invert three blocks in momentum space and cutoff the  $2 \times 2$  edge in order to multiply the  $\gamma_0$  matrices correctly.

<sup>2</sup> See appendix D from page 49 onwards for more details. The general form of the infinite propagator  $S(\vec{p}', \vec{p})$  can be deduced from the expressions given there.

$$S^{(-)}(\vec{p} + \vec{q}, \vec{p}) = \begin{pmatrix} 0 & (2^{(-)}) & (3^{(-)}) & 0 \\ (1^{(-)}) & 0 & 0 & 0 \\ 0 & 0 & 0 & (6^{(-)}) \\ 0 & (4^{(-)}) & (5^{(-)}) & 0 \end{pmatrix}, \quad (4.30)$$

with  $(1^{(\pm)}) - (6^{(\pm)})$  being  $2 \times 2$  matrices<sup>3</sup>.

## 4.2 Gap Equation

Now that we have an expression for the dressed quark propagator, we want to have a look at the gap equation. The main difference to the homogenous case is, that the momentum of propagating quarks can be changed as they scatter with the inhomogeneous condensates. This is shown in the Feynman diagram of the gap equation

$$p_{out} \leftarrow p_{in} = p_{in} \leftarrow p_{in} + p_{out} \leftarrow p_{out} \leftarrow p_{inter} \leftarrow p_{in} \quad (4.31)$$

where we can see, that the dressed quark propagators now are labeled with two different momenta. Equivalently we have

$$iS^{(\pm)}(p_{out}, p_{in}) = iS_0^{(\pm)}(p_{in}, p_{in}) + iS_0^{(\pm)}(p_{out}, p_{out})(-i\Sigma^{(\pm)})iS^{(\pm)}(p_{inter}, p_{in}). \quad (4.32)$$

We will be omitting the vector signs of the momenta in the propagator from here on. The propagators  $S_0^{\pm}$  and their inverses have the same structure as  $S^{\pm}$  and their inverses. The difference is, that  $S_0^{\pm}$  contains the bare quark mass  $m$  instead of  $M$ . We will work in the chiral limit, therefore we set  $m = 0$  MeV.

### Self energy

Before studying the gap equation further and deriving an equation for the mass gap, we want to analyze the self-energy. It is given by

$$\begin{aligned} \Sigma^{(\pm)} = & 2G_S \left( \mathbb{1} \int \frac{d^4k}{(2\pi)^4} \text{Tr}[\mathbb{1}i(S^{(+)}(k', k) + S^{(-)}(k', k))] \right. \\ & \left. \pm i\gamma^5 \int \frac{d^4k}{(2\pi)^4} \text{Tr}[i\gamma^5 i(S^{(+)}(k', k) - S^{(-)}(k', k))] \right). \end{aligned} \quad (4.33)$$

The traces have to be taken over Dirac- and color space only. We separate the different interaction channels and account for the  $i^2$  in the second term, changing the sign of it

$$\begin{aligned} \Sigma^{(\pm)} = & 2G_S \left( \mathbb{1} \int \frac{d^4k}{(2\pi)^4} (\text{Tr}[\mathbb{1}S^{(+)}(k', k)] + \text{Tr}[\mathbb{1}S^{(-)}(k', k)]) \right) \\ & \mp 2G_S \left( \gamma^5 \int \frac{d^4k}{(2\pi)^4} (\text{Tr}[\gamma^5 S^{(+)}(k', k)] - \text{Tr}[\gamma^5 S^{(-)}(k', k)]) \right). \end{aligned} \quad (4.34)$$

<sup>3</sup> For details see appendix D from page 49 onwards.

The four traces of the propagator<sup>4</sup> are almost identical

$$\text{Tr}[\mathbb{1}S^{(+)}(k', k)] = \text{Tr}[\mathbb{1}S^{(-)}(k', k)] = -\text{Tr}[\gamma^5 S^{(+)}(k', k)] = \text{Tr}[\gamma^5 S^{(-)}(k', k)]. \quad (4.35)$$

For  $k' - k = nq = 2nQ$  the trace explicitly reads

$$\text{Tr}[\mathbb{1}S^{(+)}(k', k)] = -N_c \sum_n \frac{2M(M^2 + k_\perp^2 + k_z^2 - Q^2 - (i\omega_m + \mu)^2)}{(E_{n,+}^2 - (i\omega_m + \mu)^2)(E_{n,-}^2 - (i\omega_m + \mu)^2)}. \quad (4.36)$$

With a partial fraction decomposition this can be transformed into

$$\text{Tr}[\mathbb{1}S^{(+)}(k', k)] = N_c \sum_n \frac{M}{E_{k,n}} \left[ \frac{\lambda_{+,k,n}}{(i\omega_m + \mu)^2 - E_{+,k,n}^2} + \frac{\lambda_{-,k,n}}{(i\omega_m + \mu)^2 - E_{-,k,n}^2} \right]. \quad (4.37)$$

For legibility we defined

$$\begin{aligned} E_{k,n} &= \sqrt{(k_z + 2nQ)^2 + M^2}, \quad k_\perp^2 = k_x^2 + k_y^2, \\ \lambda_{+,k,n} &= E_{k,n} + Q, \quad \lambda_{-,k,n} = E_{k,n} - Q, \\ E_{+,k,n} &= \sqrt{\lambda_{+,k,n}^2 + k_\perp^2} \quad \text{and} \quad E_{-,k,n} = \sqrt{\lambda_{-,k,n}^2 + k_\perp^2}. \end{aligned} \quad (4.38)$$

The self-energy can thus be written as

$$\begin{aligned} \Sigma^{(\pm)} &= 4N_c G_S M (\mathbb{1} \pm \gamma^5) i \int \frac{d^4k}{(2\pi)^4} \sum_n \frac{1}{E_{k,n}} \left[ \frac{\lambda_{+,k,n}}{(i\omega_m + \mu)^2 - E_{+,k,n}^2} \right. \\ &\quad \left. + \frac{\lambda_{-,k,n}}{(i\omega_m + \mu)^2 - E_{-,k,n}^2} \right]. \end{aligned} \quad (4.39)$$

The momentum integration is limited to the Brillouin zone of the reciprocal lattice. The region outside of the Brillouin zone is included by summation over  $n$ . We can drop the sum over  $n$  by expanding the momentum integration to the whole momentum space, i.e.

$$\Sigma^{(\pm)} = 4N_c G_S M (\mathbb{1} \pm \gamma^5) i \int \frac{d^4k}{(2\pi)^4} \frac{1}{E_{k,0}} \left[ \frac{\lambda_{+,k,0}}{(i\omega_m + \mu)^2 - E_{+,k,0}^2} + \frac{\lambda_{-,k,0}}{(i\omega_m + \mu)^2 - E_{-,k,0}^2} \right]. \quad (4.40)$$

Following the previous chapters, we call the occurring integral  $I_1^{inhom}(Q, M)$

$$I_1^{inhom}(Q, M) = 2i \int \frac{d^4k}{(2\pi)^4} \frac{1}{E_{k,0}} \left[ \frac{\lambda_{+,k,0}}{(i\omega_m + \mu)^2 - E_{+,k,0}^2} + \frac{\lambda_{-,k,0}}{(i\omega_m + \mu)^2 - E_{-,k,0}^2} \right]. \quad (4.41)$$

The  $k_0$ -integration of the integral  $I_1^{inhom}(Q, M)$  can be evaluated with the Matsubara formalism analogously to the homogeneous case<sup>5</sup>. The result reads

$$\begin{aligned} I_1^{inhom}(Q, M) &= \int \frac{d^3k}{(2\pi)^3} \frac{1}{E_{k,0}} \left[ \frac{\lambda_{+,k,0}}{E_{+,k,0}} (1 - n_{E_{+,k,0}} - \bar{n}_{E_{+,k,0}}) \right. \\ &\quad \left. + \frac{\lambda_{-,k,0}}{E_{-,k,0}} (1 - n_{E_{-,k,0}} - \bar{n}_{E_{-,k,0}}) \right]. \end{aligned} \quad (4.42)$$

The self energy takes the form

$$\Sigma^{(\pm)} = 2G_S N_c M (\mathbb{1} \pm \gamma^5) I_1^{inhom}(Q, M). \quad (4.43)$$

<sup>4</sup> Which can be looked up in appendix D from page 49 onwards.

<sup>5</sup> Calculated in appendix C on page 45.



---

## Mass gap

---

To derive an equation for the mass gap in the chiral limit, we take a look at the general gap equation

$$iS = iS_0 + iS_0(-i\Sigma)iS, \quad (4.44)$$

or equivalently

$$S^{-1} = S_0^{-1} - \Sigma. \quad (4.45)$$

We have omitted the  $(\pm)$ -notation here, since the mass gap is identical for both cases. Writing these expressions as matrices one can extract the formula for the mass gap

$$M = 2\sigma \quad (4.46)$$

with  $\sigma = 2N_c G_s M I_1^{inhom}(Q, M)$ . Thus the formula for the mass gap<sup>6</sup> is

$$M = 4N_c G_s M \int \frac{d^3k}{(2\pi)^3} \frac{1}{E_{k,0}} \left[ \frac{\lambda_{+,k,0}}{E_{+,k,0}} (1 - n_{E_{+,k,0}} - \bar{n}_{E_{+,k,0}}) + \frac{\lambda_{-,k,0}}{E_{-,k,0}} (1 - n_{E_{-,k,0}} - \bar{n}_{E_{-,k,0}}) \right], \quad (4.47)$$

which is divergent. To account for the divergencies, we will use the Pauli-Villars regularization scheme to treat  $\frac{\lambda_{+,k,0}}{E_{+,k,0}}$  and  $\frac{\lambda_{-,k,0}}{E_{-,k,0}}$ .

---

## 4.3 Mesons

---

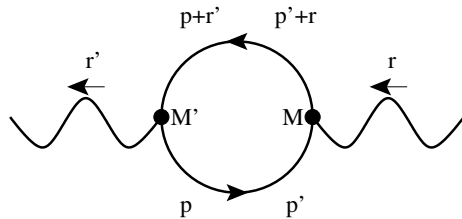
From the previous chapters we learned that the polarization loop plays an important role when it comes to calculating meson masses since it represented an essential part of the meson propagator. In the following we want to analyze the nature of the polarization loop in the inhomogeneous phase.

---

### General polarization loop

---

We want to start from a more general polarization loop and build in the constraints step by step. The Feynman diagram for a general polarization loop is



$$(4.48)$$

---

<sup>6</sup> We have shown an alternative derivation of the formula for the mass gap in appendix D on page 48.

We have an incoming meson of type  $M$  with momentum  $r$  and an outgoing meson of a possibly different type  $M'$  with momentum  $r'$ . The polarization loop consists of two inhomogeneous dressed quark propagators, which have to be  $\tilde{S}(p', p)$  and  $\tilde{S}(p + r', p' + r)$ , since we have momentum conservation at the vertices  $\Gamma_M$  and  $\Gamma_{M'}$ . Here we used the tilde to express that these propagators are general. Translating the Feynman diagram yields

$$\tilde{J}_{M',M}(r', r) = i \int \frac{d^4 p}{(2\pi)^4} \int \frac{d^4 p'}{(2\pi)^4} \text{Tr} \left[ \Gamma_{M'} \tilde{S}(p + r', p' + r) \Gamma_M \tilde{S}(p', p) \right]. \quad (4.49)$$

---

### Chiral density wave

---

Since we are working with the chiral density wave, we know that the inhomogeneous quark propagator is only non-zero if the involved momenta differ by any integer multiples of  $q = 2Q$ . We build in this constraint by using four dimensional delta-distributions and our inhomogeneous quark propagators for the chiral density wave

$$\begin{aligned} \tilde{S}(p', p) &= \sum_m S(p', p) (2\pi)^4 \delta^{(4)}(p' - (p + 2mQ)), \\ \tilde{S}(p + r', p' + r) &= \sum_n S(p + r', p' + r) (2\pi)^4 \delta^{(4)}(p + r' - (p' + r + 2nQ)) \end{aligned} \quad (4.50)$$

with  $m, n \in \mathbb{Z}$ . We plug these expressions into eq. (4.49) and get

$$\begin{aligned} \tilde{J}_{M',M}(r', r) &= i \int \frac{d^4 p}{(2\pi)^4} \int \frac{d^4 p'}{(2\pi)^4} \sum_m \sum_n \text{Tr} \left[ \Gamma_{M'} S(p + r', p' + r) \Gamma_M S(p', p) \right] \\ &\quad \times (2\pi)^4 \delta^{(4)}(p' - (p + 2mQ)) (2\pi)^4 \delta^{(4)}(p + r' - (p' + r + 2nQ)). \end{aligned} \quad (4.51)$$

We evaluate the  $p'$ -integral using the first delta-distribution  $\delta^{(4)}(p' - (p + 2mQ))$

$$\begin{aligned} \tilde{J}_{M',M}(r', r) &= i \int \frac{d^4 p}{(2\pi)^4} \sum_m \sum_n \text{Tr} \left[ \Gamma_{M'} S(p + r', p + r + 2mQ) \Gamma_M S(p + 2mQ, p) \right] \\ &\quad \times (2\pi)^4 \delta^{(4)}(p + r' - (p + r + 2mQ + 2nQ)). \end{aligned} \quad (4.52)$$

We summarize the remaining delta-distribution to  $(2\pi)^4 \delta^{(4)}(r' - (r + 2lQ))$  by introducing  $l = m + n$ . In the following we keep  $\sum_m$  and convert  $\sum_n$  into  $\sum_l$  and interpret the summation over  $l$  together with the summarized delta-distribution as

$$\tilde{J}_{M',M}(r', r) = \sum_l J_{M',M}(r', r) (2\pi)^4 \delta^{(4)}(r' - (r + 2lQ)) \quad (4.53)$$

with

$$J_{M',M}(r', r) = i \int \frac{d^4 p}{(2\pi)^4} \sum_m \text{Tr} \left[ \Gamma_{M'} S(p + r', p + r + 2mQ) \Gamma_M S(p + 2mQ, p) \right]. \quad (4.54)$$

We see that only those polarization loops are non-zero, for which the constraint  $r' - r = 2lQ$  holds. We can write down a more specified version of the polarization loop

$$(4.55)$$

with incoming meson of type  $M$  with momentum  $r$ , outgoing meson of type  $M'$  with momentum  $r + 2lQ$  and the two quark propagators  $S(p + 2mQ, p)$  and  $S(p + r + 2lQ, p + r + 2mQ)$ . Mathematically the equation reads

$$J_{M',M}(r + 2lQ, r) = i \int \frac{d^4 p}{(2\pi)^4} \sum_m \text{Tr} [\Gamma_{M'} S(p + r + 2lQ, p + r + 2mQ) \Gamma_M S(p + 2mQ, p)]. \quad (4.56)$$

---

### Employing Matsubara formalism

---

For further investigation we have to make use of the Matsubara formalism. The occurring vectors will be changed according to

$$p \rightarrow (i\omega_j + \mu, \vec{p}), \quad r \rightarrow (i\omega_k, \vec{r}), \quad Q \rightarrow (0, \vec{Q}), \quad (4.57)$$

where  $\omega_k$  is a bosonic Matsubara frequency belonging to the meson, while  $\omega_j$  is a fermionic one. We introduce these Matsubara frequencies as additional arguments of the propagators. The polarization loop then reads

$$J_{M',M}(i\omega_k; \vec{r} + 2l\vec{Q}, \vec{r}) = -T \sum_j \int \frac{d^3 p}{(2\pi)^3} \sum_m \text{Tr}[\dots], \quad (4.58)$$

with  $\text{Tr}[\dots]$  being

$$\text{Tr} [\Gamma_{M'} S(i\omega_k + i\omega_j + \mu; \vec{p} + \vec{r} + 2l\vec{Q}, \vec{p} + \vec{r} + 2m\vec{Q}) \Gamma_M S(i\omega_j + \mu; \vec{p} + 2m\vec{Q}, \vec{p})]. \quad (4.59)$$

We make use of the residue theorem to convert the sum over Matsubara frequencies  $i\omega_j$  into an integral over  $n_F(z) \cdot \text{Tr}[\dots]$  with residue  $-T$

$$J_{M',M}(i\omega_k; \vec{r} + 2l\vec{Q}, \vec{r}) = \int \frac{d^3 p}{(2\pi)^3} \frac{1}{2\pi i} \oint_{C_1} dz n_F(z) \sum_m \text{Tr}[\dots], \quad (4.60)$$

where  $\text{Tr}[\dots]$  is

$$\text{Tr} [\Gamma_{M'} S(i\omega_k + z + \mu; \vec{p} + \vec{r} + 2l\vec{Q}, \vec{p} + \vec{r} + 2m\vec{Q}) \Gamma_M S(z + \mu; \vec{p} + 2m\vec{Q}, \vec{p})] \quad (4.61)$$

and  $n_F(z)$  is the Fermi-Dirac distribution. The contour  $C_1$  runs around the fermionic Matsubara frequencies  $i\omega_j$ . The next step will be to change the contour such that it runs around the poles of the integrand. Therefore we need to evaluate the trace in detail.

---

## Analyzing the trace

---

It turns out that the trace is identical if the meson type does not change, i.e.

$$\Gamma_M = \Gamma_{M'} \in \{\mathbb{1}, i\gamma^5\}. \quad (4.62)$$

Therefore we will drop the vertices  $\Gamma_{M'}$  and  $\Gamma_M$  as well as the corresponding indices  $M', M$ . However, the traces for the different isospin flavors are not quite identical. Using the expressions for the propagators<sup>7</sup>, adjusting the respective momenta and summarizing the terms, the traces read

$$\begin{aligned} & \text{Tr} \left[ S^+(i\omega_k + z + \mu; \vec{p} + \vec{r} + 2l\vec{Q}, \vec{p} + \vec{r} + 2m\vec{Q}) S^+(z + \mu; \vec{p} + 2m\vec{Q}, \vec{p}) \right] = \\ & \frac{f_1^+(z + \mu) \cdot g_1^+(z + \mu + i\omega_k) + f_3^+(z + \mu) \cdot g_3^+(z + \mu + i\omega_k) + h_1^+(z + \mu + i\omega_k)}{(E_{+,p,m-1}^2 - p_0^2)(E_{-,p,m-1}^2 - p_0^2)(E_{+,p+r,l}^2 - (p_0 + i\omega_k)^2)(E_{-,p+r,l}^2 - (p_0 + i\omega_k)^2)} \\ & + \frac{f_2^+(z + \mu) \cdot g_2^+(z + \mu + i\omega_k) + f_4^+(z + \mu) \cdot g_4^+(z + \mu + i\omega_k) + h_2^+(z + \mu + i\omega_k)}{(E_{+,p,m+1}^2 - p_0^2)(E_{-,p,m+1}^2 - p_0^2)(E_{+,p+r,l}^2 - (p_0 + i\omega_k)^2)(E_{-,p+r,l}^2 - (p_0 + i\omega_k)^2)} \end{aligned} \quad (4.63)$$

for the up quark and

$$\begin{aligned} & \text{Tr} \left[ S^-(i\omega_k + z + \mu; \vec{p} + \vec{r} + 2l\vec{Q}, \vec{p} + \vec{r} + 2m\vec{Q}) S^-(z + \mu; \vec{p} + 2m\vec{Q}, \vec{p}) \right] = \\ & \frac{f_1^-(z + \mu) \cdot g_1^-(z + \mu + i\omega_k) + f_3^-(z + \mu) \cdot g_3^-(z + \mu + i\omega_k) + h_1^-(z + \mu + i\omega_k)}{(E_{+,p,m}^2 - p_0^2)(E_{-,p,m}^2 - p_0^2)(E_{+,p+r,l-1}^2 - (p_0 + i\omega_k)^2)(E_{-,p+r,l-1}^2 - (p_0 + i\omega_k)^2)} \\ & + \frac{f_2^-(z + \mu) \cdot g_2^-(z + \mu + i\omega_k) + f_4^-(z + \mu) \cdot g_4^-(z + \mu + i\omega_k) + h_2^-(z + \mu + i\omega_k)}{(E_{+,p,m}^2 - p_0^2)(E_{-,p,m}^2 - p_0^2)(E_{+,p+r,l+1}^2 - (p_0 + i\omega_k)^2)(E_{-,p+r,l+1}^2 - (p_0 + i\omega_k)^2)} \end{aligned} \quad (4.64)$$

for the down quark. We defined several functions<sup>8</sup> to keep the numerator legible. The denominator has been summarized using the definitions given in eq. (4.38). Additionally we have defined  $p_0 = z + \mu$ . The indices  $l \pm 1$  and  $m \pm 1$  represent the fact that the inhomogeneous propagator couples neighbouring momenta with each other.

---

## Evaluating the polarization loop

---

We are now ready to evaluate the  $z$ -integration of eq. (4.60) with the residue theorem.<sup>9</sup> Corresponding to the results we found, we split the polarization loop into an unregularized and a medium part

$$J(r_0, \vec{r} + 2l\vec{Q}, \vec{r}) = \int \frac{d^3p}{(2\pi)^3} \frac{1}{8Q} \sum_m (J_m^{unreg}(r_0, \vec{r} + 2l\vec{Q}, \vec{r}) + J_m^{med}(r_0, \vec{r} + 2l\vec{Q}, \vec{r})), \quad (4.65)$$

<sup>7</sup> Given in appendix D from page 49 onwards.

<sup>8</sup> They have been noted down in detail in appendix D on pages 53 and 54.

<sup>9</sup> Details and results of the calculation are given in appendix D from page 52 onwards.

where we made the continuous extension  $i\omega_k \rightarrow r_0$ . In order to perform numerical calculations, we need to make a few adjustments to the polarization loop. For simplicity we want to study the case of resting mesons, i.e.  $\vec{r} = 0$ . Due to the energies occurring in the Fermi distribution functions, the medium part converges for high momenta. We avoided referring to the unregularized part as vacuum part, since it is still dependent on  $\mu$ . However, there are no Fermi distribution functions taking care of high momenta thus it needs to be regularized, which will be discussed shortly. The expression for the polarization loop we want to calculate numerically reads

$$J_l(r_0, M) = \int \frac{d^3p}{(2\pi)^3} \frac{1}{8Q} \sum_m (J_{l,m}^{reg}(r_0, M) + J_{l,m}^{med}(r_0, M)). \quad (4.66)$$

The  $M$  in the argument, which we have omitted so far to avoid confusion, denominates the constituent quark mass, not the meson type. We dropped the arguments  $\vec{r} + 2l\vec{Q}$  and  $\vec{r}$  and noted down  $m$  and  $l$  as indices instead.

---

#### 4.4 Numerical Results

---

Before presenting our results, we want to discuss the regularization of the integrals. Since we are dealing with the chiral density wave modulation, which distinguishes the  $z$ -direction of the momentum from the other two directions, we will use cylindrical coordinates for the integration in the mass gap formula (cf. eq. (4.47))

$$\int d^3k \rightarrow \int k_\perp dk_\perp d\phi dk_z \quad (4.67)$$

as well as for the polarization loop (cf. eq. (4.66))

$$\int d^3p \rightarrow \int p_\perp dp_\perp d\phi dp_z. \quad (4.68)$$

The polarization loop is divergent, since its integrand is proportional to  $p_\perp^2$ . The denominator and numerator both are of order  $M^6$  and  $p_z^6$ . However, the denominator is of order  $p_\perp^5$ , while the numerator is of order  $p_\perp^6$ . An additional factor of  $p_\perp$  originates from the cylindrical volume element. The integration over  $\phi$  is straight forward due to the rotational symmetry of the chiral density wave and yields a factor  $2\pi$ . All calculations are done for temperature  $T = 1$  MeV

---

#### Regularization

---

To acquire results comparable to [19], we use the same regularization to treat the formula for the mass gap and the polarization loop. The factors  $\frac{\lambda_{+,k,0}}{E_{+,k,0}}$  and  $\frac{\lambda_{-,k,0}}{E_{-,k,0}}$  in eq. (4.47) as well as  $J_{l,m}^{unreg}(r_0, M)$  are regularized using the replacement

$$f^{reg}(M) = \sum_{n=0}^3 c_n f^{unreg}(\sqrt{M^2 + n\Lambda^2}), \quad (4.69)$$

with  $c_0 = 1$ ,  $c_1 = -3$ ,  $c_2 = 3$  and  $c_3 = -1$ . The regulator is  $\Lambda = 757.048$  MeV and the coupling of the quarks is given by  $G_S \Lambda^2 = 6.002$ . These parameters are tuned to a pion-decay constant of  $f_\pi = 88$  MeV, the vacuum constituent quark mass of  $M = 300$  MeV and zero bare quark mass  $m$ . The coefficients  $c_n$  are chosen such that

$$\sum_n^3 c_n = 0 \quad (4.70)$$

to cancel out the divergencies.

---

### Quark masses

---

First we want to take a look at the constituent quark masses. They were calculated by iterating eq. (4.47) numerically, until the relative alteration of  $M$  deceeded a certain treshold. The results are listed in Table 4.1. We have calculated the constituent quark mass for different chemical potentials  $\mu$  and compared them to [19, 27].

$\mu$ [MeV]	$Q$ [MeV]	$M$ [MeV]	$M_{exp}$ [MeV]
300	0.001	299.884	299.982
305	0.020	298.295	298.395
310	0.001	293.652	293.652
315	192.762	100.365	101.319
320	207.552	85.709	85.606
325	220.096	71.735	71.666
330	231.249	58.612	58.428
335	241.205	45.184	44.856
340	250.652	30.289	29.413
345	262.768	0.224	0.215
350	247.879	0.427	0.411

**Table 4.1.:** Constituent quark masses for different chemical potentials  $\mu$ .  $Q$  has been aquired by minimizing the corresponding grandcanonical potential [28].  $M$  is the value calculated, the expected value  $M_{exp}$  is from [19, 27, 28].

The values correspond very well to results found in [19, 27]. As  $\mu$  increases, we observe a sudden increase in  $Q$  which corresponds to the phase transition from the homogeneous to the inhomogeneous phase. The decrease of constituent quark mass  $M$  shows the restauration of the chiral symmetry.

---

### Polarization loop

---

Next we analyzed the polarization loop

$$J_l(r_0, M) = \frac{1}{4\pi^2} \int dp_\perp dp_z \frac{p_\perp}{8Q} \sum_m (J_{l,m}^{reg}(r_0, M) + J_{l,m}^{med}(r_0, M)) \quad (4.71)$$

numerically for two different values of  $\mu$ . At the same time we restricted the indices  $l$  and  $m$  to two cases and set the meson energy to  $r_0 = 0$  MeV. As a reminder, index  $l$  represents the difference of incoming and outgoing meson momenta while index  $m$  represents the change in the momenta of the propagating quarks. The integration covers the whole momentum space in principle. Nevertheless we introduce bounds  $p_{z,max}$  and  $p_{\perp,max}$  for the integrations. By keeping one integration bound constant and varying the other one, we will be able to determine whether or not the polarization loop converges.

In Figure 4.1 we have shown the integrand of the polarization loop

$$\frac{p_{\perp}}{8Q}(J_{l,m}^{reg}(0, M) + J_{l,m}^{med}(0, M)) \quad (4.72)$$

for  $\mu = 305$  MeV as a function of the momenta  $p_z = p_{\perp}$ . According to Table 4.1 we have  $Q = 0.02$  MeV and  $M = 298.295$  MeV.

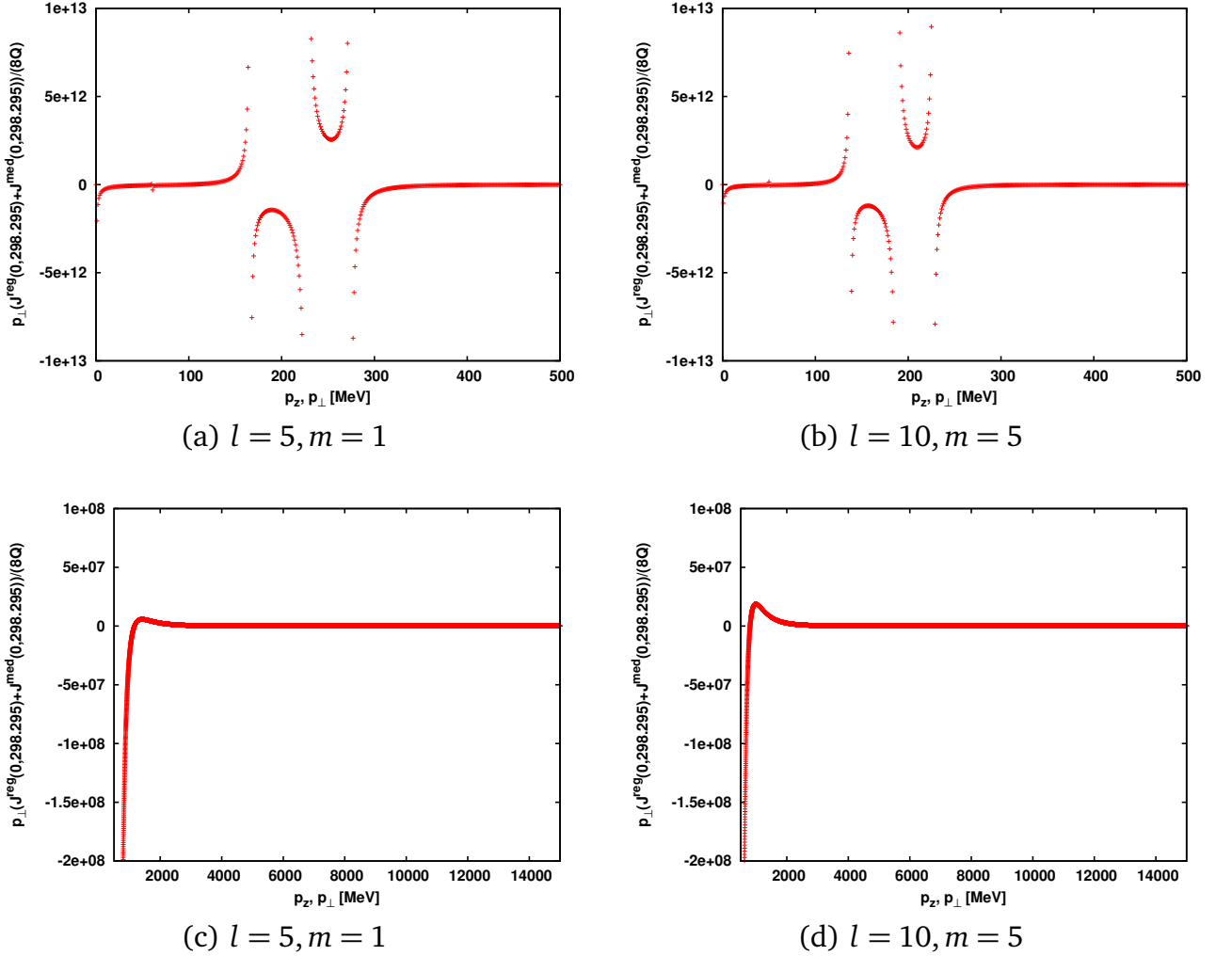


**Figure 4.1.:** Integrand of polarization loop as function of momenta  $p_z = p_{\perp}$  for  $\mu = 305$  MeV,  $Q = 0.02$  MeV and  $M = 298.295$  MeV. The integrand has three singularities in the region of low momenta while it approaches zero for high momenta.

Subfigures 4.1(a) and 4.1(c) show the integrand for  $l = 5$  and  $m = 1$ , while Subfigures 4.1(b) and 4.1(d) show the case  $l = 10$  and  $m = 5$ . In the region of low momenta we observe three singularities in both cases. As the momenta increase, the integrand falls off and converges to zero.

The integration for various combinations of  $p_{z,max}$  and  $p_{\perp,max}$  failed since the implemented procedure for the numerical integration did not converge. We assume this is due to the occurring singularities and could be solved by refining the numerical procedure.

In Figures 4.2 and 4.3 we have plotted the polarization loop for  $\mu = 325$  MeV. Accordingly we have  $Q = 220.099$  MeV and  $M = 71.735$  MeV. Figure 4.2 shows our results for three different but constant  $p_{\perp,max}$ .

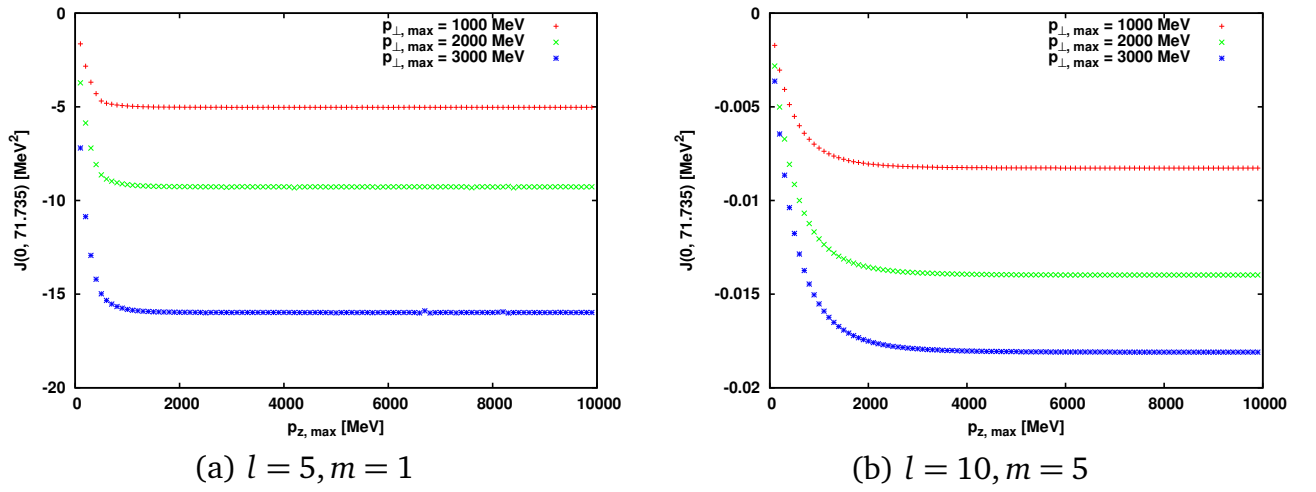


**Figure 4.2.:** Polarization loop for  $\mu = 325$  MeV,  $Q = 220.099$  MeV and  $M = 71.735$  MeV.  $p_{\perp,max}$  is kept constant while  $p_{z,max}$  is varied. The polarization loop converges in Subfigure (a) at about 1000 MeV and in Subfigure (b) at about 3000 MeV.

We observe that the polarization loop converges relatively quick to a certain value in both cases. The absolute value increases with  $p_{\perp,max}$  while it decreases with  $l$  and  $m$ . Recalling that we actually would have to sum over  $m$ , this behaviour indicates that summands with higher  $m$  contribute less than summands with low  $m$ , thus allowing to expect that the sum may converge.

In Subfigures 4.3(a) and (b) we have shown the polarization loop for three different values of  $p_{z,max}$ . While in the case of  $l = 5$ , and  $m = 1$  all three lines overlap, one line splits in the case of  $l = 10$  and  $m = 5$ . In Subfigures 4.3(c) and (d) we additionally plotted the integrand of the polarization loop. Contrary to the case of constant  $p_{\perp,max}$ , the polarization loop and its integrand both diverge, which was not expected.

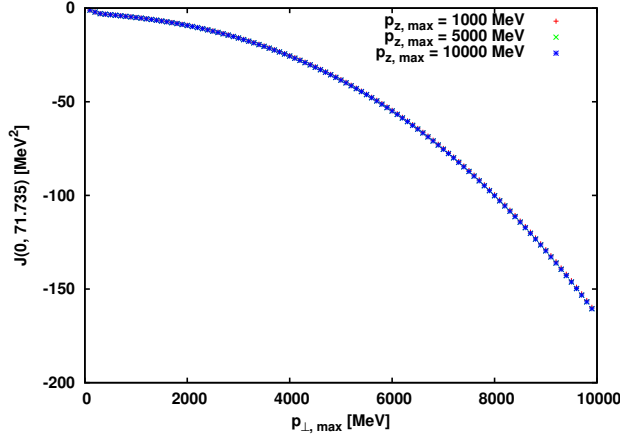
A careful look at the analytical expressions<sup>10</sup> revealed the reason for this behaviour. The integrand of the polarization loop has terms of the form

$$(E_{\pm,p,m\pm 1}^2 - E_{\pm,p,l}^2)(E_{\mp,p,m\pm 1}^2 - E_{\pm,p,l}^2) \quad (4.73)$$

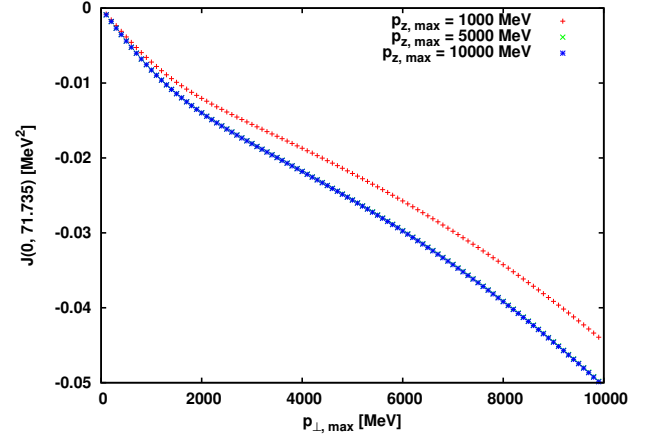
<sup>10</sup> Given in appendix D from page 53 onwards.



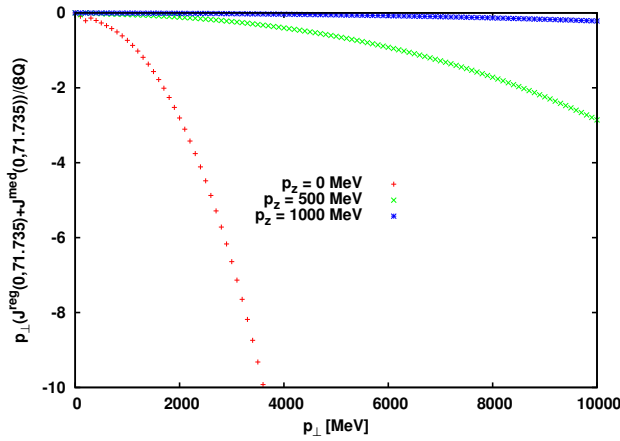
in every denominator. Since these energies contain  $p_{\perp}$  (cf. eq. (4.38)), a factor of  $p_{\perp}^4$  is cancelled out of every denominator, leaving the integrand proportional to  $p_{\perp}^6$  rather than  $p_{\perp}^2$ . This is a much stronger divergency than anticipated and needs to be taken care of.



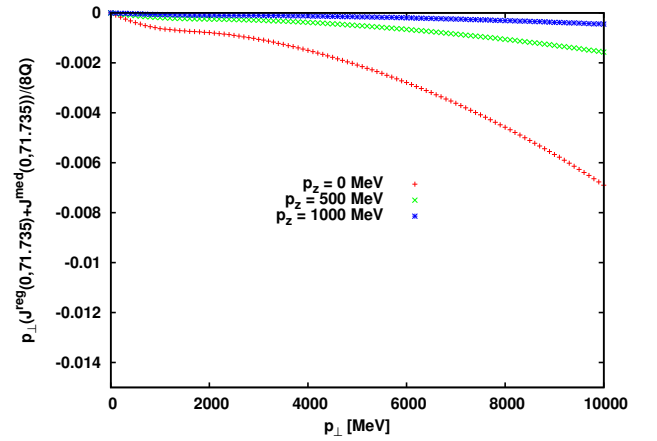
(a) Polarization loop for  $l = 5, m = 1$



(b) Polarization loop for  $l = 10, m = 5$



(c) Integrand for  $l = 5, m = 1$



(d) Integrand for  $l = 10, m = 5$

**Figure 4.3.:** Polarization loop and integrand for  $\mu = 325\text{MeV}$ ,  $Q = 220.099\text{ MeV}$  and  $M = 71.735\text{ MeV}$ .  $p_z$  and  $p_{z,max}$  are kept constant while  $p_{\perp}$  and  $p_{\perp,max}$  are varied. In Subfigure (a) all three lines overlap while one line splits in Subfigure (b). The integrand of the polarization loop diverges, accordingly the polarization loop diverges.

### Change in regularization

Following our findings so far, we adjust the regularization scheme by enhancing it with four additional regulatory terms. Our new scheme is

$$f^{reg}(M) = \sum_{n=0}^7 c_n f^{unreg}(\sqrt{M^2 + n\Lambda^2}), \quad (4.74)$$

with  $c_0 = 1$ ,  $c_1 = -7$ ,  $c_2 = 21$ ,  $c_3 = -35$ ,  $c_4 = 35$ ,  $c_5 = -21$ ,  $c_6 = 7$ ,  $c_7 = -1$ ,  $\Lambda = 956.373$  MeV and  $G_S \Lambda^2 = 11.6538$  [28]. These parameters have been fitted to the same conditions as the previous parameters.

---

### Polarization loop

---

We calculated the polarization loops for the same scenarios as before. In Figure 4.4 we have shown the integrand for  $\mu = 305$  MeV, accordingly  $Q = 0.652$  MeV and  $M = 297.867$  MeV [28].

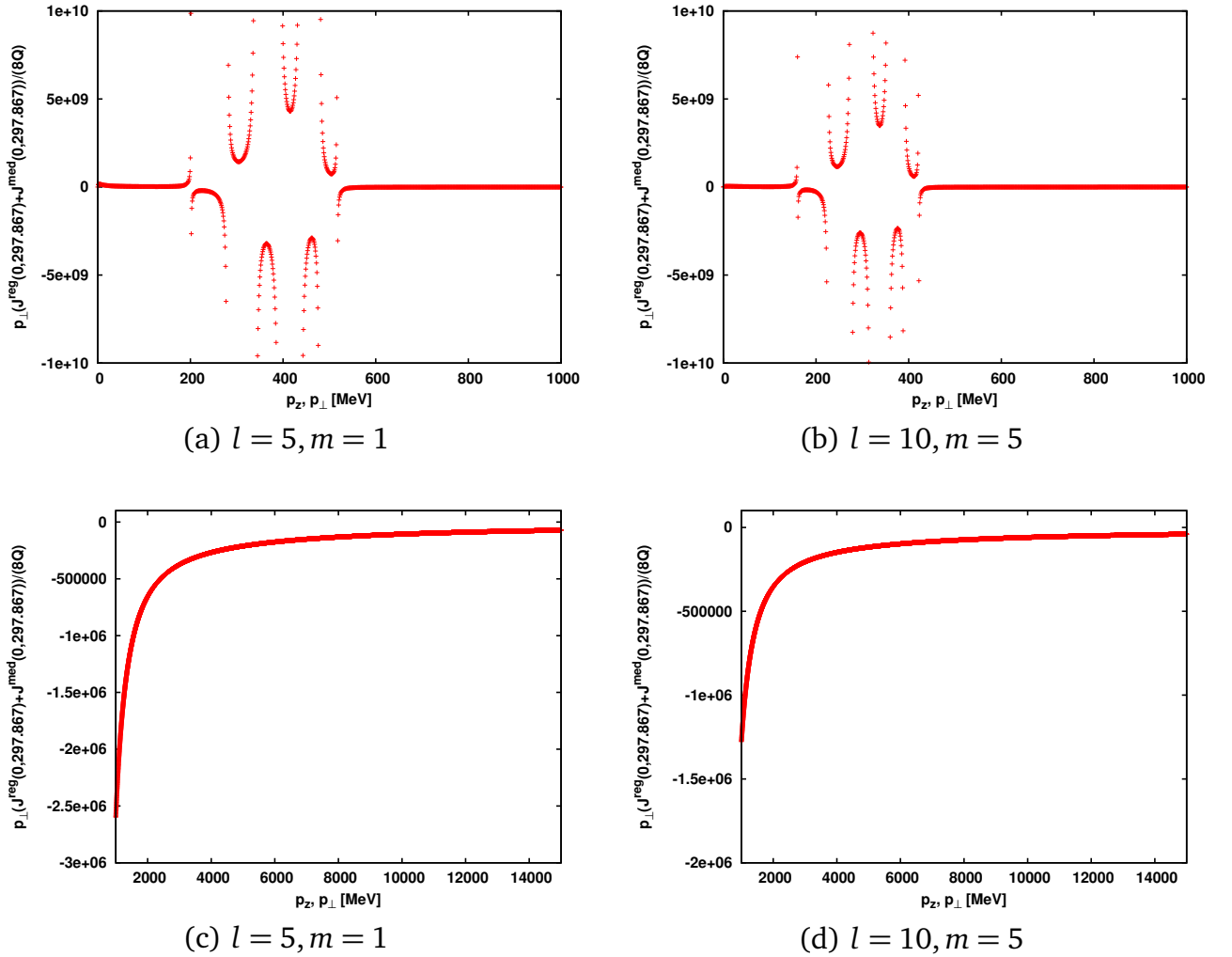


**Figure 4.4.:** Integrand of polarization loop as function of momenta  $p_z = p_\perp$  for  $\mu = 305$  MeV,  $Q = 0.652$  MeV and  $M = 297.867$  MeV. The integrand now has seven singularities at low momenta while still approaching zero for high momenta.

Qualitatively the behaviour of the integrand remained the same. For low momenta we now have seven singularities. Recalling the case of the previous regulation, where we had three singularities and three regulatory terms, this result is quite peculiar. It seems that every regulatory term

adds a singularity. We suppose that certain combinations of  $p_z$ ,  $M$ ,  $m$  and  $l$  generate a sign flip in the denominators of the integrand of the polarization loops which contain terms of the form

$$(E_{\pm,p,m\pm 1}^2 - E_{\pm,p,l}^2)(E_{\mp,p,m\pm 1}^2 - E_{\pm,p,l}^2). \quad (4.75)$$

These singularities should be determinable analytically and then should be considered when improving the numerical procedure.

In Figures 4.5 and 4.6 we have plotted the polarization loop for  $\mu = 325$  MeV,  $Q = 220.235$  MeV and  $M = 69.871$  MeV [28]. Figure 4.5 shows the results for three different but constant  $p_{\perp,max}$ . The polarization loop remains convergent, although the absolute values have increased and the convergence is reached at higher values of  $p_{z,max}$ . This is most likely due to the higher coefficients of the regulatory terms.

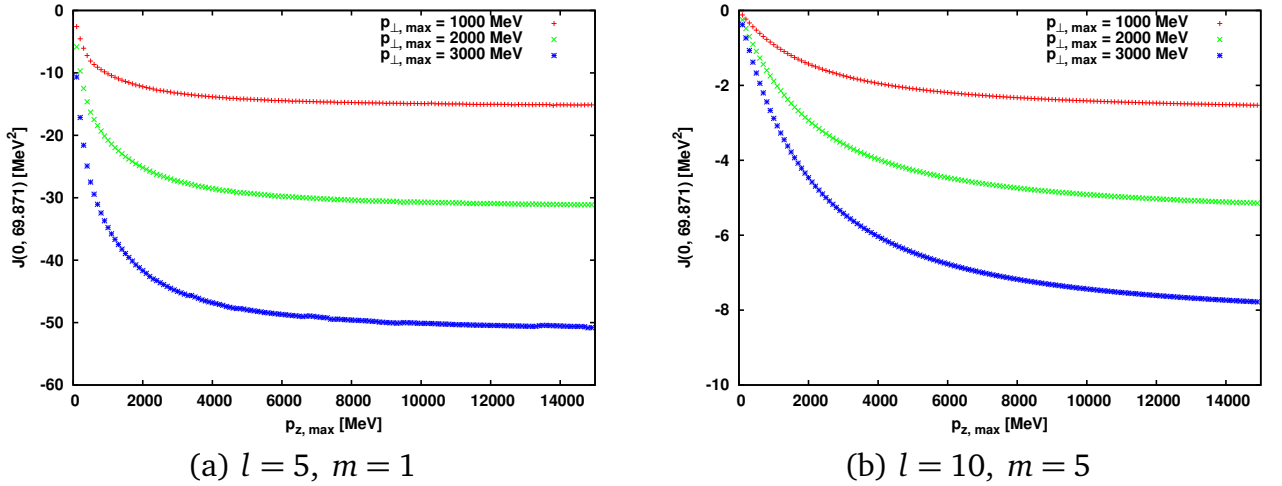
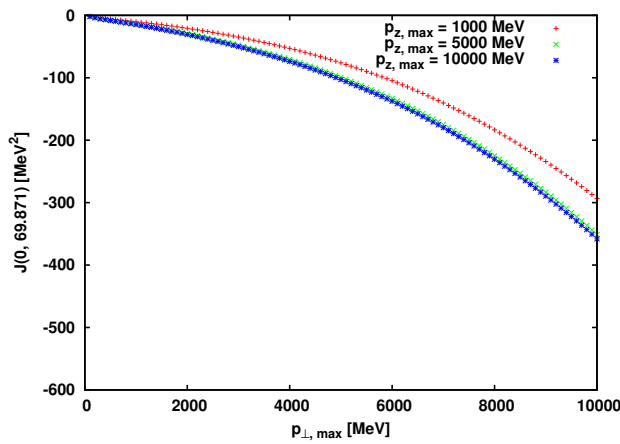
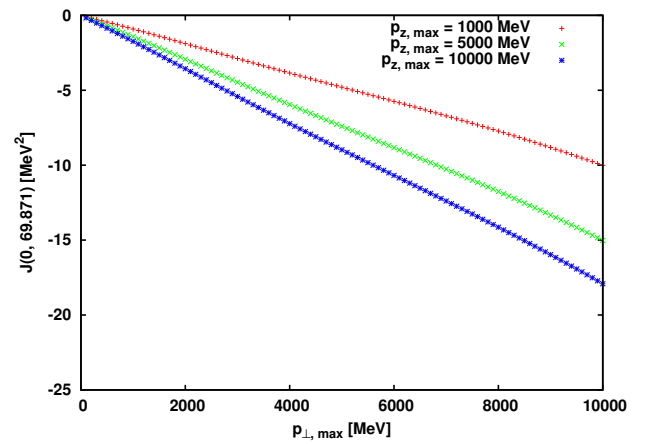


**Figure 4.5.:** Polarization loop for  $\mu = 325$  MeV,  $Q = 220.235$  MeV and  $M = 69.871$  MeV.  $p_{\perp,max}$  is kept constant while  $p_{z,max}$  is varied. The polarisation loop converges in both cases although the values for  $p_{z,max}$  at which convergence is reached have increased.

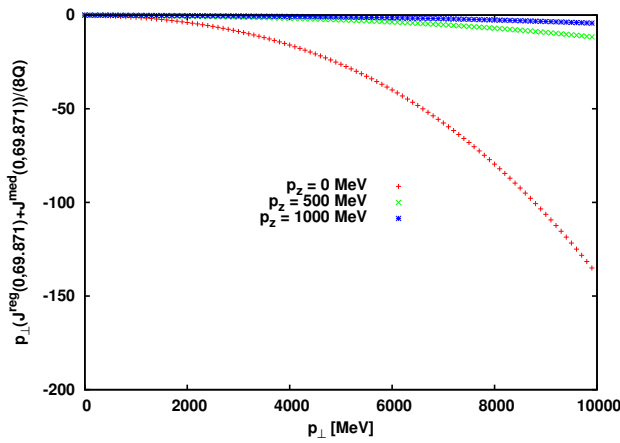
In Figure 4.6 we have shown the polarization loop for constant  $p_{z,max}$  and its integrand for constant  $p_z$ . The absolute values have also increased, while the divergent character remained.



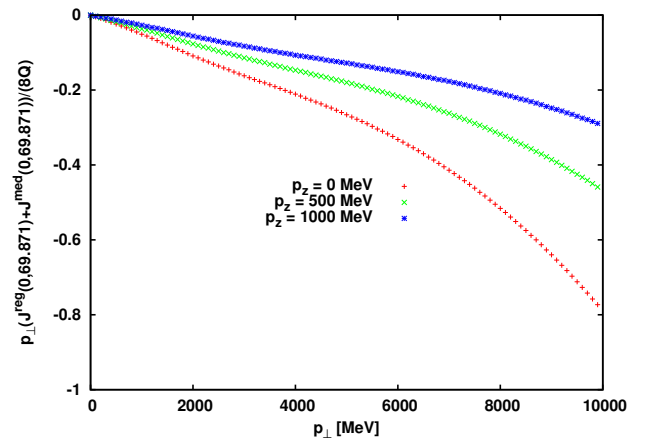
(a) Polarization loop for  $l = 5$ ,  $m = 1$



(b) Polarization loop for  $l = 10$ ,  $m = 5$



(c) Integrand for  $l = 5$ ,  $m = 1$



(d) Integrand for  $l = 10$ ,  $m = 5$

**Figure 4.6.:** Polarization loop and integrand for  $\mu = 325$  MeV,  $Q = 220.235$  MeV and  $M = 69.871$  MeV.  $p_z$  and  $p_{z,max}$  are kept constant while  $p_\perp$  and  $p_{\perp,max}$  are varied. The polarization loop and its integrand remain divergent.

---

## 5 Summary, Conclusion and Outlook

---

### Summary

---

In chapter 2 we introduced the NJL model in vacuum. We briefly discussed the NJL Lagrangian, its symmetries and the Feynman rules for this fermionic effective quantum field theory. We then had our first look at one of the main features of this theory, namely the dynamically generated constituent quark mass, which occurs due to the spontaneous chiral symmetry breaking. Since we encountered an integral with divergencies, we discussed how to regularize such integrals. Next we described mesons as states of quark-antiquark scattering via the Bethe-Salpeter equation. We concluded with the numerical calculation of quark and meson masses.

In chapter 3 we moved our discussion from the vacuum to the medium. We saw that in order to include a finite temperature  $T$  and chemical potential  $\mu$  we had to employ the Matsubara formalism. We repeated most calculations of the previous chapter in the new mathematical framework and presented again some results regarding quark and meson masses.

In chapter 4 we started to discuss inhomogeneous phases. This was done by promoting the condensates, which were constant up to that point, to be functions of the three-dimensional space. In the course of the calculation we made some assumptions and choices to simplify the problem. For the simplest case of inhomogeneous modulation, the chiral density wave, we explicitly derived the dressed quark propagator. We analyzed the gap equation and derived a formula for the mass gap. Numerical values for the constituent quark mass were calculated. We derived a numerically evaluable expression for the polarization loop of the Bethe-Salpeter equation and showed some numerical calculations.

---

### Conclusion

---

To verify the applicability of the inhomogeneous quark propagator derived in this work, we compared the results we gained using it with existing results [19, 27]. We have shown<sup>1</sup> that the formula for the mass gap derived from the grandcanonical potential [19] is the same formula as derived from the quark propagators (cf. eq. (4.47)). Furthermore, using the same regularization scheme as in [19, 24], we were able to calculate agreeing results for the constituent quark mass using the quark propagator instead of the grandcanonical potential. Values for the size of the Brillouin zone  $Q$  still had to be determined by minimizing the corresponding thermodynamical potential [28].

Regarding the investigation of mesons in inhomogeneous phases, we were able to derive quite lengthy, but numerically evaluable expressions for the polarization loop, which plays a crucial role in calculating meson masses. We analyzed the polarization loop numerically for two different, but simple scenarios. At low  $Q$  the numerical integration necessary to calculate the

---

<sup>1</sup> See appendix D on page 48

---

polarization loop failed. We suppose that this is due to the singularities which are caused by the regulatory terms and the low value of  $Q$ . These should be calculable analytically and considered in the procedure of numerical integration.

At a much higher  $Q$  the singularities were not present and we were able to perform the numerical integration. We then examined the polarization loop concerning its convergence. It converged respecting  $p_z$ , while it diverged respecting  $p_\perp$ . These characteristics did not change after an update to our regularization scheme. It is yet to be determined why these divergencies are occurring.

---

## Outlook

---

We think that the singularities and divergencies of the polarization loop are the most pressing problems requiring further numerical and analytical investigations of the polarization loop. During the discourse of mesons in an inhomogeneous phase we made several simplifications. For instance we only calculated the polarization loop for certain values of  $l$  and  $m$  while actually one has to calculate the sum over  $m$ . It has yet to be determined if the summation leads to more reliable results. A reconsideration of the regularization scheme is another possibility.

If these problems are solved, it would be interesting to look at the polarization loop in the inhomogeneous phase with  $l = 0$ ,  $m = 0$  and  $Q \rightarrow 0$  to learn whether or not one recovers the polarization loop for the homogeneous case. Further on, one could consider mixed interaction channels  $\Gamma_M \neq \Gamma_{M'}$  and non-zero momenta and energies of the incoming and outgoing mesons, since ultimately the motivation of this thesis was the study of meson masses in the chiral density wave modulated inhomogeneous phase, which remains to be done. Another step could be to investigate the inhomogeneous phase with non-zero bare quark masses.

---

# Appendices

---

## A Miscellaneous

---

### Conventions

---

We used natural units in this thesis

$$\hbar = c = k_B = 1. \quad (\text{A.1})$$

For the Dirac matrices we used the chiral or Weyl representation

$$\gamma^0 = \begin{pmatrix} 0 & \mathbb{1} \\ \mathbb{1} & 0 \end{pmatrix}, \quad \gamma^k = \begin{pmatrix} 0 & \sigma^k \\ -\sigma^k & 0 \end{pmatrix}, \quad \gamma^5 = \begin{pmatrix} -\mathbb{1} & 0 \\ 0 & \mathbb{1} \end{pmatrix}, \quad (\text{A.2})$$

$$\gamma^0 \gamma^k = \begin{pmatrix} -\sigma^k & 0 \\ 0 & \sigma^k \end{pmatrix}, \quad \gamma^0 \gamma^5 = \begin{pmatrix} 0 & \mathbb{1} \\ -\mathbb{1} & 0 \end{pmatrix}, \quad (\text{A.3})$$

with the Pauli matrices

$$\sigma^1 = \begin{pmatrix} 0 & 1 \\ 1 & 0 \end{pmatrix}, \quad \sigma^2 = \begin{pmatrix} 0 & -i \\ i & 0 \end{pmatrix}, \quad \sigma^3 = \begin{pmatrix} 1 & 0 \\ 0 & -1 \end{pmatrix}. \quad (\text{A.4})$$



---

## B Vacuum Calculations

---

### Self-Energy

---

Detailed evaluation of self-energy. The self-energy reads

$$\Sigma = 2G_S \left( \mathbb{1} \int \frac{d^4k}{(2\pi)^4} \text{Tr}[\mathbb{1}iS(k)] + i\gamma^5\tau_a \int \frac{d^4k}{(2\pi)^4} \text{Tr}[i\gamma^5\tau_a iS(k)] \right) \quad (\text{B.1})$$

In the first term we apply the definition of the propagator, while the second term is zero, since the trace over an odd number of Pauli matrices vanishes.

$$\Sigma = 2G_S \mathbb{1} \int \frac{d^4k}{(2\pi)^4} \text{Tr} \left[ \mathbb{1}i \frac{\not{k} + M}{k^2 - M^2 + i\epsilon} \right] \quad (\text{B.2})$$

Now we make use of  $\not{k} = \gamma^\mu k_\mu$  and the fact that traces over an odd number of  $\gamma$ -matrices vanish as well.

$$\Sigma = 2G_S \mathbb{1}i \int \frac{d^4k}{(2\pi)^4} \text{Tr}[\mathbb{1}] \frac{M}{k^2 - M^2 + i\epsilon} \quad (\text{B.3})$$

The trace is to be taken in color-, flavor- and Dirac-space yielding the factor  $4N_f N_c$ . In general  $\Sigma$  is a matrix. In this case, it is diagonal and all entries are the same. Therefore we drop the  $\mathbb{1}$  in front of the integral. The final expression reads

$$\Sigma = 8N_f N_c G_S M I_1^{\nu ac}(M), \quad (\text{B.4})$$

with the integral

$$I_1^{\nu ac}(M) = i \int \frac{d^4k}{(2\pi)^4} \frac{1}{k^2 - M^2 + i\epsilon}. \quad (\text{B.5})$$

This integral can be further evaluated analytically, which is done on page 42.

---

### Bethe-Salpeter equation

---

Here we present the derivation of eq. 2.24 from the Bethe-Salpeter equation, which reads

$$iT_M = iK_M + iK_M(-i\Pi_M)iT_M. \quad (\text{B.6})$$

First we replace the elements of the equation, which are matrices, by the expressions given in eq. 2.21, 2.22 and 2.23

$$\Gamma_M it(q)\Gamma_M = \Gamma_M 2iG_S \Gamma_M + \Gamma_M 2iG_S \Gamma_M(-i\Pi_M)\Gamma_M it(q)\Gamma_M. \quad (\text{B.7})$$

---

After accounting for two of the imaginary units in the second term we have

$$\Gamma_M it(q) \Gamma_M = \Gamma_M 2iG_S \Gamma_M + \Gamma_M 2G_S \Gamma_M \Pi_M \Gamma_M it(q) \Gamma_M \quad (\text{B.8})$$

where we can use  $J_M(q) = \Gamma_M \Pi_M \Gamma_M$  to get

$$\Gamma_M it(q) \Gamma_M = \Gamma_M 2iG_S \Gamma_M + \Gamma_M 2G_S J_M(q) it(q) \Gamma_M. \quad (\text{B.9})$$

This matrix equation has to hold, regardless of which interaction vertex we choose. Therefore we can neglect all  $\Gamma_M$  here

$$it(q) = 2iG_S + 2G_S J_M(q) it(q). \quad (\text{B.10})$$

With a few steps we can resolve this equation for  $it(q)$

$$it(q) - 2G_S J_M(q) it(q) = 2iG_S, \quad (\text{B.11})$$

$$(1 - 2G_S J_M(q)) it(q) = 2iG_S, \quad (\text{B.12})$$

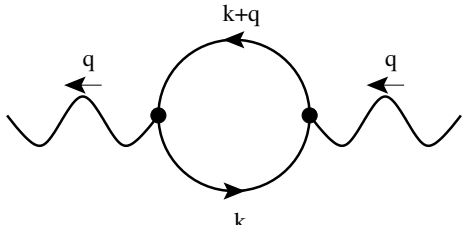
$$it(q) = \frac{2iG_S}{1 - 2G_S J_M(q)}. \quad (\text{B.13})$$

---

## Polarization Loop

---

The Feynman diagram of the  $\pi$ -polarization loop and its translation into a mathematical form is given by

$$\begin{aligned}
 -iJ_{\pi_a}(q^2) &= \text{Diagram} \\
 &= - \int \frac{d^4k}{(2\pi)^4} \text{Tr}[i\gamma^5 \tau_a iS(k+q) i\gamma^5 \tau_a iS(k)] \\
 &= -i^2 N_f N_c \int \frac{d^4k}{(2\pi^4)} \text{Tr}_{\text{Dirac}}[i\gamma^5 S(k+q) i\gamma^5 S(k)].
 \end{aligned} \quad (\text{B.14})$$


where  $N_f$  and  $N_c$  come from the trace in flavor and color space. We apply the definition of the propagators and get

$$J_{\pi_a}(q^2) = N_f N_c i \int \frac{d^4k}{(2\pi^4)} \text{Tr} \left[ \frac{i\gamma^5 (\not{k} + \not{q} + M) i\gamma^5 (\not{k} + M)}{((k+q)^2 - M^2 + i\epsilon)(k^2 - M^2 + i\epsilon)} \right]. \quad (\text{B.15})$$

Since the denominator is a scalar expression, we can factor it out

$$J_{\pi_a}(q^2) = N_f N_c i \int \frac{d^4 k}{(2\pi^4)} \frac{\text{Tr}[i\gamma^5(\not{k} + \not{q} + M)i\gamma^5(\not{k} + M)]}{((k+q)^2 - M^2 + i\epsilon)(k^2 - M^2 + i\epsilon)}. \quad (\text{B.16})$$

In the next step we commute the second  $\gamma^5$  with the first factor, generating minus signs for  $\not{k}$  and  $\not{q}$ . We absorb the  $-1$  from  $i^2$  into the first factor and use  $(\gamma^5)^2 = \mathbb{1}$ , which results in

$$J_{\pi_a}(q^2) = N_f N_c i \int \frac{d^4 k}{(2\pi^4)} \frac{\text{Tr}[(\not{k} + \not{q} - M)(\not{k} + M)]}{((k+q)^2 - M^2 + i\epsilon)(k^2 - M^2 + i\epsilon)}. \quad (\text{B.17})$$

Now we use the following rules for computing traces with gamma-matrices

$$\text{Tr}[\not{a}] = 0 \quad \text{and} \quad \text{Tr}[\not{a}\not{b}] = 4(a \cdot b), \quad (\text{B.18})$$

which leave us with

$$J_{\pi_a}(q^2) = 4N_f N_c i \int \frac{d^4 k}{(2\pi^4)} \frac{k^2 + qk - M^2}{((k+q)^2 - M^2 + i\epsilon)(k^2 - M^2 + i\epsilon)}. \quad (\text{B.19})$$

Now we expand the numerator of the integrand by adding  $+qk - qk + q^2 - q^2$

$$J_{\pi_a}(q^2) = 4N_f N_c i \int \frac{d^4 k}{(2\pi^4)} \frac{k^2 + qk - M^2 + qk - qk + q^2 - q^2}{((k+q)^2 - M^2 + i\epsilon)(k^2 - M^2 + i\epsilon)}. \quad (\text{B.20})$$

Rearranging and summarizing the nominator leaves us with

$$J_{\pi_a}(q^2) = 4N_f N_c i \int \frac{d^4 k}{(2\pi^4)} \frac{((k+q)^2 - M^2) - qk - q^2}{((k+q)^2 - M^2 + i\epsilon)(k^2 - M^2 + i\epsilon)} \quad (\text{B.21})$$

which can be further simplified to

$$J_{\pi_a}(q^2) = 4N_f N_c i \int \frac{d^4 k}{(2\pi^4)} \left( \frac{1}{k^2 - M^2 + i\epsilon} - \frac{qk + q^2}{((k+q)^2 - M^2 + i\epsilon)(k^2 - M^2 + i\epsilon)} \right). \quad (\text{B.22})$$

It can be shown that this expression is the same as

$$J_{\pi_a}(q^2) = 4N_f N_c i \int \frac{d^4 k}{(2\pi^4)} \left( \frac{1}{k^2 - M^2 + i\epsilon} - \frac{q^2}{2((k+q)^2 - M^2 + i\epsilon)(k^2 - M^2 + i\epsilon)} \right). \quad (\text{B.23})$$

We recognize the integral  $I_1^{\text{vac}}(M)$  and define the second term as the integral  $I_2^{\text{vac}}(q, M)$

$$J_{\pi_a}(q^2, M) = 4N_f N_c I_1^{\text{vac}}(M) - 2N_f N_c q^2 I_2^{\text{vac}}(q, M). \quad (\text{B.24})$$

In the same fashion one can derive the expression for the  $\sigma$ -polarization loop

$$J_{\sigma}(q^2, M) = 4N_f N_c I_1^{\text{vac}}(M) - 2N_f N_c (q^2 - 4M^2) I_2^{\text{vac}}(q, M). \quad (\text{B.25})$$

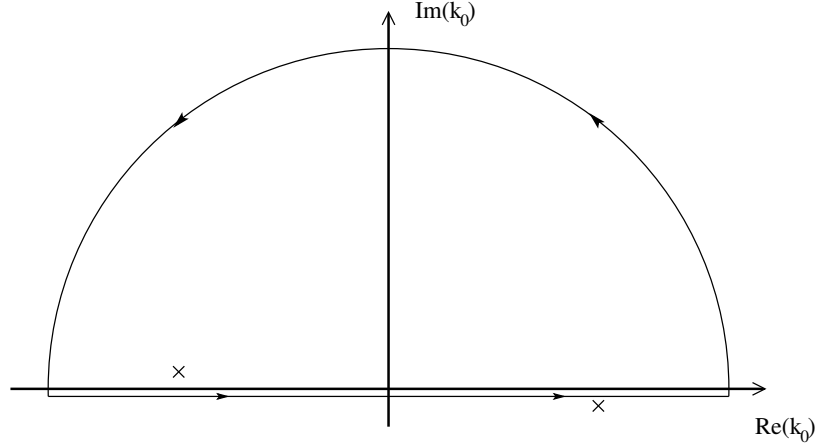


**Figure B.1.:** Integration path for applying the residue theorem for the integral  $I_1^{\text{vac}}(M)$ . Poles of the integrand are marked by small crosses.

---

### The Integral $I_1^{\text{vac}}(M)$

---

Here we present the analytical simplification of the integral  $I_1^{\text{vac}}(M)$

$$I_1^{\text{vac}}(M) = i \int \frac{d^4k}{(2\pi)^4} \frac{1}{k^2 - M^2 + i\epsilon}. \quad (\text{B.26})$$

First we separate the 0-component of the four-vector  $k$  and its integration

$$I_1^{\text{vac}}(M) = i \int \frac{d^3k}{(2\pi)^3} \int_{-\infty}^{+\infty} \frac{dk_0}{2\pi} \frac{1}{k_0^2 - \vec{k}^2 - M^2 + i\epsilon}. \quad (\text{B.27})$$

Now we use  $E_k = \sqrt{k^2 + M^2}$ .

$$I_1^{\text{vac}}(M) = i \int \frac{d^3k}{(2\pi)^3} \int_{-\infty}^{+\infty} \frac{dk_0}{2\pi} \frac{1}{k_0^2 - E_k^2 + i\epsilon} \quad (\text{B.28})$$

Before performing the integration, we factorize the denominator. This step can best be reconstructed, by calculating it backwards and neglecting the term with  $(i\epsilon)^2$ . However, we have the following expression with  $\epsilon' = \frac{\epsilon}{2E_k}$

$$I_1^{\text{vac}}(M) = i \int \frac{d^3k}{(2\pi)^3} \int_{-\infty}^{+\infty} \frac{dk_0}{2\pi} \frac{1}{(k_0 + E_k - i\epsilon')(k_0 - E_k + i\epsilon')}. \quad (\text{B.29})$$

The  $k_0$ -integral has two poles  $k_0 = \pm(-E_k + i\epsilon')$  and can be solved with the residue theorem. As depicted in Figure B.1 we choose to close the integration contour in the upper half plane. Then only the pole  $k_0 = -E_k + i\epsilon'$  contributes to the integral. After applying the residue theorem and sending  $\epsilon \rightarrow 0$  we are left with

$$I_1^{\text{vac}}(M) = \int \frac{d^3k}{(2\pi)^3} \frac{1}{2E_k}. \quad (\text{B.30})$$

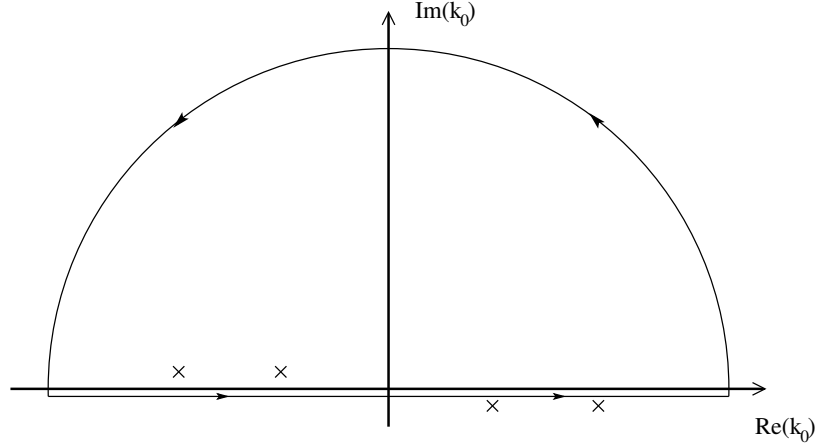


**Figure B.2.:** Integration path for applying the residue theorem for the integral  $I_2^{vac}(q)$ . Poles of the integrand are marked by small crosses.

We employ spherical coordinates onto the three-dimensional integral, since it only depends on  $k^2 \equiv \vec{k}^2$ , and calculate the angular part, resulting in

$$I_1^{vac}(M) = \frac{1}{4\pi^2} \int_0^\infty dk \frac{k^2}{\sqrt{k^2 + M^2}}. \quad (\text{B.31})$$

The remaining part, which is divergent, can now be treated by implementing one of the regularization schemes discussed in section 2.2.

---

### The Integral $I_2^{vac}(q, M)$

---

Here we present the analytical simplification of the integral  $I_2^{vac}(q, M)$ . Most steps will be analogous to the calculation of  $I_1^{vac}(M)$ . The integral reads

$$I_2^{vac}(q, M) = i \int \frac{d^4k}{(2\pi)^4} \frac{1}{[k^2 - M^2 + i\epsilon][(k+q)^2 - M^2 + i\epsilon]}. \quad (\text{B.32})$$

We rewrite the demoninator by introducing energies  $E_k = \sqrt{\vec{k}^2 + M^2}$  and  $E_{k,q} = \sqrt{(\vec{k} + \vec{q})^2 + M^2}$

$$I_2^{vac}(q, M) = i \int \frac{d^4k}{(2\pi)^4} \frac{1}{[k_0^2 - E_k^2 + i\epsilon][(k_0 + q_0)^2 - E_{k,q}^2 + i\epsilon]}. \quad (\text{B.33})$$

In the next step we perform a partial fraction decomposition and use  $i = (-i)^{-1}$  which leaves us with

$$I_2^{vac}(q, M) = - \int \frac{d^3k}{(2\pi)^3} \int \frac{dk_0}{2\pi i} \frac{1}{4E_k E_{k,q}} \left( \frac{1}{k_0 - E_k + i\epsilon'} - \frac{1}{k_0 + E_k - i\epsilon'} \right) \times \left( \frac{1}{k_0 + q_0 - E_{k,q} + i\epsilon'} - \frac{1}{k_0 + q_0 + E_{k,q} - i\epsilon'} \right). \quad (\text{B.34})$$

The  $k_0$ -integration can again be done with the residue theorem. Therefore we close the integration path in the upper half plane as shown in Figure B.2. Then the poles  $k_0 = -E_k + i\epsilon'$  and  $k_0 = -q_0 - E_{k,q} + i\epsilon'$  contribute and we get

$$I_2^{\text{vac}}(q, M) = \int \frac{d^3k}{(2\pi)^3} \frac{1}{4E_k E_{k,q}} \left( \frac{1}{q_0 - E_k - E_{k,q}} - \frac{1}{q_0 + E_k + E_{k,q}} \right). \quad (\text{B.35})$$

We further simplify the expression by reducing the integrand to a common denominator.

$$I_2^{\text{vac}}(q, M) = \int \frac{d^3k}{(2\pi)^3} \frac{1}{4E_k E_{k,q}} \left( \frac{q_0 + E_k + E_{k,q} - (q_0 - E_k - E_{k,q})}{(q_0 - E_k - E_{k,q})(q_0 + E_k + E_{k,q})} \right) \quad (\text{B.36})$$

Summarizing the nominator and denominator and introducing the sum of energies  $s_E = E_k + E_{k,q}$  we get

$$I_2^{\text{vac}}(q, M) = \int \frac{d^3k}{(2\pi)^3} \frac{1}{2E_k E_{k,q}} \frac{s_E}{q_0^2 - s_E^2}. \quad (\text{B.37})$$

Employing spherical coordinates and calculating the angular part of the integral leads us to

$$I_2^{\text{vac}}(q, M) = \frac{1}{4\pi^2} \int_0^\infty dk \frac{k^2}{E_k E_{k,q}} \frac{s_E}{q_0^2 - s_E^2}. \quad (\text{B.38})$$

This expression has to be regularized in order to deliver reliable results.

---

## C Medium Calculations

---

### The Integral $I_1^{med}(M)$

---

Here we present the calculation of the integral  $I_1^{med}(M)$

$$I_1^{med}(M) = -T \sum_n \int \frac{d^3k}{(2\pi)^3} \frac{1}{(i\omega_n + \mu)^2 - E_k^2}. \quad (C.1)$$

The first step is a partial fraction decomposition into

$$I_1^{med}(M) = \int \frac{d^3k}{(2\pi)^3} \frac{1}{2E_k} \left[ -T \sum_n \left( \frac{1}{i\omega_n + \mu - E_k} - \frac{1}{i\omega_n + \mu + E_k} \right) \right]. \quad (C.2)$$

We apply the residue theorem backwards, to convert the sum over Matsubara frequencies into an integral. Therefore we introduce an additional function in the integrand, which has poles at the Matsubara frequencies with residue  $-T$ .

$$I_1^{med}(M) = \int \frac{d^3k}{(2\pi)^3} \frac{1}{2E_k} \frac{1}{2\pi i} \int dz \frac{1}{e^{\frac{z}{T}} + 1} \left( \frac{1}{z + \mu - E_k} - \frac{1}{z + \mu + E_k} \right) \quad (C.3)$$

We deform the integration contour as depicted in Figure C.1 and perform the integration via residue theorem with the two poles  $a_{1/2} = \pm E_k - \mu$ , which results in

$$I_1^{med}(M) = \int \frac{d^3k}{(2\pi)^3} \frac{1}{2E_k} - \int \frac{d^3k}{(2\pi)^3} \frac{1}{2E_k} (n_k + \bar{n}_k). \quad (C.4)$$

We recognize the vacuum version of the integral  $I_1^{vac}(M)$  in the first term, and split up vacuum and medium part of  $I_1^{med}(M)$

$$I_1^{med}(M) = \int \frac{d^3k}{(2\pi)^3} (f^{vac}(E_k) - f^{med}(E_k)), \quad (C.5)$$

with

$$f^{vac}(E_k) = \frac{1}{2E_k} \quad \text{and} \quad f^{med}(E_k) = \frac{n_k + \bar{n}_k}{2E_k}. \quad (C.6)$$

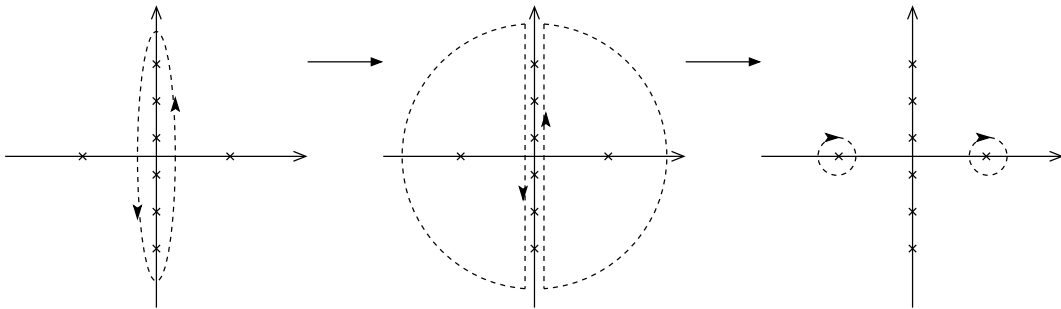


**Figure C.1.:** Deformation of the contour of integral  $I_1^{med}(M)$ . The small crosses indicate poles.

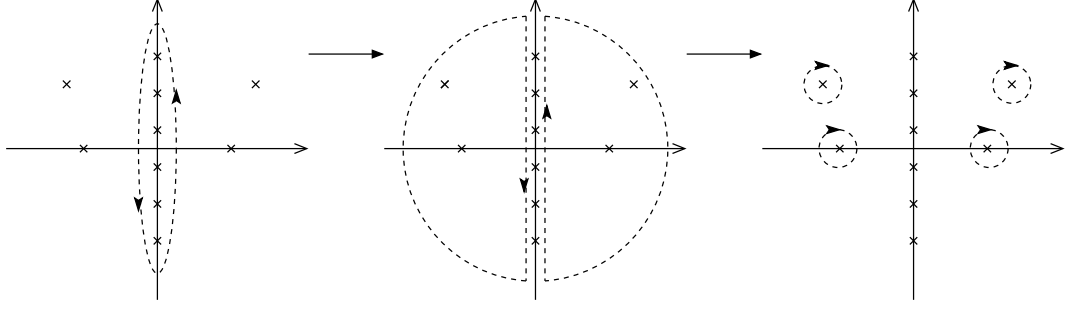


**Figure C.2.:** Deformation of the contour of integral  $I_2^{med}(i\omega_n, \vec{q})$ . The small crosses indicate poles.

---

### The Integral $I_2^{med}(i\omega_n, \vec{q}, M)$

---

Here we want to present the simplification of  $I_2^{med}(i\omega_n, \vec{q}, M)$  taken from [29].

$$\begin{aligned}
 I_2^{med}(i\omega_n, \vec{q}, M) &= -T \int \frac{d^3k}{(2\pi)^3} \sum_m \frac{1}{(i\omega_m + \mu) - \vec{k}^2 - M^2} \frac{1}{(i\omega_m + i\omega_n + \mu)^2 - (\vec{k} + \vec{q})^2 - M^2} \\
 &= -T \int \frac{d^3k}{(2\pi)^3} \sum_m \frac{1}{(i\omega_m + \mu) - E_k^2} \frac{1}{(i\omega_m + i\omega_n + \mu)^2 - E_{k,q}^2} \quad (C.7)
 \end{aligned}$$

Applying the residue theorem backwards we arrive at

$$I_2^{med}(i\omega_n, \vec{q}, M) = \int \frac{d^3k}{(2\pi)^3} \frac{1}{2\pi i} \int dz \underbrace{\frac{1}{e^{\frac{z}{T}} + 1}}_{\equiv n_F(z)} \left( \frac{1}{((z + \mu)^2 - E_k^2 + \mu)} \frac{1}{(z + \mu + i\omega_n)^2 - E_{k,q}^2} \right) \quad (C.8)$$

where the integral over  $z$  corresponds to the infinite Matsubara sum. As shown in figure C.2, the integration path can be deformed so much that only the four poles  $z = \pm E_k - \mu$  and  $z = \pm E_{k,q} - \mu - i\omega_n$  of the integrand contribute. Applying the residue theorem again results in

$$\begin{aligned}
 I_2^{med}(i\omega_n, \vec{q}, M) &= - \int \frac{d^3k}{(2\pi)^3} \frac{1}{4E_k E_{k,q}} \left[ \frac{n_F(E_k - \mu)}{(E_k + i\omega_n - E_{k,q})(E_k + i\omega_n + E_{k,q})} \right. \\
 &\quad - \frac{n_F(-E_k - \mu)}{(-E_k + i\omega_n - E_{k,q})(-E_k + i\omega_n + E_{k,q})} \\
 &\quad + \frac{n_F(E_{k,q} - i\omega_n - \mu)}{(E_{k,q} - i\omega_n - E_k)(E_{k,q} - i\omega_n + E_k)} \\
 &\quad \left. - \frac{n_F(-E_{k,q} - i\omega_n - \mu)}{(E_{k,q} - i\omega_n - E_k)(-E_{k,q} - i\omega_n + E_k)} \right]. \quad (C.9)
 \end{aligned}$$



Using  $n_F(x \pm i\omega_n) = n_F(x)$  and substituting  $k \rightarrow -k - q$  in the last two terms, we get

$$\begin{aligned}
I_2^{med}(i\omega_n, \vec{q}, M) = & - \int \frac{d^3k}{(2\pi)^3} \frac{1}{4E_k E_{k,q}} \left[ \frac{n_F(E_k - \mu)}{(E_k + i\omega_n - E_{k,q})(E_k + i\omega_n + E_{k,q})} \right. \\
& - \frac{n_F(-E_k - \mu)}{(E_k - i\omega_n + E_{k,q})(E_k - i\omega_n - E_{k,q})} \\
& + \frac{n_F(E_k - \mu)}{(E_k - i\omega_n - E_{k,q})(E_k - i\omega_n + E_{k,q})} \\
& \left. - \frac{n_F(-E_k - \mu)}{(E_k + i\omega_n + E_{k,q})(E_k + i\omega_n - E_{k,q})} \right]. \tag{C.10}
\end{aligned}$$

By using  $n_F(-x) = 1 - n_F(x)$  and defining  $n_k \equiv n_F(E_k - \mu)$  resp.  $\bar{n}_k \equiv n_F(E_k + \mu)$  this can be rearranged into following form

$$I_2^{med}(i\omega_n, \vec{q}, M) = \int \frac{d^3k}{(2\pi)^2} \left[ \left( \frac{1}{E_k} - \frac{n_k + \bar{n}_k}{2E_k E_{k,q}} s_E \right) \frac{1}{(i\omega_n)^2 - s_E^2} - \frac{n_k + \bar{n}_k}{2E_k E_{k,q}} d_E \frac{1}{(i\omega_n)^2 - d_E^2} \right] \tag{C.11}$$

with the sum  $s_E = E_{k,q} + E_k$  and the difference  $d_E = E_{k,q} - E_k$  of the energies.

---

## D Inhomogeneous Phase Calculations

---

### Alternative derivation of formula for mass gap

---

In section 4.2 we have shown the derivation of the mass gap from the gap equation. We want to present here an alternative method of derivation, using the grandcanonical potential of the system taken from [19]. Equation (3.17) on page 24 reads

$$\Omega = -N_f N_c \int \frac{d^2 k_\perp}{(2\pi)^2} \int_0^q \frac{dk_z}{(2\pi)} \sum_{\lambda_n > 0} \left( \underbrace{E_n + T \log(1 + e^{-\frac{E_n - \mu}{T}}) + T \log(1 + e^{-\frac{E_n + \mu}{T}})}_{f(E_n)} \right) + \frac{M^2}{4G_S}. \quad (\text{D.1})$$

with

$$\begin{aligned} E_n &= \text{sgn}(\lambda_n) \sqrt{\lambda_n^2 + k_\perp^2}, \quad \lambda_n = \pm \left( \sqrt{k_n^2 + M^2} \pm Q \right) \\ k_n &= k_z + 2nQ, \quad Q = \frac{q}{2}, \quad k_\perp^2 = k_x^2 + k_y^2 \end{aligned} \quad (\text{D.2})$$

The sum in the grandcanonical potential runs over positive eigenvalues, so only  $\lambda_n = + \left( \sqrt{k_n^2 + M^2} \pm Q \right)$  are needed. We subdivide them further into  $\lambda_{n,+} = \left( \sqrt{k_n^2 + M^2} + Q \right)$  and  $\lambda_{n,-} = \left( \sqrt{k_n^2 + M^2} - Q \right)$ . The potential can then be rewritten as

$$\Omega = -N_f N_c \int \frac{d^2 k_\perp}{(2\pi)^2} \int_0^q \frac{dk_z}{(2\pi)} \sum_n (f(E_{n,+}) + f(E_{n,-})) + \frac{M^2}{4G_S}. \quad (\text{D.3})$$

The potential contains a momentum integration over the Brillouin zone times the sum over all positive eigenvalues. This can be changed to an infinite momentum integration by dropping the sum over the eigenvalues

$$\Omega = -N_f N_c \int \frac{d^2 k_\perp}{(2\pi)^2} \int \frac{dk_z}{(2\pi)} [f(E_+) + f(E_-)] + \frac{M^2}{4G_S}. \quad (\text{D.4})$$

To obtain equation for the mass gap, the following condition has to be fulfilled

$$\frac{d\Omega}{dM} \stackrel{!}{=} 0. \quad (\text{D.5})$$

Calculating the derivative results in

$$M = 2N_f N_c G_S M \int \frac{d^3 k}{(2\pi)^3} \frac{1}{E} \left[ \frac{\lambda_+}{E_+} (1 - n_{E_+} - \bar{n}_{E_+}) + \frac{\lambda_-}{E_-} (1 - n_{E_-} - \bar{n}_{E_-}) \right] \quad (\text{D.6})$$

with

$$\begin{aligned} E &= \sqrt{k_z^2 + M^2}, \\ \lambda_+ &= E + Q, \quad \lambda_- = E - Q \\ E_+ &= \sqrt{\lambda_+^2 + k_\perp^2} \quad \text{and} \quad E_- = \sqrt{\lambda_-^2 + k_\perp^2}. \end{aligned} \quad (\text{D.7})$$

If we plug in  $N_f = 2$  and we have the same result as in section 4.2. Please keep in mind that we used the notation of [19] here.

---

## Inhomogeneous quark propagator

---

On the following pages we have noted down the inhomogeneous quark propagator and its inverse. For legibility we have only shown one block. All other blocks<sup>1</sup> have the same structure, but additional factors of  $q$ , i.e.  $p_z + 2q$ ,  $p_z + 3q$ , etc.

---

<sup>1</sup> Denoted by  $\cdot$ .



$$\mathbf{1}^{(+)} = \frac{1}{C_{-1}} \left( \begin{array}{c} M^2[(p_z - q) - (i\omega_m + \mu)] + [(\bar{p} - \bar{q})^2 - (i\omega_m + \mu)^2] [p_z - (i\omega_m + \mu)] \\ (p_x + ip_y) [M^2 + (\bar{p} - \bar{q})^2 - (i\omega_m + \mu)^2] \\ - M^2[(p_z - q) + (i\omega_m + \mu)] - [(\bar{p} - \bar{q})^2 - (i\omega_m + \mu)^2] [p_z + (i\omega_m + \mu)] \end{array} \right) \quad (\text{D.11})$$

$$\mathbf{1}^{(-)} = \frac{1}{\bar{p}^2 - (i\omega_m + \mu)^2} \left( \begin{array}{c} -p_z - ip_y \\ -p_x + ip_y \end{array} \begin{array}{c} -p_x + ip_y \\ p_z - (i\omega_m + \mu) \end{array} \right) \quad \mathbf{6}^{(-)} = \frac{1}{(\bar{p} + \bar{q})^2 - (i\omega_m + \mu)^2} \left( \begin{array}{c} (p_z + q) - (i\omega_m + \mu) \\ p_x + ip_y \end{array} \begin{array}{c} p_x - ip_y \\ (p_z + q) + (i\omega_m + \mu) \end{array} \right) \quad (\text{D.12})$$

$$\mathbf{2}^{(\pm)} = \frac{1}{C_1} \left( \begin{array}{c} \mp M^2[(p_z + q) \pm (i\omega_m + \mu)] \mp [(\bar{p} + \bar{q})^2 - (i\omega_m + \mu)^2] [p_z \pm (i\omega_m + \mu)] \\ \mp (p_x + ip_y) [M^2 + (\bar{p} + \bar{q})^2 - (i\omega_m + \mu)^2] \\ \pm M^2[(p_z + q) \mp (i\omega_m + \mu)] \pm [(\bar{p} + \bar{q})^2 - (i\omega_m + \mu)^2] [p_z \mp (i\omega_m + \mu)] \end{array} \right) \quad (\text{D.13})$$

$$\mathbf{3}^{(\pm)} = \frac{1}{C_1} \left( \begin{array}{c} -M[M^2 + \bar{p} \cdot (\bar{p} + \bar{q}) - (i\omega_m + \mu)^2] \pm q(i\omega_m + \mu) \\ -M(p_x + ip_y)q \end{array} \begin{array}{c} M(p_x - ip_y)q \\ -M[M^2 + \bar{p} \cdot (\bar{p} + \bar{q}) - (i\omega_m + \mu)^2] \mp q(i\omega_m + \mu) \end{array} \right) \quad (\text{D.14})$$

$$\mathbf{4}^{(\pm)} = \frac{1}{C_1} \left( \begin{array}{c} -M[M^2 + \bar{p} \cdot (\bar{p} + \bar{q}) - (i\omega_m + \mu)^2] \pm q(i\omega_m + \mu) \\ M(p_x + ip_y)q \end{array} \begin{array}{c} -M(p_x - ip_y)q \\ -M[M^2 + \bar{p} \cdot (\bar{p} + \bar{q}) - (i\omega_m + \mu)^2] \mp q(i\omega_m + \mu) \end{array} \right) \quad (\text{D.15})$$

$$\mathbf{5}^{(\pm)} = \frac{1}{C_1} \left( \begin{array}{c} \pm M^2[p_z \mp (i\omega_m + \mu)] \pm [p_z^2 - (i\omega_m + \mu)^2] [(p_z + q) \mp (i\omega_m + \mu)] \\ \pm (p_x + ip_y) [M^2 + p_z^2 - (i\omega_m + \mu)^2] \\ \mp M^2[p_z \pm (i\omega_m + \mu)] \mp [p_z^2 - (i\omega_m + \mu)^2] [(p_z + q) \pm (i\omega_m + \mu)] \end{array} \right) \quad (\text{D.16})$$

$$\mathbf{6}^{(+)} = \frac{1}{C_2} \left( \begin{array}{c} -M^2[(p_z + 2q) + (i\omega_m + \mu)] - [(\bar{p} + 2\bar{q})^2 - (i\omega_m + \mu)^2] [(p_z + q) + (i\omega_m + \mu)] \\ -(p_x + ip_y) [M^2 + (\bar{p} + 2\bar{q})^2 - (i\omega_m + \mu)^2] \\ - (p_x - ip_y) [M^2 + (\bar{p} + 2\bar{q})^2 - (i\omega_m + \mu)^2] \\ M^2[(p_z + 2q) - (i\omega_m + \mu)] + [(\bar{p} + 2\bar{q})^2 - (i\omega_m + \mu)^2] [(p_z + q) - (i\omega_m + \mu)] \end{array} \right) \quad (\text{D.17})$$

with

$$\begin{aligned} C_{-1} &= M^4 + 2M^2[\bar{p} \cdot (\bar{p} - \bar{q})] + [\bar{p}^2 - (i\omega_m + \mu)^2][(\bar{p} - \bar{q})^2 - (i\omega_m + \mu)^2] \\ C_1 &= M^4 + 2M^2[\bar{p} \cdot (\bar{p} + \bar{q})] + [\bar{p}^2 - (i\omega_m + \mu)^2][(\bar{p} + \bar{q})^2 - (i\omega_m + \mu)^2] \\ C_2 &= M^4 + 2M^2[(\bar{p} + \bar{q}) \cdot (\bar{p} + 2\bar{q})] + [\bar{p}^2 - (i\omega_m + \mu)^2][(\bar{p} + 2\bar{q})^2 - (i\omega_m + \mu)^2] \end{aligned} \quad (\text{D.18})$$

## Inhomogeneous mesons

Here we present the  $z$ -integration of eq. (4.60). Changing the contour from  $C_1$ , which runs around the fermionic Matsubara frequencies, to  $C_2$ , which runs around the poles of the traces given in the Table D.1 and considering the difference in the two isospin flavors, the polarization loops read

$$J^\pm(i\omega_k; \vec{r} + 2l\vec{Q}, \vec{r}) = \int \frac{d^3p}{(2\pi)^3} \frac{1}{2\pi i} \oint_{C_2} dz n_F(z) \sum_m \text{Tr}[\dots] \quad (\text{D.19})$$

where  $\text{Tr}[\dots]$  is

$$\text{Tr} \left[ S^\pm(i\omega_k + z + \mu; \vec{p} + \vec{r} + 2l\vec{Q}, \vec{p} + \vec{r} + 2m\vec{Q}) S^\pm(z + \mu; \vec{p} + 2m\vec{Q}, \vec{p}) \right]. \quad (\text{D.20})$$

We dropped  $\Gamma_{M'}$ ,  $\Gamma_M$  and the indices  $M'$ ,  $M$ , since we found that the traces are the same as long as the meson types does not change.

poles for up quark	poles for down quark
$a_{1/2}^+ = \pm E_{+,p,m-1} - \mu$	$a_{1/2}^- = \pm E_{+,p,m} - \mu$
$a_{3/4}^+ = \pm E_{-,p,m-1} - \mu$	$a_{3/4}^- = \pm E_{-,p,m} - \mu$
$a_{5/6}^+ = \pm E_{+,p+r,l} - i\omega_k - \mu$	$a_{5/6}^- = \pm E_{+,p+r,l-1} - i\omega_k - \mu$
$a_{7/8}^+ = \pm E_{-,p+r,l} - i\omega_k - \mu$	$a_{7/8}^- = \pm E_{-,p+r,l-1} - i\omega_k - \mu$
$a_{9/10}^+ = \pm E_{+,p,m+1} - \mu$	$a_{9/10}^- = \pm E_{+,p,m} - \mu$
$a_{11/12}^+ = \pm E_{-,p,m+1} - \mu$	$a_{11/12}^- = \pm E_{-,p,m} - \mu$
$a_{13/14}^+ = \pm E_{+,p+r,l} - i\omega_k - \mu$	$a_{13/14}^- = \pm E_{+,p+r,l+1} - i\omega_k - \mu$
$a_{15/16}^+ = \pm E_{-,p+r,l} - i\omega_k - \mu$	$a_{15/16}^- = \pm E_{-,p+r,l+1} - i\omega_k - \mu$

**Table D.1.:** Poles occuring in the traces of the polarization loop for both isospin flavors.

The  $z$ -integration is done using the residue theorem

$$\oint_{C_2} f(z) dz = 2\pi i \sum_{i=1}^n \text{Res}(f, a_i) \quad (\text{D.21})$$

Since the traces consists of sums of fractions, we will use an alternative way of calculating the residues.

$$f(z) = \frac{g(z)}{h(z)} \text{ with } g(a_i) \neq 0, h(a_i) = 0, h'(a_i) \neq 0 \Rightarrow \text{Res}(f, a_i) = \frac{g(a_i)}{h'(a_i)} \quad (\text{D.22})$$

After the integration the polarization loops are given by the formulas we have noted down on the following pages. The first version is the direct result, the second version has been treated with

$$n_F(x) = 1 - n_F(x) \quad (\text{D.23})$$

and arranged according to whether the term has a factor of  $n_F(x)$  in front of it or not. We have done this based on the homogeneous case, where we identified the the terms with  $n_F(x)$  as medium parts of the expression, which did not need regularization.

$$\begin{aligned}
f_1^+(z + \mu) &= M^2[p_z + (2m - 3)Q - (z + \mu)] + [p_z + (2m - 1)Q - (z + \mu)][p_x^2 + p_y^2 + (p_z + (2m - 3)Q)^2 - (z + \mu)^2] \\
f_2^+(z + \mu) &= M^2[p_z + (2m + 3)Q - (z + \mu)] + [p_z + (2m + 1)Q - (z + \mu)][p_x^2 + p_y^2 + (p_z + (2m + 3)Q)^2 - (z + \mu)^2] \\
f_3^+(z + \mu) &= -M^2[p_z + (2m - 3)Q + (z + \mu)] - [p_z + (2m - 1)Q + (z + \mu)][p_x^2 + p_y^2 + (p_z + (2m - 3)Q)^2 - (z + \mu)^2] \\
f_4^+(z + \mu) &= -M^2[p_z + (2m + 3)Q + (z + \mu)] - [p_z + (2m + 1)Q + (z + \mu)][p_x^2 + p_y^2 + (p_z + (2m + 3)Q)^2 - (z + \mu)^2] \\
g_1^+(z + \mu + i\omega_k) &= -M^2[p_z + r_z + (2l + 1)Q + (z + \mu + i\omega_k)] - [p_z + r_z + (2l - 1)Q + (z + \mu + i\omega_k)][(p_x + r_x)^2 + (p_y + r_y)^2 + (p_z + r_z + (2l + 1)Q)^2 - (z + \mu + i\omega_k)^2] \\
g_2^+(z + \mu + i\omega_k) &= -M^2[p_z + r_z + (2l - 1)Q + (z + \mu + i\omega_k)] - [p_z + r_z + (2l + 1)Q + (z + \mu + i\omega_k)][(p_x + r_x)^2 + (p_y + r_y)^2 + (-p_z - r_z - (2l - 1)Q)^2 - (z + \mu + i\omega_k)^2] \\
g_3^+(z + \mu + i\omega_k) &= M^2[p_z + r_z + (2l + 1)Q - (z + \mu + i\omega_k)] + [p_z + r_z + (2l - 1)Q - (z + \mu + i\omega_k)][(p_x + r_x)^2 + (p_y + r_y)^2 + (p_z + r_z + (2l + 1)Q)^2 - (z + \mu + i\omega_k)^2] \\
g_4^+(z + \mu + i\omega_k) &= M^2[p_z + r_z + (2l - 1)Q - (z + \mu + i\omega_k)] + [p_z + r_z + (2l + 1)Q - (z + \mu + i\omega_k)][(p_x + r_x)^2 + (p_y + r_y)^2 + (-p_z - r_z - (2l - 1)Q)^2 - (z + \mu + i\omega_k)^2] \\
h_1^+(z + \mu + i\omega_k) &= -2[(p_x + r_x)p_x + (p_y + r_y)p_y][M^2 + p_x^2 + p_y^2 + (p_z + (2m - 3)Q)^2 - (z + \mu)^2] + (p_x + r_x)^2 + (p_y + r_y)^2 + (p_z + (2l + 1)Q)^2 - (z + \mu + i\omega_k)^2] \\
h_2^+(z + \mu + i\omega_k) &= -2[(p_x + r_x)p_x + (p_y + r_y)p_y][M^2 + p_x^2 + p_y^2 + (p_z + (2m + 3)Q)^2 - (z + \mu)^2] + (p_x + r_x)^2 + (p_y + r_y)^2 + (p_z + (2l - 1)Q)^2 - (z + \mu + i\omega_k)^2]
\end{aligned}$$

$$\begin{aligned}
f_1^-(z + \mu) &= M^2[p_z + (2m + 1)Q - (z + \mu)] + [p_z + (2m - 1)Q - (z + \mu)][p_x^2 + p_y^2 + (p_z + (2m + 1)Q)^2 - (z + \mu)^2] \\
f_2^-(z + \mu) &= M^2[p_z + (2m - 1)Q - (z + \mu)] + [p_z + (2m + 1)Q - (z + \mu)][p_x^2 + p_y^2 + (p_z + (2m - 1)Q)^2 - (z + \mu)^2] \\
f_3^-(z + \mu) &= -M^2[p_z + (2m + 1)Q + (z + \mu)] - [p_z + (2m - 1)Q + (z + \mu)][p_x^2 + p_y^2 + (p_z + (2m + 1)Q)^2 - (z + \mu)^2] \\
f_4^-(z + \mu) &= -M^2[p_z + (2m - 1)Q + (z + \mu)] - [p_z + (2m + 1)Q + (z + \mu)][p_x^2 + p_y^2 + (p_z + (2m - 1)Q)^2 - (z + \mu)^2] \\
g_1^-(z + \mu + i\omega_k) &= -M^2[p_z + r_z + (2l - 3)Q + (z + \mu + i\omega_k)] - [p_z + r_z + (2l - 1)Q + (z + \mu + i\omega_k)][(p_x + r_x)^2 + (p_y + r_y)^2 + (p_z + r_z + (2l - 3)Q)^2 - (z + \mu + i\omega_k)^2] \\
g_2^-(z + \mu + i\omega_k) &= -M^2[p_z + r_z + (2l + 3)Q + (z + \mu + i\omega_k)] - [p_z + r_z + (2l + 1)Q + (z + \mu + i\omega_k)][(p_x + r_x)^2 + (p_y + r_y)^2 + (p_z + r_z + (2l + 3)Q)^2 - (z + \mu + i\omega_k)^2] \\
g_3^-(z + \mu + i\omega_k) &= M^2[p_z + r_z + (2l - 3)Q - (z + \mu + i\omega_k)] + [p_z + r_z + (2l - 1)Q - (z + \mu + i\omega_k)][(p_x + r_x)^2 + (p_y + r_y)^2 + (p_z + r_z + (2l - 3)Q)^2 - (z + \mu + i\omega_k)^2] \\
g_4^-(z + \mu + i\omega_k) &= M^2[p_z + r_z + (2l + 3)Q - (z + \mu + i\omega_k)] + [p_z + r_z + (2l + 1)Q - (z + \mu + i\omega_k)][(p_x + r_x)^2 + (p_y + r_y)^2 + (p_z + r_z + (2l + 3)Q)^2 - (z + \mu + i\omega_k)^2] \\
h_1^-(z + \mu + i\omega_k) &= -2[(p_x + r_x)p_x + (p_y + r_y)p_y][M^2 + p_x^2 + p_y^2 + (p_z + (2m + 1)Q)^2 - (z + \mu)] + (p_x + r_x)^2 + (p_y + r_y)^2 + (p_z + (2l - 3)Q)^2 - (z + \mu + i\omega_k)^2 \\
h_2^-(z + \mu + i\omega_k) &= -2[(p_x + r_x)p_x + (p_y + r_y)p_y][M^2 + p_x^2 + p_y^2 + (p_z + (2m - 1)Q)^2 - (z + \mu)] + (p_x + r_x)^2 + (p_y + r_y)^2 + (p_z + (2l + 3)Q)^2 - (z + \mu + i\omega_k)^2
\end{aligned}$$



$$J_m^+(\mathbf{i}\omega_k; \vec{r} + 2l\vec{Q}, \vec{r}) = \int \frac{d^3p}{(2\pi)^3} \quad (\text{D.24})$$

$$\begin{aligned}
& n_F(E_{+,p,m-1} - \mu) \frac{f_1^+(E_{+,p,m-1})g_1^+(E_{+,p,m-1} + \mathbf{i}\omega_k) + f_3^+(E_{+,p,m-1})g_3^+(E_{+,p,m-1} + \mathbf{i}\omega_k) + h_1^+(E_{+,p,m-1} + \mathbf{i}\omega_k)}{E_{p,m-1}E_{+,p,m-1}[E_{-,p+r,l}^2 - (E_{+,p,m-1} + \mathbf{i}\omega_k)^2][E_{+,p+r,l}^2 - (E_{+,p,m-1} + \mathbf{i}\omega_k)^2]} \\
& - n_F(-E_{+,p,m-1} - \mu) \frac{f_1^+(-E_{+,p,m-1})g_1^+(-E_{+,p,m-1} + \mathbf{i}\omega_k) + f_3^+(-E_{+,p,m-1})g_3^+(-E_{+,p,m-1} + \mathbf{i}\omega_k) + h_1^+(-E_{+,p,m-1} + \mathbf{i}\omega_k)}{E_{p,m-1}E_{+,p,m-1}[E_{-,p+r,l}^2 - (E_{+,p,m-1} - \mathbf{i}\omega_k)^2][E_{+,p+r,l}^2 - (E_{+,p,m-1} - \mathbf{i}\omega_k)^2]} \\
& - n_F(E_{-,p,m-1} - \mu) \frac{f_1^+(E_{-,p,m-1})g_1^+(E_{-,p,m-1} + \mathbf{i}\omega_k) + f_3^+(E_{-,p,m-1})g_3^+(E_{-,p,m-1} + \mathbf{i}\omega_k) + h_1^+(E_{-,p,m-1} + \mathbf{i}\omega_k)}{E_{p,m-1}E_{-,p,m-1}[E_{-,p+r,l}^2 - (E_{-,p,m-1} + \mathbf{i}\omega_k)^2][E_{+,p+r,l}^2 - (E_{-,p,m-1} + \mathbf{i}\omega_k)^2]} \\
& + n_F(-E_{-,p,m-1} - \mu) \frac{f_1^+(-E_{-,p,m-1})g_1^+(-E_{-,p,m-1} + \mathbf{i}\omega_k) + f_3^+(-E_{-,p,m-1})g_3^+(-E_{-,p,m-1} + \mathbf{i}\omega_k) + h_1^+(-E_{-,p,m-1} + \mathbf{i}\omega_k)}{E_{p,m-1}E_{-,p,m-1}[E_{-,p+r,l}^2 - (E_{-,p,m-1} - \mathbf{i}\omega_k)^2][E_{+,p+r,l}^2 - (E_{-,p,m-1} - \mathbf{i}\omega_k)^2]} \\
& + n_F(E_{+,p+r,l} - \mathbf{i}\omega_k - \mu) \frac{f_1^+(E_{+,p+r,l} - \mathbf{i}\omega_k)g_1^+(E_{+,p+r,l}) + f_3^+(E_{+,p+r,l} - \mathbf{i}\omega_k)g_3^+(E_{+,p+r,l}) + h_1^+(E_{+,p+r,l})}{E_{p+r,l}E_{+,p+r,l}[E_{-,p,m-1}^2 - (E_{+,p+r,l} - \mathbf{i}\omega_k)^2][E_{+,p+m-1}^2 - (E_{+,p+r,l} - \mathbf{i}\omega_k)^2]} \\
& - n_F(-E_{+,p+r,l} - \mathbf{i}\omega_k - \mu) \frac{f_1^+(-E_{+,p+r,l} - \mathbf{i}\omega_k)g_1^+(-E_{+,p+r,l}) + f_3^+(-E_{+,p+r,l} - \mathbf{i}\omega_k)g_3^+(-E_{+,p+r,l}) + h_1^+(-E_{+,p+r,l})}{E_{p+r,l}E_{+,p+r,l}[E_{-,p,m-1}^2 - (E_{+,p+r,l} + \mathbf{i}\omega_k)^2][E_{+,p+m-1}^2 - (E_{+,p+r,l} + \mathbf{i}\omega_k)^2]} \\
& - n_F(E_{-,p+r,l} - \mathbf{i}\omega_k - \mu) \frac{f_1^+(E_{-,p+r,l} - \mathbf{i}\omega_k)g_1^+(E_{-,p+r,l}) + f_3^+(E_{-,p+r,l} - \mathbf{i}\omega_k)g_3^+(E_{-,p+r,l}) + h_1^+(E_{-,p+r,l})}{E_{p+r,l}E_{-,p+r,l}[E_{-,p,m-1}^2 - (E_{-,p+r,l} - \mathbf{i}\omega_k)^2][E_{+,p+m-1}^2 - (E_{-,p+r,l} - \mathbf{i}\omega_k)^2]} \\
& + n_F(-E_{-,p+r,l} - \mathbf{i}\omega_k - \mu) \frac{f_1^+(-E_{-,p+r,l} - \mathbf{i}\omega_k)g_1^+(-E_{-,p+r,l}) + f_3^+(-E_{-,p+r,l} - \mathbf{i}\omega_k)g_3^+(-E_{-,p+r,l}) + h_1^+(-E_{-,p+r,l})}{E_{p+r,l}E_{-,p+r,l}[E_{-,p,m-1}^2 - (E_{-,p+r,l} + \mathbf{i}\omega_k)^2][E_{+,p+m-1}^2 - (E_{-,p+r,l} + \mathbf{i}\omega_k)^2]}
\end{aligned}$$

$$\begin{aligned}
& +n_F(E_{+,p,m+1} - \mu) \frac{f_2^+(E_{+,p,m+1})g_2^+(E_{+,p,m+1} + i\omega_k) + f_4^+(E_{+,p,m+1})g_4^+(E_{+,p,m+1} + i\omega_k) + h_2^+(E_{+,p,m+1} + i\omega_k)}{E_{p,m+1}E_{+,p,m+1}[E_{-,p+r,l}^2 - (E_{+,p,m+1} + i\omega_k)^2][E_{+,p+r,l}^2 - (E_{+,p,m+1} + i\omega_k)^2]} \\
& -n_F(-E_{+,p,m+1} - \mu) \frac{f_2^+(-E_{+,p,m+1})g_2^+(-E_{+,p,m+1} + i\omega_k) + f_4^+(-E_{+,p,m+1})g_4^+(-E_{+,p,m+1} + i\omega_k) + h_2^+(-E_{+,p,m+1} + i\omega_k)}{E_{p,m+1}E_{+,p,m+1}[E_{-,p+r,l}^2 - (E_{+,p,m+1} - i\omega_k)^2][E_{+,p+r,l}^2 - (E_{+,p,m+1} - i\omega_k)^2]} \\
& -n_F(E_{-,p,m+1} - \mu) \frac{f_2^+(E_{-,p,m+1})g_2^+(E_{-,p,m+1} + i\omega_k) + f_4^+(E_{-,p,m+1})g_4^+(E_{-,p,m+1} + i\omega_k) + h_2^+(E_{-,p,m+1} + i\omega_k)}{E_{p,m+1}E_{-,p,m+1}[E_{-,p+r,l}^2 - (E_{-,p,m+1} + i\omega_k)^2][E_{+,p+r,l}^2 - (E_{-,p,m+1} + i\omega_k)^2]} \\
& +n_F(-E_{-,p,m+1} - \mu) \frac{f_2^+(-E_{-,p,m+1})g_2^+(-E_{-,p,m+1} + i\omega_k) + f_4^+(-E_{-,p,m+1})g_4^+(-E_{-,p,m+1} + i\omega_k) + h_2^+(-E_{-,p,m+1} + i\omega_k)}{E_{p,m+1}E_{-,p,m+1}[E_{-,p+r,l}^2 - (E_{-,p,m+1} - i\omega_k)^2][E_{+,p+r,l}^2 - (E_{-,p,m+1} - i\omega_k)^2]} \\
& +n_F(E_{+,p+r,l} - i\omega_k - \mu) \frac{f_2^+(E_{+,p+r,l} - i\omega_k)g_2^+(E_{+,p+r,l} + i\omega_k) + f_4^+(E_{+,p+r,l} - i\omega_k)g_4^+(E_{+,p+r,l} + i\omega_k) + h_2^+(E_{+,p+r,l})}{E_{p+r,l}E_{+,p+r,l}[E_{-,p,m+1}^2 - (E_{+,p+r,l} - i\omega_k)^2][E_{+,p,m+1}^2 - (E_{+,p+r,l} - i\omega_k)^2]} \\
& -n_F(-E_{+,p+r,l} - i\omega_k - \mu) \frac{f_2^+(-E_{+,p+r,l} - i\omega_k)g_2^+(-E_{+,p+r,l} + i\omega_k) + f_4^+(-E_{+,p+r,l} - i\omega_k)g_4^+(-E_{+,p+r,l} + i\omega_k) + h_2^+(-E_{+,p+r,l})}{E_{p+r,l}E_{+,p+r,l}[E_{-,p,m+1}^2 - (E_{+,p+r,l} - i\omega_k)^2][E_{+,p,m+1}^2 - (E_{+,p+r,l} - i\omega_k)^2]} \\
& -n_F(E_{-,p+r,l} - i\omega_k - \mu) \frac{f_2^+(E_{-,p+r,l} - i\omega_k)g_2^+(E_{-,p+r,l} + i\omega_k) + f_4^+(E_{-,p+r,l} - i\omega_k)g_4^+(E_{-,p+r,l} + i\omega_k) + h_2^+(E_{-,p+r,l})}{E_{p+r,l}E_{-,p+r,l}[E_{-,p,m+1}^2 - (E_{-,p+r,l} - i\omega_k)^2][E_{+,p,m+1}^2 - (E_{-,p+r,l} - i\omega_k)^2]} \\
& +n_F(-E_{-,p+r,l} - i\omega_k - \mu) \frac{f_2^+(-E_{-,p+r,l} - i\omega_k)g_2^+(-E_{-,p+r,l} + i\omega_k) + f_4^+(-E_{-,p+r,l} - i\omega_k)g_4^+(-E_{-,p+r,l} + i\omega_k) + h_2^+(-E_{-,p+r,l})}{E_{p+r,l}E_{-,p+r,l}[E_{-,p,m+1}^2 - (E_{-,p+r,l} - i\omega_k)^2][E_{+,p,m+1}^2 - (E_{-,p+r,l} - i\omega_k)^2]}
\end{aligned}$$

$$J_m^+(i\omega_k; \vec{r} + 2l\vec{Q}, \vec{r}) = \int \frac{d^3p}{(2\pi)^3} \quad (\text{D.25})$$

$$\begin{aligned}
& \frac{f_1^+(-E_{-p,m-1})g_1^+(-E_{-p,m-1} + i\omega_k) + f_3^+(-E_{-p,m-1})g_3^+(-E_{-p,m-1} + i\omega_k) + h_1^+(-E_{-p,m-1} + i\omega_k)}{E_{p,m-1}E_{-p,m-1}[E_{-p,p+r,l}^2 - (E_{-p,m-1} - i\omega_k)^2][E_{+p,p+r,l}^2 - (E_{-p,m-1} - i\omega_k)^2]} \\
& + \frac{f_1^+(-E_{-p,p+r,l} - i\omega_k)g_1^+(-E_{-p,p+r,l}) + f_3^+(-E_{-p,p+r,l} - i\omega_k)g_3^+(-E_{-p,p+r,l}) + h_1^+(-E_{-p,p+r,l})}{E_{p+r,l}E_{-p,p+r,l}[E_{-p,m-1}^2 - (E_{-p,p+r,l} + i\omega_k)^2][E_{+p,m-1}^2 - (E_{-p,p+r,l} + i\omega_k)^2]} \\
& + \frac{f_2^+(-E_{-p,m+1})g_2^+(-E_{-p,m+1} + i\omega_k) + f_4^+(-E_{-p,m+1})g_4^+(-E_{-p,m+1} + i\omega_k) + h_2^+(-E_{-p,m+1} + i\omega_k)}{E_{p,m+1}E_{-p,m+1}[E_{-p,p+r,l}^2 - (E_{-p,m+1} - i\omega_k)^2][E_{+p,p+r,l}^2 - (E_{-p,m+1} - i\omega_k)^2]} \\
& + \frac{f_2^+(-E_{-p,p+r,l} - i\omega_k)g_2^+(-E_{-p,p+r,l}) + f_4^+(-E_{-p,p+r,l} - i\omega_k)g_4^+(-E_{-p,p+r,l}) + h_2^+(-E_{-p,p+r,l})}{E_{p+r,l}E_{-p,p+r,l}[E_{-p,m+1}^2 - (E_{-p,p+r,l} + i\omega_k)^2][E_{+p,m+1}^2 - (E_{-p,p+r,l} + i\omega_k)^2]} \\
& + \frac{f_1^+(-E_{+p,m-1})g_1^+(-E_{+p,m-1} + i\omega_k) + f_3^+(-E_{+p,m-1})g_3^+(-E_{+p,m-1} + i\omega_k) + h_1^+(-E_{+p,m-1} + i\omega_k)}{E_{p,m-1}E_{+p,m-1}[E_{-p,p+r,l}^2 - (E_{+p,m-1} - i\omega_k)^2][E_{+p,p+r,l}^2 - (E_{+p,m-1} - i\omega_k)^2]} \\
& + \frac{f_1^+(-E_{+p,p+r,l} - i\omega_k)g_1^+(-E_{+p,p+r,l}) + f_3^+(-E_{+p,p+r,l} - i\omega_k)g_3^+(-E_{+p,p+r,l}) + h_1^+(-E_{+p,p+r,l})}{E_{p+r,l}E_{+p,p+r,l}[E_{-p,m-1}^2 - (E_{+p,p+r,l} + i\omega_k)^2][E_{+p,m-1}^2 - (E_{+p,p+r,l} + i\omega_k)^2]} \\
& + \frac{f_2^+(-E_{+p,m+1})g_2^+(-E_{+p,m+1} + i\omega_k) + f_4^+(-E_{+p,m+1})g_4^+(-E_{+p,m+1} + i\omega_k) + h_2^+(-E_{+p,m+1} + i\omega_k)}{E_{p,m+1}E_{+p,m+1}[E_{-p,p+r,l}^2 - (E_{+p,m+1} - i\omega_k)^2][E_{+p,p+r,l}^2 - (E_{+p,m+1} - i\omega_k)^2]} \\
& + \frac{f_2^+(-E_{+p,p+r,l} - i\omega_k)g_2^+(-E_{+p,p+r,l}) + f_4^+(-E_{+p,p+r,l} - i\omega_k)g_4^+(-E_{+p,p+r,l}) + h_2^+(-E_{+p,p+r,l})}{E_{p+r,l}E_{+p,p+r,l}[E_{-p,m+1}^2 - (E_{+p,p+r,l} + i\omega_k)^2][E_{+p,m+1}^2 - (E_{+p,p+r,l} + i\omega_k)^2]}
\end{aligned}$$

$$\begin{aligned}
& +n_F(E_{+,p,m-1} - \mu) \frac{f_1^+(E_{+,p,m-1})g_1^+(E_{+,p,m-1} + i\omega_k) + f_3^+(E_{+,p,m-1})g_3^+(E_{+,p,m-1} + i\omega_k) + h_1^+(E_{+,p,m-1} + i\omega_k)}{E_{p,m-1}E_{+,p,m-1}[E_{-,p+r,l}^2 - (E_{+,p,m-1} + i\omega_k)^2][E_{+,p+r,l}^2 - (E_{+,p,m-1} + i\omega_k)^2]} \\
& +n_F(E_{+,p,m-1} + \mu) \frac{f_1^+(-E_{+,p,m-1})g_1^+(-E_{+,p,m-1} + i\omega_k) + f_3^+(-E_{+,p,m-1})g_3^+(-E_{+,p,m-1} + i\omega_k) + h_1^+(-E_{+,p,m-1} + i\omega_k)}{E_{p,m-1}E_{+,p,m-1}[E_{-,p+r,l}^2 - (E_{+,p,m-1} - i\omega_k)^2][E_{+,p+r,l}^2 - (E_{+,p,m-1} - i\omega_k)^2]} \\
& +n_F(E_{+,p,m+1} - \mu) \frac{f_2^+(E_{+,p,m+1})g_2^+(E_{+,p,m+1} + i\omega_k) + f_4^+(E_{+,p,m+1})g_4^+(E_{+,p,m+1} + i\omega_k) + h_2^+(E_{+,p,m+1} + i\omega_k)}{E_{p,m+1}E_{+,p,m+1}[E_{-,p+r,l}^2 - (E_{+,p,m+1} + i\omega_k)^2][E_{+,p+r,l}^2 - (E_{+,p,m+1} + i\omega_k)^2]} \\
& +n_F(E_{+,p,m+1} + \mu) \frac{f_2^+(-E_{+,p,m+1})g_2^+(-E_{+,p,m+1} + i\omega_k) + f_4^+(-E_{+,p,m+1})g_4^+(-E_{+,p,m+1} + i\omega_k) + h_2^+(-E_{+,p,m+1} + i\omega_k)}{E_{p,m+1}E_{+,p,m+1}[E_{-,p+r,l}^2 - (E_{+,p,m+1} - i\omega_k)^2][E_{+,p+r,l}^2 - (E_{+,p,m+1} - i\omega_k)^2]} \\
& -n_F(E_{-,p,m-1} - \mu) \frac{f_1^+(E_{-,p,m-1})g_1^+(E_{-,p,m-1} + i\omega_k) + f_3^+(E_{-,p,m-1})g_3^+(E_{-,p,m-1} + i\omega_k) + h_1^+(E_{-,p,m-1} + i\omega_k)}{E_{p,m-1}E_{-,p,m-1}[E_{-,p+r,l}^2 - (E_{-,p,m-1} + i\omega_k)^2][E_{+,p+r,l}^2 - (E_{-,p,m-1} + i\omega_k)^2]} \\
& -n_F(E_{-,p,m-1} + \mu) \frac{f_1^+(-E_{-,p,m-1})g_1^+(-E_{-,p,m-1} + i\omega_k) + f_3^+(-E_{-,p,m-1})g_3^+(-E_{-,p,m-1} + i\omega_k) + h_1^+(-E_{-,p,m-1} + i\omega_k)}{E_{p,m-1}E_{-,p,m-1}[E_{-,p+r,l}^2 - (E_{-,p,m-1} - i\omega_k)^2][E_{+,p+r,l}^2 - (E_{-,p,m-1} - i\omega_k)^2]} \\
& -n_F(E_{-,p,m+1} - \mu) \frac{f_2^+(E_{-,p,m+1})g_2^+(E_{-,p,m+1} + i\omega_k) + f_4^+(E_{-,p,m+1})g_4^+(E_{-,p,m+1} + i\omega_k) + h_2^+(E_{-,p,m+1} + i\omega_k)}{E_{p,m+1}E_{-,p,m+1}[E_{-,p+r,l}^2 - (E_{-,p,m+1} + i\omega_k)^2][E_{+,p+r,l}^2 - (E_{-,p,m+1} + i\omega_k)^2]} \\
& -n_F(E_{-,p,m+1} + \mu) \frac{f_2^+(-E_{-,p,m+1})g_2^+(-E_{-,p,m+1} + i\omega_k) + f_4^+(-E_{-,p,m+1})g_4^+(-E_{-,p,m+1} + i\omega_k) + h_2^+(-E_{-,p,m+1} + i\omega_k)}{E_{p,m+1}E_{-,p,m+1}[E_{-,p+r,l}^2 - (E_{-,p,m+1} - i\omega_k)^2][E_{+,p+r,l}^2 - (E_{-,p,m+1} - i\omega_k)^2]}
\end{aligned}$$

$$\begin{aligned}
& +n_F(E_{+,p+r,l} - i\omega_k - \mu) \frac{f_1^+(E_{+,p+r,l} - i\omega_k)g_1^+(E_{+,p+r,l}) + f_3^+(E_{+,p+r,l} - i\omega_k)g_3^+(E_{+,p+r,l}) + h_1^+(E_{+,p+r,l})}{E_{p+r,l}E_{+,p+r,l}[E_{-,p,m-1}^2 - (E_{+,p+r,l} - i\omega_k)^2][E_{+,p,m-1}^2 - (E_{+,p+r,l} - i\omega_k)^2]} \\
& +n_F(E_{+,p+r,l} + i\omega_k + \mu) \frac{f_1^+(-E_{+,p+r,l} - i\omega_k)g_1^+(-E_{+,p+r,l}) + f_3^+(-E_{+,p+r,l} - i\omega_k)g_3^+(-E_{+,p+r,l}) + h_1^+(-E_{+,p+r,l})}{E_{p+r,l}E_{+,p+r,l}[E_{-,p,m-1}^2 - (E_{+,p+r,l} + i\omega_k)^2][E_{+,p,m-1}^2 - (E_{+,p+r,l} + i\omega_k)^2]} \\
& +n_F(E_{+,p+r,l} - i\omega_k - \mu) \frac{f_2^+(E_{+,p+r,l} - i\omega_k)g_2^+(E_{+,p+r,l}) + f_4^+(E_{+,p+r,l} - i\omega_k)g_4^+(E_{+,p+r,l}) + h_2^+(E_{+,p+r,l})}{E_{p+r,l}E_{+,p+r,l}[E_{-,p,m+1}^2 - (E_{+,p+r,l} - i\omega_k)^2][E_{+,p,m+1}^2 - (E_{+,p+r,l} - i\omega_k)^2]} \\
& +n_F(E_{+,p+r,l} + i\omega_k + \mu) \frac{f_2^+(-E_{+,p+r,l} - i\omega_k)g_2^+(-E_{+,p+r,l}) + f_4^+(-E_{+,p+r,l} - i\omega_k)g_4^+(-E_{+,p+r,l}) + h_2^+(-E_{+,p+r,l})}{E_{p+r,l}E_{+,p+r,l}[E_{-,p,m+1}^2 - (E_{+,p+r,l} + i\omega_k)^2][E_{+,p,m+1}^2 - (E_{+,p+r,l} + i\omega_k)^2]} \\
& -n_F(E_{-,p+r,l} - i\omega_k - \mu) \frac{f_1^+(E_{-,p+r,l} - i\omega_k)g_1^+(E_{-,p+r,l}) + f_3^+(E_{-,p+r,l} - i\omega_k)g_3^+(E_{-,p+r,l}) + h_1^+(E_{-,p+r,l})}{E_{p+r,l}E_{-,p+r,l}[E_{-,p,m-1}^2 - (E_{-,p+r,l} - i\omega_k)^2][E_{+,p,m-1}^2 - (E_{-,p+r,l} - i\omega_k)^2]} \\
& -n_F(E_{-,p+r,l} + i\omega_k + \mu) \frac{f_1^+(-E_{-,p+r,l} - i\omega_k)g_1^+(-E_{-,p+r,l}) + f_3^+(-E_{-,p+r,l} - i\omega_k)g_3^+(-E_{-,p+r,l}) + h_1^+(-E_{-,p+r,l})}{E_{p+r,l}E_{-,p+r,l}[E_{-,p,m-1}^2 - (E_{-,p+r,l} + i\omega_k)^2][E_{+,p,m-1}^2 - (E_{-,p+r,l} + i\omega_k)^2]} \\
& -n_F(E_{-,p+r,l} - i\omega_k - \mu) \frac{f_2^+(E_{-,p+r,l} - i\omega_k)g_2^+(E_{-,p+r,l}) + f_4^+(E_{-,p+r,l} - i\omega_k)g_4^+(E_{-,p+r,l}) + h_2^+(E_{-,p+r,l})}{E_{p+r,l}E_{-,p+r,l}[E_{-,p}^2 - (E_{-,p+r,l} - i\omega_k)^2][E_{+,p,m+1}^2 - (E_{-,p+r,l} - i\omega_k)^2]} \\
& -n_F(E_{-,p+r,l} + i\omega_k + \mu) \frac{f_2^+(-E_{-,p+r,l} - i\omega_k)g_2^+(-E_{-,p+r,l}) + f_4^+(-E_{-,p+r,l} - i\omega_k)g_4^+(-E_{-,p+r,l}) + h_2^+(-E_{-,p+r,l})}{E_{p+r,l}E_{-,p+r,l}[E_{-,p}^2 - (E_{-,p+r,l} + i\omega_k)^2][E_{+,p,m+1}^2 - (E_{-,p+r,l} + i\omega_k)^2]}
\end{aligned}$$

$$J_{\vec{m}}^-(i\omega_k; \vec{r} + 2l\vec{Q}, \vec{r}) = \int \frac{d^3p}{(2\pi)^3} \quad (\text{D.26})$$

$$\begin{aligned}
& n_F(E_{+,p,m} - \mu) \frac{f_1^-(E_{+,p,m})g_1^-(E_{+,p,m} + i\omega_k) + f_3^-(E_{+,p,m})g_3^-(E_{+,p,m} + i\omega_k) + h_1^-(E_{+,p,m} + i\omega_k)}{E_{p,m}E_{+,p,m}[E_{-,p+r,l-1}^2(-E_{+,p,m} + i\omega_k)^2][E_{+,p+r,l-1}^2(-E_{+,p,m} + i\omega_k)^2]} \\
& - n_F(-E_{+,p,m} - \mu) \frac{f_1^-(E_{+,p,m})g_1^-(E_{+,p,m} + i\omega_k) + f_3^-(E_{+,p,m})g_3^-(E_{+,p,m} + i\omega_k) + h_1^-(E_{+,p,m} + i\omega_k)}{E_{p,m}E_{+,p,m}[E_{-,p+r,l-1}^2(-E_{+,p,m} - i\omega_k)^2][E_{+,p+r,l-1}^2(-E_{+,p,m} - i\omega_k)^2]} \\
& - n_F(E_{-,p,m} - \mu) \frac{f_1^-(E_{-,p,m})g_1^-(E_{-,p,m} + i\omega_k) + f_3^-(E_{-,p,m})g_3^-(E_{-,p,m} + i\omega_k) + h_1^-(E_{-,p,m} + i\omega_k)}{E_{p,m}E_{-,p,m}[E_{-,p+r,l-1}^2(-E_{-,p,m} + i\omega_k)^2][E_{+,p+r,l-1}^2(-E_{-,p,m} + i\omega_k)^2]} \\
& + n_F(-E_{-,p,m} - \mu) \frac{f_1^-(E_{-,p,m})g_1^-(E_{-,p,m} + i\omega_k) + f_3^-(E_{-,p,m})g_3^-(E_{-,p,m} + i\omega_k) + h_1^-(E_{-,p,m} + i\omega_k)}{E_{p,m}E_{-,p,m}[E_{-,p+r,l-1}^2(-E_{-,p,m} - i\omega_k)^2][E_{+,p+r,l-1}^2(-E_{-,p,m} - i\omega_k)^2]} \\
& + n_F(E_{+,p+r,l-1} - i\omega_k - \mu) \frac{f_1^-(E_{+,p+r,l-1} - i\omega_k)g_1^-(E_{+,p+r,l-1}) + f_3^-(E_{+,p+r,l-1} - i\omega_k)g_3^-(E_{+,p+r,l-1}) + h_1^-(E_{+,p+r,l-1})}{E_{p+r,l-1}E_{+,p+r,l-1}[E_{-,p,m}^2(-E_{+,p+r,l-1} - i\omega_k)^2][E_{+,p,m}^2(-E_{+,p+r,l-1} - i\omega_k)^2]} \\
& - n_F(-E_{+,p+r,l-1} - i\omega_k - \mu) \frac{f_1^-(E_{+,p+r,l-1} - i\omega_k)g_1^-(E_{+,p+r,l-1}) + f_3^-(E_{+,p+r,l-1} - i\omega_k)g_3^-(E_{+,p+r,l-1}) + h_1^-(E_{+,p+r,l-1})}{E_{p+r,l-1}E_{+,p+r,l-1}[E_{-,p,m}^2(-E_{+,p+r,l-1} - i\omega_k)^2][E_{+,p,m}^2(-E_{+,p+r,l-1} - i\omega_k)^2]} \\
& - n_F(E_{-,p+r,l-1} - i\omega_k - \mu) \frac{f_1^-(E_{-,p+r,l-1} - i\omega_k)g_1^-(E_{-,p+r,l-1}) + f_3^-(E_{-,p+r,l-1} - i\omega_k)g_3^-(E_{-,p+r,l-1}) + h_1^-(E_{-,p+r,l-1})}{E_{p+r,l-1}E_{-,p+r,l-1}[E_{-,p,m}^2(-E_{-,p+r,l-1} - i\omega_k)^2][E_{+,p,m}^2(-E_{-,p+r,l-1} - i\omega_k)^2]} \\
& + n_F(-E_{-,p+r,l-1} - i\omega_k - \mu) \frac{f_1^-(E_{-,p+r,l-1} - i\omega_k)g_1^-(E_{-,p+r,l-1}) + f_3^-(E_{-,p+r,l-1} - i\omega_k)g_3^-(E_{-,p+r,l-1}) + h_1^-(E_{-,p+r,l-1})}{E_{p+r,l-1}E_{-,p+r,l-1}[E_{-,p,m}^2(-E_{-,p+r,l-1} - i\omega_k)^2][E_{+,p,m}^2(-E_{-,p+r,l-1} - i\omega_k)^2]}
\end{aligned}$$

$$\begin{aligned}
& +n_F(E_{+,p,m} - \mu) \frac{f_2^-(E_{+,p,m})g_2^-(E_{+,p,m} + i\omega_k) + f_4^-(E_{+,p,m})g_4^-(E_{+,p,m} + i\omega_k) + h_2^-(E_{+,p,m} + i\omega_k)}{E_{p,m}E_{+,p,m}[E_{-,p+r,l+1}^2 - (E_{+,p,m} + i\omega_k)^2][E_{+,p+r,l+1}^2 - (E_{+,p,m} + i\omega_k)^2]} \\
& -n_F(-E_{+,p,m} - \mu) \frac{f_2^-(E_{+,p,m})g_2^-(E_{+,p,m} + i\omega_k) + f_4^-(E_{+,p,m})g_4^-(E_{+,p,m} + i\omega_k) + h_2^-(E_{+,p,m} + i\omega_k)}{E_{p,m}E_{+,p,m}[E_{-,p+r,l+1}^2 - (E_{+,p,m} - i\omega_k)^2][E_{+,p+r,l+1}^2 - (E_{+,p,m} - i\omega_k)^2]} \\
& -n_F(E_{-,p,m} - \mu) \frac{f_2^-(E_{-,p,m})g_2^-(E_{-,p,m} + i\omega_k) + f_4^-(E_{-,p,m})g_4^-(E_{-,p,m} + i\omega_k) + h_2^-(E_{-,p,m} + i\omega_k)}{E_{p,m}E_{-,p,m}[E_{-,p+r,l+1}^2 - (E_{-,p,m} + i\omega_k)^2][E_{+,p+r,l+1}^2 - (E_{-,p,m} + i\omega_k)^2]} \\
& +n_F(-E_{-,p,m} - \mu) \frac{f_2^-(E_{-,p,m})g_2^-(E_{-,p,m} + i\omega_k) + f_4^-(E_{-,p,m})g_4^-(E_{-,p,m} + i\omega_k) + h_2^-(E_{-,p,m} + i\omega_k)}{E_{p,m}E_{-,p,m}[E_{-,p+r,l+1}^2 - (E_{-,p,m} - i\omega_k)^2][E_{+,p+r,l+1}^2 - (E_{-,p,m} - i\omega_k)^2]} \\
& +n_F(E_{+,p+r,l+1} - i\omega_k - \mu) \frac{f_2^-(E_{+,p+r,l+1} - i\omega_k)g_2^-(E_{+,p+r,l+1}) + f_4^-(E_{+,p+r,l+1} - i\omega_k)g_4^-(E_{+,p+r,l+1}) + h_2^-(E_{+,p+r,l+1})}{E_{p+r,l+1}E_{+,p+r,l+1}[E_{-,p,m}^2 - (E_{+,p+r,l+1} - i\omega_k)^2][E_{+,p,m}^2 - (E_{+,p+r,l+1} - i\omega_k)^2]} \\
& -n_F(-E_{+,p+r,l+1} - i\omega_k - \mu) \frac{f_2^-(E_{+,p+r,l+1} - i\omega_k)g_2^-(E_{+,p+r,l+1}) + f_4^-(E_{+,p+r,l+1} - i\omega_k)g_4^-(E_{+,p+r,l+1}) + h_2^-(E_{+,p+r,l+1})}{E_{p+r,l+1}E_{+,p+r,l+1}[E_{-,p,m}^2 - (E_{+,p+r,l+1} - i\omega_k)^2][E_{+,p,m}^2 - (E_{+,p+r,l+1} - i\omega_k)^2]} \\
& -n_F(E_{-,p+r,l+1} - i\omega_k - \mu) \frac{f_2^-(E_{-,p+r,l+1} - i\omega_k)g_2^-(E_{-,p+r,l+1}) + f_4^-(E_{-,p+r,l+1} - i\omega_k)g_4^-(E_{-,p+r,l+1}) + h_2^-(E_{-,p+r,l+1})}{E_{p+r,l+1}E_{-,p+r,l+1}[E_{-,p,m}^2 - (E_{-,p+r,l+1} - i\omega_k)^2][E_{+,p,m}^2 - (E_{-,p+r,l+1} - i\omega_k)^2]} \\
& +n_F(-E_{-,p+r,l+1} - i\omega_k - \mu) \frac{f_2^-(E_{-,p+r,l+1} - i\omega_k)g_2^-(E_{-,p+r,l+1}) + f_4^-(E_{-,p+r,l+1} - i\omega_k)g_4^-(E_{-,p+r,l+1}) + h_2^-(E_{-,p+r,l+1})}{E_{p+r,l+1}E_{-,p+r,l+1}[E_{-,p,m}^2 - (E_{-,p+r,l+1} - i\omega_k)^2][E_{+,p,m}^2 - (E_{-,p+r,l+1} - i\omega_k)^2]}
\end{aligned}$$

$$J_m^-(i\omega_k; \vec{r} + 2l\vec{Q}, \vec{r}) = \int \frac{d^3p}{(2\pi)^3} \quad (\text{D.27})$$

$$\begin{aligned}
& \frac{f_1^-(-E_{+,p,m})g_1^-(-E_{+,p,m} + i\omega_k) + f_3^-(-E_{+,p,m})g_3^-(-E_{+,p,m} + i\omega_k) + h_1^-(-E_{+,p,m} + i\omega_k)}{E_{p,m}E_{+,p,m}[E_{-,p+p+r,l-1}^2 - (E_{+,p,m} - i\omega_k)^2][E_{+,p+p+r,l-1}^2 - (E_{+,p,m} - i\omega_k)^2]} \\
& + \frac{f_1^-(-E_{+,p+p+r,l-1} - i\omega_k)g_1^-(-E_{+,p+p+r,l-1}) + f_3^-(-E_{+,p+p+r,l-1} - i\omega_k)g_3^-(-E_{+,p+p+r,l-1}) + h_1^-(-E_{+,p+p+r,l-1})}{E_{p+p+r,l-1}E_{+,p+p+r,l-1}[E_{-,p,m}^2 - (E_{+,p+p+r,l-1} + i\omega_k)^2][E_{+,p,m}^2 - (E_{+,p+p+r,l-1} + i\omega_k)^2]} \\
& + \frac{f_2^-(-E_{+,p,m})g_2^-(-E_{+,p,m} + i\omega_k) + f_4^-(-E_{+,p,m})g_4^-(-E_{+,p,m} + i\omega_k) + h_2^-(-E_{+,p,m} + i\omega_k)}{E_{p,m}E_{+,p,m}[E_{-,p+p+r,l+1}^2 - (E_{+,p,m} - i\omega_k)^2][E_{+,p+p+r,l+1}^2 - (E_{+,p,m} - i\omega_k)^2]} \\
& + \frac{f_2^-(-E_{+,p+p+r,l+1} - i\omega_k)g_2^-(-E_{+,p+p+r,l+1}) + f_4^-(-E_{+,p+p+r,l+1} - i\omega_k)g_4^-(-E_{+,p+p+r,l+1}) + h_2^-(-E_{+,p+p+r,l+1})}{E_{p+p+r,l+1}E_{+,p+p+r,l+1}[E_{-,p,m}^2 - (E_{+,p+p+r,l+1} + i\omega_k)^2][E_{+,p,m}^2 - (E_{+,p+p+r,l+1} + i\omega_k)^2]} \\
& + \frac{f_1^-(-E_{-,p,m})g_1^-(-E_{-,p,m} + i\omega_k) + f_3^-(-E_{-,p,m})g_3^-(-E_{-,p,m} + i\omega_k) + h_1^-(-E_{-,p,m} + i\omega_k)}{E_{p,m}E_{-,p,m}[E_{-,p+p+r,l-1}^2 - (E_{-,p,m} - i\omega_k)^2][E_{+,p+p+r,l-1}^2 - (E_{-,p,m} - i\omega_k)^2]} \\
& + \frac{f_1^-(-E_{-,p+p+r,l-1} - i\omega_k)g_1^-(-E_{-,p+p+r,l-1}) + f_3^-(-E_{-,p+p+r,l-1} - i\omega_k)g_3^-(-E_{-,p+p+r,l-1}) + h_1^-(-E_{-,p+p+r,l-1})}{E_{p+p+r,l-1}E_{-,p+p+r,l-1}[E_{-,p,m}^2 - (E_{-,p+p+r,l-1} + i\omega_k)^2][E_{+,p,m}^2 - (E_{-,p+p+r,l-1} + i\omega_k)^2]} \\
& + \frac{f_2^-(-E_{-,p,m})g_2^-(-E_{-,p,m} + i\omega_k) + f_4^-(-E_{-,p,m})g_4^-(-E_{-,p,m} + i\omega_k) + h_2^-(-E_{-,p,m} + i\omega_k)}{E_{p,m}E_{-,p,m}[E_{-,p+p+r,l+1}^2 - (E_{-,p,m} - i\omega_k)^2][E_{+,p+p+r,l+1}^2 - (E_{-,p,m} - i\omega_k)^2]} \\
& + \frac{f_2^-(-E_{-,p+p+r,l+1} - i\omega_k)g_2^-(-E_{-,p+p+r,l+1}) + f_4^-(-E_{-,p+p+r,l+1} - i\omega_k)g_4^-(-E_{-,p+p+r,l+1}) + h_2^-(-E_{-,p+p+r,l+1})}{E_{p+p+r,l+1}E_{-,p+p+r,l+1}[E_{-,p,m}^2 - (E_{-,p+p+r,l+1} + i\omega_k)^2][E_{+,p,m}^2 - (E_{-,p+p+r,l+1} + i\omega_k)^2]}
\end{aligned}$$



$$\begin{aligned}
& +n_F(E_{+,p,m} - \mu) \frac{f_1^-(E_{+,p,m})g_1^-(E_{+,p,m} + i\omega_k) + f_3^-(E_{+,p,m})g_3^-(E_{+,p,m} + i\omega_k) + h_1^-(E_{+,p,m} + i\omega_k)}{E_{p,m}E_{+,p,m}[E_{-,p+r,l-1}^2 - (E_{+,p,m} + i\omega_k)^2][E_{+,p+r,l-1}^2 - (E_{+,p,m} + i\omega_k)^2]} \\
& +n_F(E_{+,p,m} - \mu) \frac{f_1^-(E_{+,p,m})g_1^-(E_{+,p,m} + i\omega_k) + f_3^-(E_{+,p,m})g_3^-(E_{+,p,m} + i\omega_k) + h_1^-(E_{+,p,m} + i\omega_k)}{E_{p,m}E_{+,p,m}[E_{-,p+r,l-1}^2 - (E_{+,p,m} - i\omega_k)^2][E_{+,p+r,l-1}^2 - (E_{+,p,m} - i\omega_k)^2]} \\
& +n_F(E_{+,p,m} - \mu) \frac{f_2^-(E_{+,p,m})g_2^-(E_{+,p,m} + i\omega_k) + f_4^-(E_{+,p,m})g_4^-(E_{+,p,m} + i\omega_k) + h_2^-(E_{+,p,m} + i\omega_k)}{E_{p,m}E_{+,p,m}[E_{-,p+r,l+1}^2 - (E_{+,p,m} + i\omega_k)^2][E_{+,p+r,l+1}^2 - (E_{+,p,m} + i\omega_k)^2]} \\
& +n_F(E_{+,p,m} - \mu) \frac{f_2^-(E_{+,p,m})g_2^-(E_{+,p,m} + i\omega_k) + f_4^-(E_{+,p,m})g_4^-(E_{+,p,m} + i\omega_k) + h_2^-(E_{+,p,m} + i\omega_k)}{E_{p,m}E_{+,p,m}[E_{-,p+r,l+1}^2 - (E_{+,p,m} - i\omega_k)^2][E_{+,p+r,l+1}^2 - (E_{+,p,m} - i\omega_k)^2]} \\
& -n_F(E_{-,p,m} - \mu) \frac{f_1^-(E_{-,p,m})g_1^-(E_{-,p,m} + i\omega_k) + f_3^-(E_{-,p,m})g_3^-(E_{-,p,m} + i\omega_k) + h_1^-(E_{-,p,m} + i\omega_k)}{E_{p,m}E_{-,p,m}[E_{-,p+r,l-1}^2 - (E_{-,p,m} + i\omega_k)^2][E_{+,p+r,l-1}^2 - (E_{-,p,m} + i\omega_k)^2]} \\
& -n_F(E_{-,p,m} - \mu) \frac{f_1^-(E_{-,p,m})g_1^-(E_{-,p,m} + i\omega_k) + f_3^-(E_{-,p,m})g_3^-(E_{-,p,m} + i\omega_k) + h_1^-(E_{-,p,m} + i\omega_k)}{E_{p,m}E_{-,p,m}[E_{-,p+r,l-1}^2 - (E_{-,p,m} - i\omega_k)^2][E_{+,p+r,l-1}^2 - (E_{-,p,m} - i\omega_k)^2]} \\
& -n_F(E_{-,p,m} - \mu) \frac{f_2^-(E_{-,p,m})g_2^-(E_{-,p,m} + i\omega_k) + f_4^-(E_{-,p,m})g_4^-(E_{-,p,m} + i\omega_k) + h_2^-(E_{-,p,m} + i\omega_k)}{E_{p,m}E_{-,p,m}[E_{-,p+r,l+1}^2 - (E_{-,p,m} + i\omega_k)^2][E_{+,p+r,l+1}^2 - (E_{-,p,m} + i\omega_k)^2]} \\
& -n_F(E_{-,p,m} - \mu) \frac{f_2^-(E_{-,p,m})g_2^-(E_{-,p,m} + i\omega_k) + f_4^-(E_{-,p,m})g_4^-(E_{-,p,m} + i\omega_k) + h_2^-(E_{-,p,m} + i\omega_k)}{E_{p,m}E_{-,p,m}[E_{-,p+r,l+1}^2 - (E_{-,p,m} - i\omega_k)^2][E_{+,p+r,l+1}^2 - (E_{-,p,m} - i\omega_k)^2]}
\end{aligned}$$

$$\begin{aligned}
& +n_F(E_{+,p+r,l-1} - i\omega_k - \mu) \frac{f_1^-(E_{+,p+r,l-1} - i\omega_k)g_1^-(E_{+,p+r,l-1}) + f_3^-(E_{+,p+r,l-1} - i\omega_k)g_3^-(E_{+,p+r,l-1}) + h_1^-(E_{+,p+r,l-1})}{E_{p+r,l-1}E_{+,p+r,l-1}[E_{-,p,m}^- - (E_{+,p+r,l-1} - i\omega_k)^2][E_{+,p,p}^- - (E_{+,p+r,l-1} - i\omega_k)^2]} \\
& +n_F(E_{+,p+r,l-1} - i\omega_k - \mu) \frac{f_1^-(E_{+,p+r,l-1} - i\omega_k)g_1^-(E_{+,p+r,l-1}) + f_3^-(E_{+,p+r,l-1} - i\omega_k)g_3^-(E_{+,p+r,l-1}) + h_1^-(E_{+,p+r,l-1})}{E_{p+r,l-1}E_{+,p+r,l-1}[E_{-,p,m}^- - (E_{+,p+r,l-1} + i\omega_k)^2][E_{+,p,m}^- - (E_{+,p+r,l-1} + i\omega_k)^2]} \\
& +n_F(E_{+,p+r,l+1} - i\omega_k - \mu) \frac{f_2^-(E_{+,p+r,l+1} - i\omega_k)g_2^-(E_{+,p+r,l+1}) + f_4^-(E_{+,p+r,l+1} - i\omega_k)g_4^-(E_{+,p+r,l+1}) + h_2^-(E_{+,p+r,l+1})}{E_{p+r,l+1}E_{+,p+r,l+1}[E_{-,p,m}^- - (E_{+,p+r,l+1} - i\omega_k)^2][E_{+,p,m}^- - (E_{+,p+r,l+1} - i\omega_k)^2]} \\
& +n_F(E_{+,p+r,l+1} - i\omega_k - \mu) \frac{f_2^-(E_{+,p+r,l+1} - i\omega_k)g_2^-(E_{+,p+r,l+1}) + f_4^-(E_{+,p+r,l+1} - i\omega_k)g_4^-(E_{+,p+r,l+1}) + h_2^-(E_{+,p+r,l+1})}{E_{p+r,l+1}E_{+,p+r,l+1}[E_{-,p,m}^- - (E_{+,p+r,l+1} + i\omega_k)^2][E_{+,p,m}^- - (E_{+,p+r,l+1} + i\omega_k)^2]} \\
& -n_F(E_{-,p+r,l-1} - i\omega_k - \mu) \frac{f_1^-(E_{-,p+r,l-1} - i\omega_k)g_1^-(E_{-,p+r,l-1}) + f_3^-(E_{-,p+r,l-1} - i\omega_k)g_3^-(E_{-,p+r,l-1}) + h_1^-(E_{-,p+r,l-1})}{E_{p+r,l-1}E_{-,p+r,l-1}[E_{-,p,m}^- - (E_{-,p+r,l-1} - i\omega_k)^2][E_{+,p,m}^- - (E_{-,p+r,l-1} - i\omega_k)^2]} \\
& -n_F(E_{-,p+r,l-1} - i\omega_k - \mu) \frac{f_1^-(E_{-,p+r,l-1} - i\omega_k)g_1^-(E_{-,p+r,l-1}) + f_3^-(E_{-,p+r,l-1} - i\omega_k)g_3^-(E_{-,p+r,l-1}) + h_1^-(E_{-,p+r,l-1})}{E_{p+r,l-1}E_{-,p+r,l-1}[E_{-,p,m}^- - (E_{-,p+r,l-1} + i\omega_k)^2][E_{+,p,m}^- - (E_{-,p+r,l-1} + i\omega_k)^2]} \\
& -n_F(E_{-,p+r,l+1} - i\omega_k - \mu) \frac{f_2^-(E_{-,p+r,l+1} - i\omega_k)g_2^-(E_{-,p+r,l+1}) + f_4^-(E_{-,p+r,l+1} - i\omega_k)g_4^-(E_{-,p+r,l+1}) + h_2^-(E_{-,p+r,l+1})}{E_{p+r,l+1}E_{-,p+r,l+1}[E_{-,p,m}^- - (E_{-,p+r,l+1} - i\omega_k)^2][E_{+,p,m}^- - (E_{-,p+r,l+1} - i\omega_k)^2]} \\
& -n_F(E_{-,p+r,l+1} - i\omega_k - \mu) \frac{f_2^-(E_{-,p+r,l+1} - i\omega_k)g_2^-(E_{-,p+r,l+1}) + f_4^-(E_{-,p+r,l+1} - i\omega_k)g_4^-(E_{-,p+r,l+1}) + h_2^-(E_{-,p+r,l+1})}{E_{p+r,l+1}E_{-,p+r,l+1}[E_{-,p,m}^- - (E_{-,p+r,l+1} + i\omega_k)^2][E_{+,p,m}^- - (E_{-,p+r,l+1} + i\omega_k)^2]}
\end{aligned}$$

---

## Bibliography

---

- [1] M. Gell-Mann. A schematic model of baryons and mesons. *Phys. Lett.*, 8(3):214 – 215, 1964.
- [2] H. Fritzsche, M. Gell-Mann, and H. Leutwyler. Advantages of the color octet gluon picture. *Phys. Lett.*, B47:365 – 368, 1973.
- [3] K. G. Wilson. Confinement of quarks. *Phys. Rev. D*, 10:2445–2459, 1974.
- [4] David J. Gross and Frank Wilczek. Ultraviolet behavior of non-abelian gauge theories. *Phys. Rev. Lett.*, 30:1343–1346, 1973.
- [5] H. David Politzer. Reliable perturbative results for strong interactions? *Phys. Rev. Lett.*, 30:1346–1349, 1973.
- [6] V. Koch. Aspects of chiral symmetry. *Int. J. Mod. Phys*, E:203–256, 1997.
- [7] [https://www-alt.gsi.de/forschung/fair\\_experiments/CBM/Phasendiagram.jpg](https://www-alt.gsi.de/forschung/fair_experiments/CBM/Phasendiagram.jpg), December 2012.
- [8] P. Braun-Munzinger and J. Wambach. The phase diagram of strongly-interacting matter. *Rev. Mod. Phys.*, 81:1031–1050, 2008.
- [9] A. Bazavov, T. Bhattacharya, M. Cheng, C. DeTar, and H.-T. Ding et al. (HotQCD collaboration). Chiral and deconfinement aspects of the QCD transition. *Phys. Rev. D*, 85:054503, 2012.
- [10] F. Karsch. Lattice QCD at high temperature and density. *Lect. Notes Phys.*, 583:209 – 249, 2002.
- [11] C. Allton, S. Ejiri, S. Hands, O. Kaczmarek, F. Karsch, E. Laermann, and C. Schmidt. The equation of state for two flavor QCD at nonzero chemical potential. *Phys. Rev.*, D 68, 2003.
- [12] M. Buballa. NJL-model analysis of dense quark matter. *Physics Reports*, 407(4–6):205 – 376, 2005.
- [13] K. Fukushima and T. Hatsuda. The phase diagram of dense QCD. *Rept. Prog. Phys.*, 74(014001), 2011.
- [14] M. G. Alford, A. Schmitt, K. Rajagopal, and T. Schäfer. Color superconductivity in dense quark matter. *Rev. Mod. Phys.*, 80:1455–1515, 2008.
- [15] A. W. Overhauser. Structure of nuclear matter. *Phys. Rev. Lett.*, 4:415–418, 1960.
- [16] Y. Nambu and G. Jona-Lasinio. Dynamical model of elementary particles based on an analogy with superconductivity. i. *Phys. Rev.*, 122:345–358, 1961.
- [17] Y. Nambu and G. Jona-Lasinio. Dynamical model of elementary particles based on an analogy with superconductivity. ii. *Phys. Rev.*, 124:246–254, 1961.

- 
- [18] S. Carignano and M. Buballa. Inhomogeneous islands and continents in the Nambu–Jona-Lasinio model. *Acta Phys.Polon.Supp.*, 5:641–658, 2012.
- [19] S. Carignano. *Inhomogeneous chiral symmetry breaking phases*. PhD thesis, TU Darmstadt, 2012.
- [20] M. E. Peskin and D. V. Schroeder. *An Introduction to Quantum Field Theory*. Westview Press, 1995.
- [21] W. Pauli and F. Villars. On the invariant regularization in relativistic quantum theory. *Rev. Mod. Phys.*, 21:434–444, 1949.
- [22] E. E. Salpeter and H. A. Bethe. A relativistic equation for bound-state problems. *Phys. Rev.*, 84:1232–1242, 1951.
- [23] M. Oertel. *Investigation of meson loop effects in the Nambu-Jona-Lasinio model*. PhD thesis, TU Darmstadt, 2000.
- [24] S. Moeller. Pion-Pion Scattering and Shear-Viscosity in the Nambu-Jona-Lasinio Model. Master’s thesis, TU Darmstadt, 2012.
- [25] J. I. Kapusta and C. Gale. *Finite Temperature Field Theory. Principles and Applications*. Cambridge University Press, 2006.
- [26] E. Nakano and T. Tatsumi. Chiral symmetry and density waves in quark matter. *Phys. Rev. D*, 71(114006), 2005.
- [27] M. Schramm. Inhomogeneous Phases in the Vector Interaction Extended Nambu–Jona-Lasinio Model. Master’s thesis, TU Darmstadt, 2013.
- [28] M. Schramm. Private communication, TU Darmstadt, 2013.
- [29] K. Heckmann. *Transport coefficients of strongly interacting matter*. PhD thesis, TU Darmstadt, 2011.